Constraints on the Symmetry Energy Parameters from Proton Scattering Experiments at RCNP

Atsushi Tamii

Research Center for Nuclear Physics (RCNP)
Osaka University, Japan

RCNP-E299, E282 and E316 collaborations

1st RAON User Workshop
April 3-5, 2019, Daejeon, Korea

Symmetry Energy of the Nuclear EOS

is important for nuclear physics and nuclear-astrophysics

Core-collapse supernova

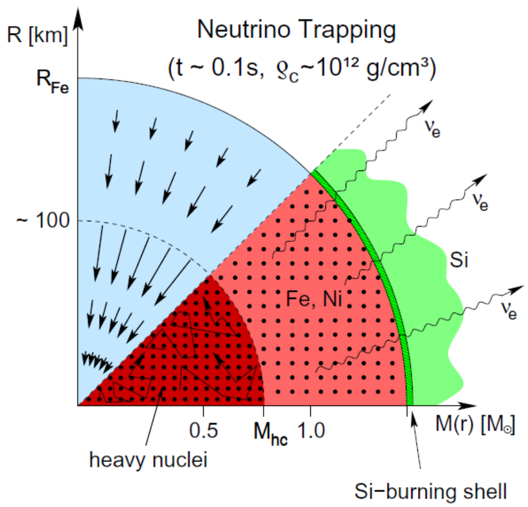

Langanke and Martinez-Pinedo

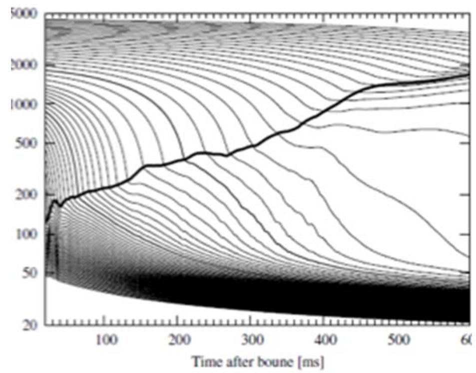

Y. Suwa et al., ApJ764, 99 (2013).

Nucleosynthesis

Neutron star mass vs radius

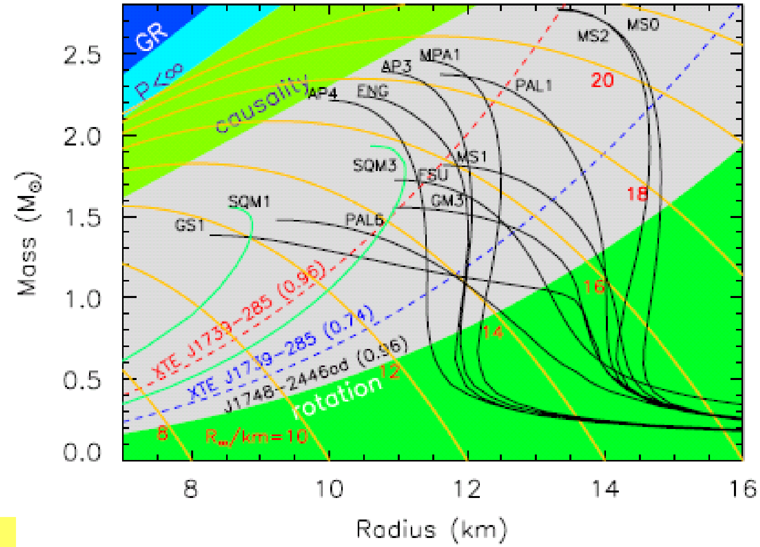

Lattimer et al., Phys. Rep. 442, 109(2007)

Neutron Star Merger Gravitational Wave

https://www.youtube.com/watch?v=IZhNWh_lFuI

Neutron star cooling

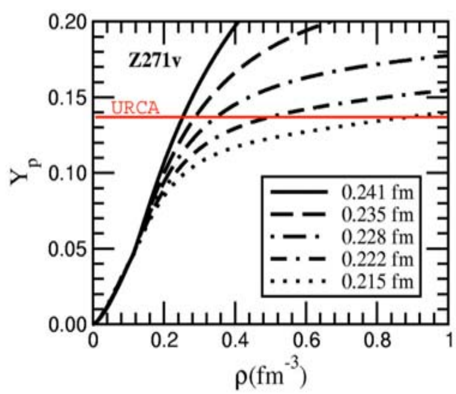

Lattimer and Prakash, Science 304, 536 (2004).

Neutron star structure

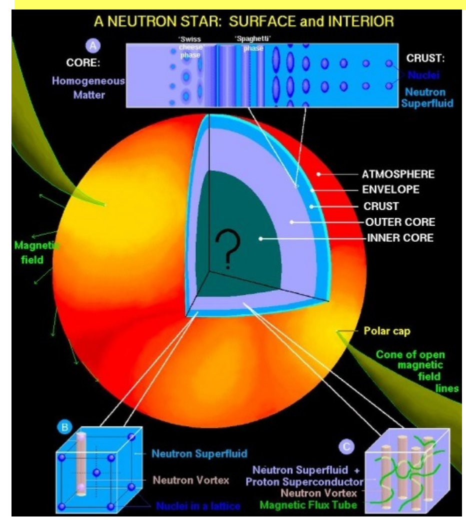

http://www.astro.umd.edu/~miller/nstar.html

Symmetry Energy from Electric Dipole Response of Nuclei

Atsushi Tamii

Research Center for Nuclear Physics (RCNP)
Osaka University, Japan

from the studies with the Grand Raiden spectrometer at RCNP

Workshop on Nuclear Equation of State in the Context of Neutron Star Merger

5th Joint Meeting of the APS Division of Nuclear Physics and the Physical Society of Japan, October 23–27, 2018, Waikoloa, Hawaii

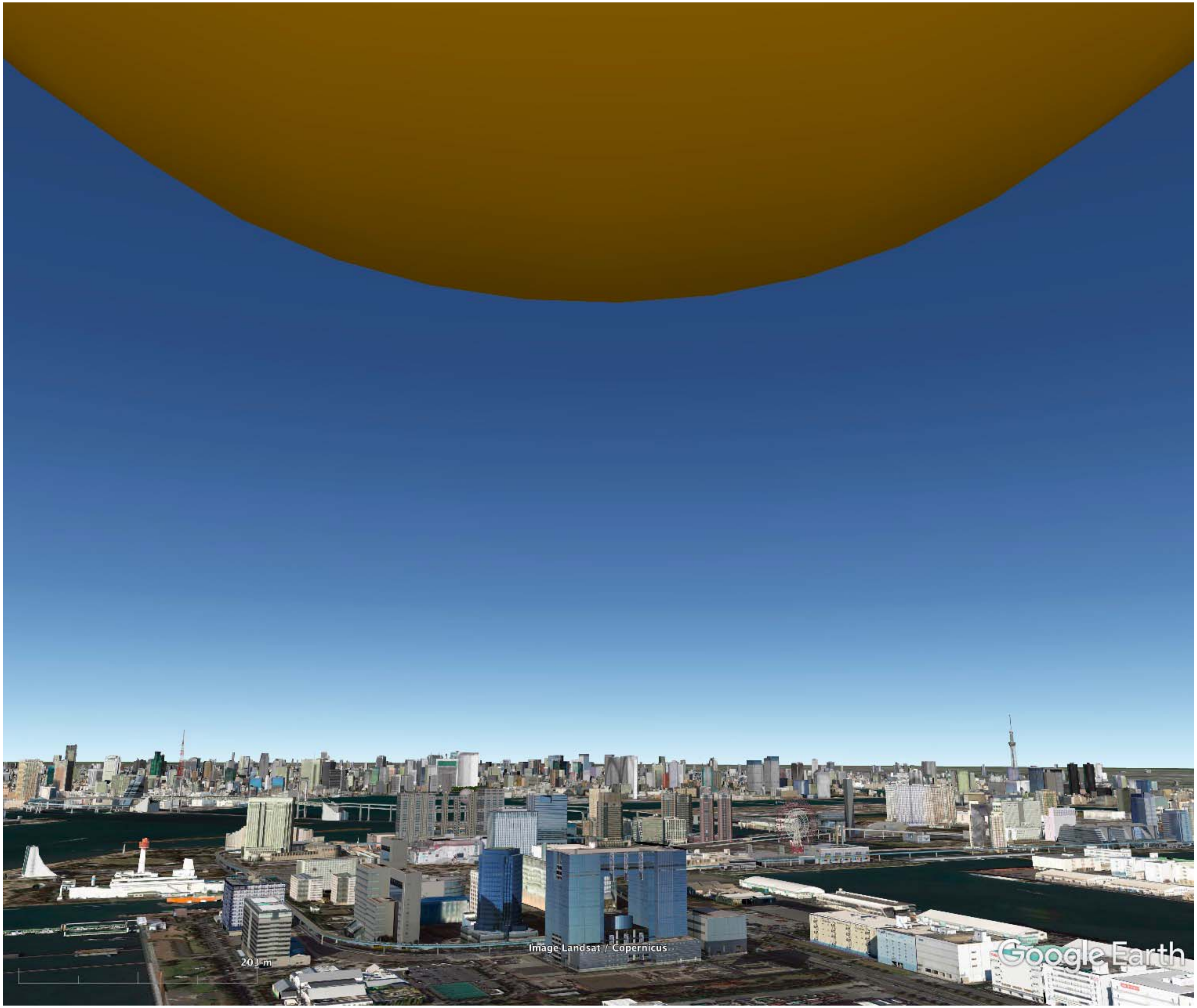
Image Landsat / Copernicus
203 m
Google Earth

Outline

1. Electric dipole response of nuclei and the symmetry energy

2. Experimental methods

3. Results and discussions on the symmetry energy parameters

4. (Other on going studies on the electric dipole response)

Outline of Our Work

Purpose

Symmetry energy of nuclear EOS at $\leqq \rho_0$

Method

An observable that is sensitive to the density difference between *p* and *n* in heavy nuclei

Experiment

Measured electric dipole response of Nuc

Results

Constraints on symmetry energy

$N \gtrsim Z$
$\rho \lesssim \rho_0$
$T=0$
p and n

Ordinary nuclear matter

Starting point to further exotic conditions

Nuclei as a Micro Physics Laboratory

Study of nuclear properties

- Systematic properties of nuclei and nuclear matter
- Properties of individual nuclides, excited states, and reactions

Experimental Methods

- Stable nuclei (target): higher resolution, statistics, and accuracy
- Unstable nuclei (beam): exotic nuclei, broader systematics

Nucleus

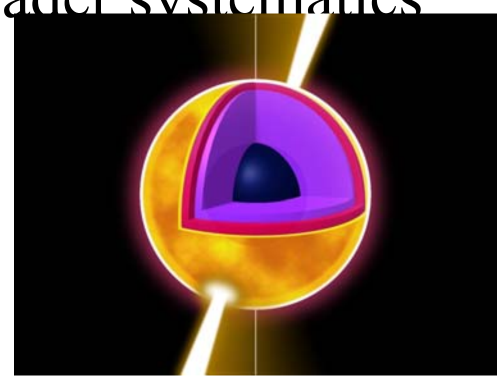

Neutron Star

Strategy

I will focuses on the properties of the nuclear matter in the conditions of

$N \gtrsim Z$	$\longrightarrow$	*neutron matter*
$\rho \lesssim \rho_0$	$\longrightarrow$	*higher density*
$T = 0$	$\longrightarrow$	*finite temperature*
p and n	$\longrightarrow$	*strangeness*

Ordinary nuclear matter

Starting point for the studies of the more exotic conditions

Strategy

High-quality data of nuclear responses

e.g. electric dipole response

Theoretical models

Mean-field models

Parameters of the nuclear equation of states

e.g. J and L

Electric Dipole Response of Nuclei and the Nuclear Symmetry Energy

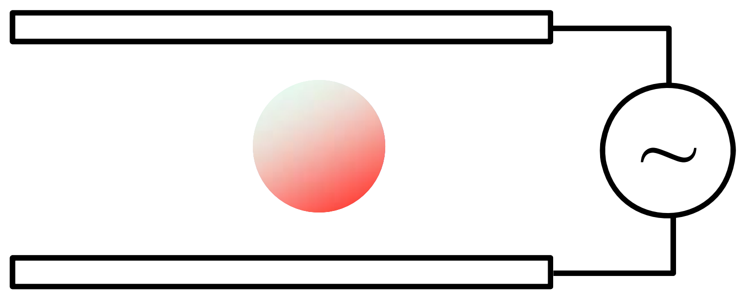

Nuclear Equation of State: How?

How can we study the EOS?

Thermodynamics

Give a “small perturbation” to the system

then observe how the system changes

→ responses

$$\kappa = -\frac{1}{V}\left(\frac{dV}{dp}\right)_S$$ adiabatic compressibility

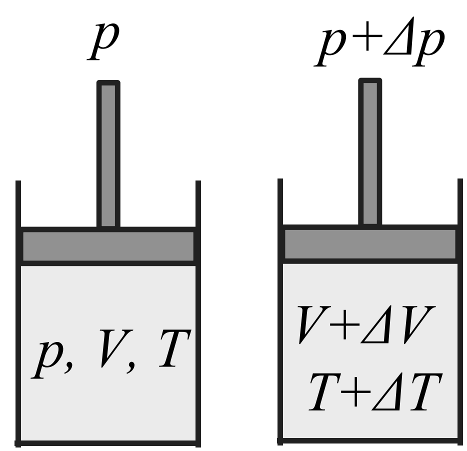

equilibrium

Nuclear EOS

Give a small perturbation by an external field

then observe how the system changes

→ nuclear responses

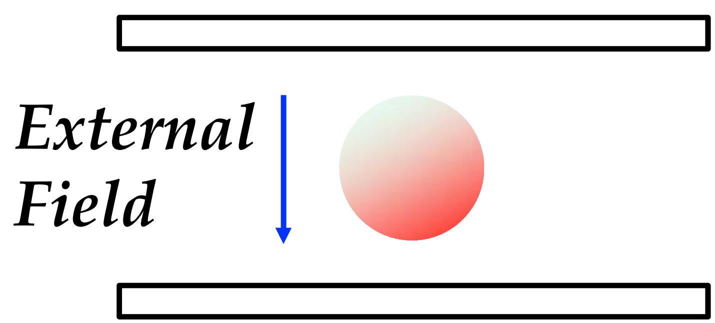

Electric Dipole Response

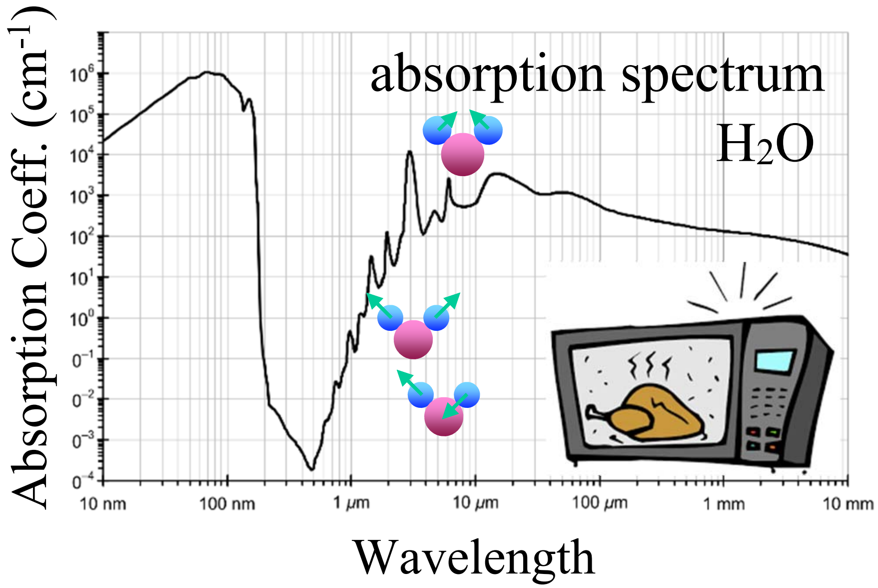

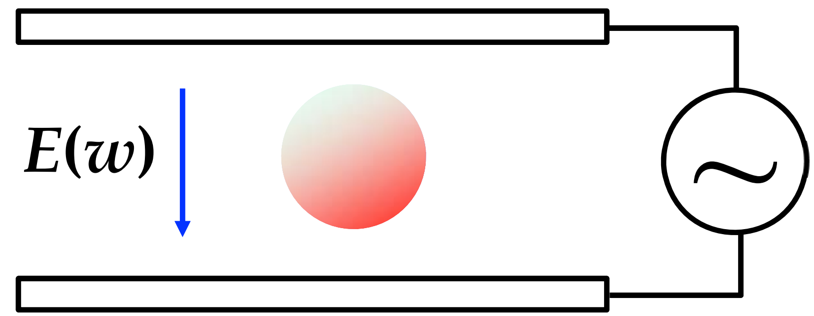

dielectric material
in an oscillating electric field

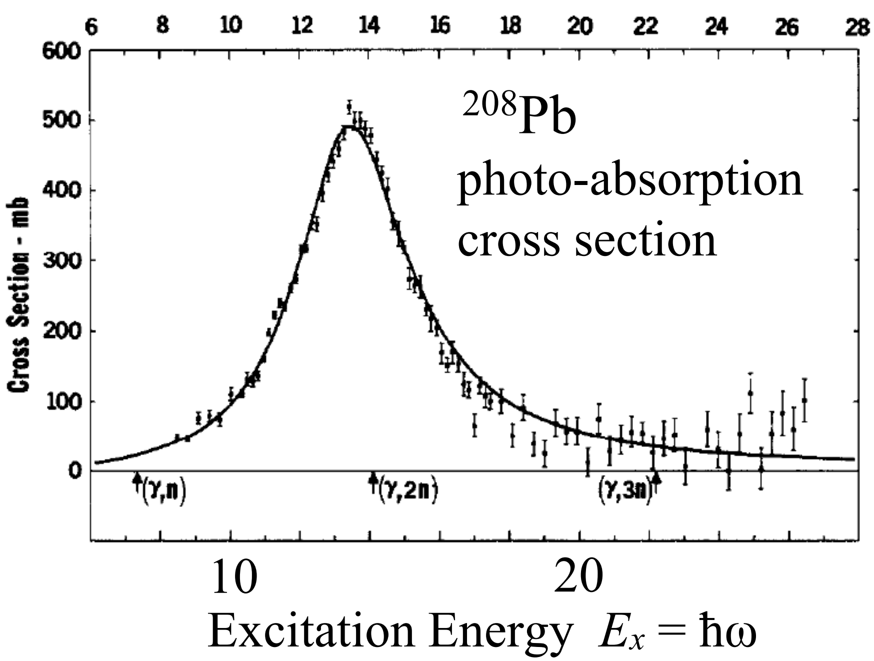

Electric Dipole (E1)
Reduced Transition Probability

$$\frac{dB(E1)}{dE_x} = \frac{9\hbar c}{16\pi^3 e^2}\frac{\sigma_{abs}^{E1}}{E_x}$$

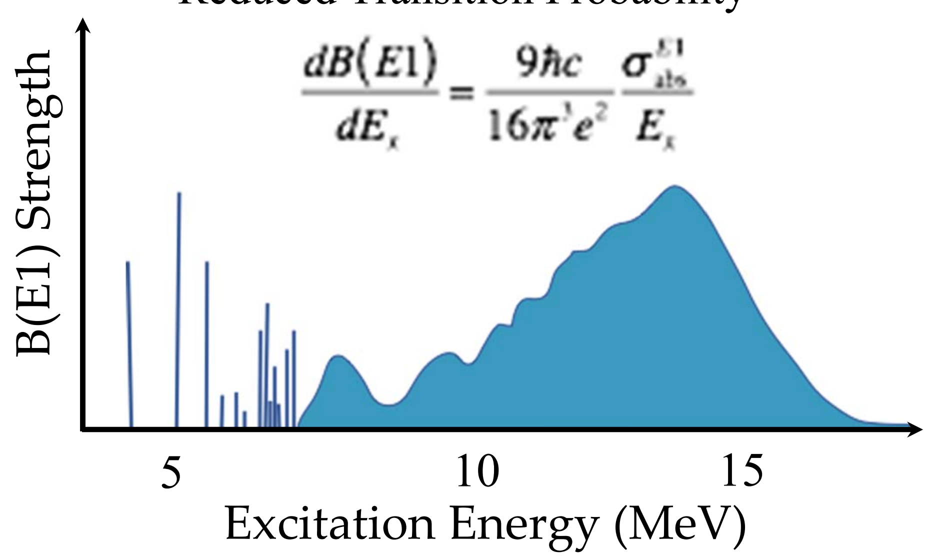

Electric Dipole Response of Nuclei

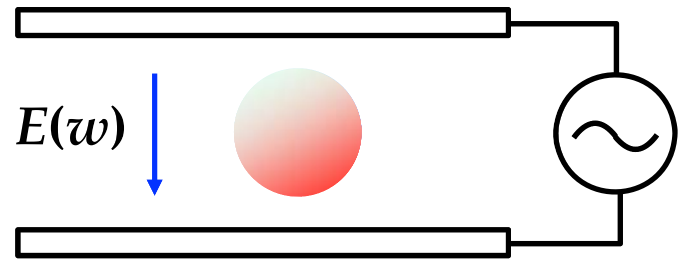

dielectric material
in an oscillating electric field

Electric Dipole Response of Nuclei

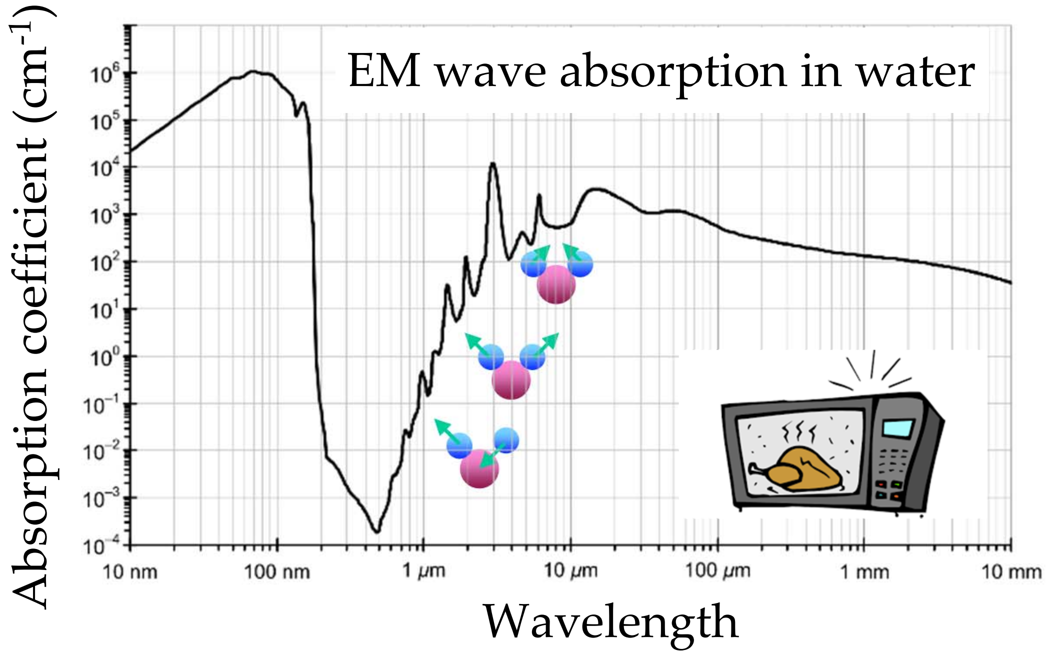

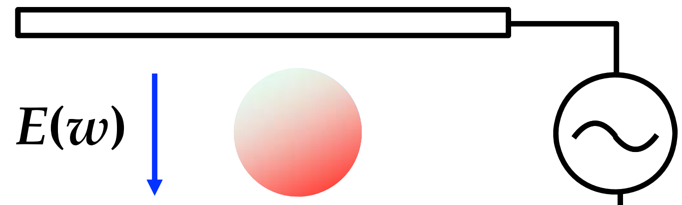

dielectric material
in an oscillating electric field

Electric Dipole Response of Nuclei

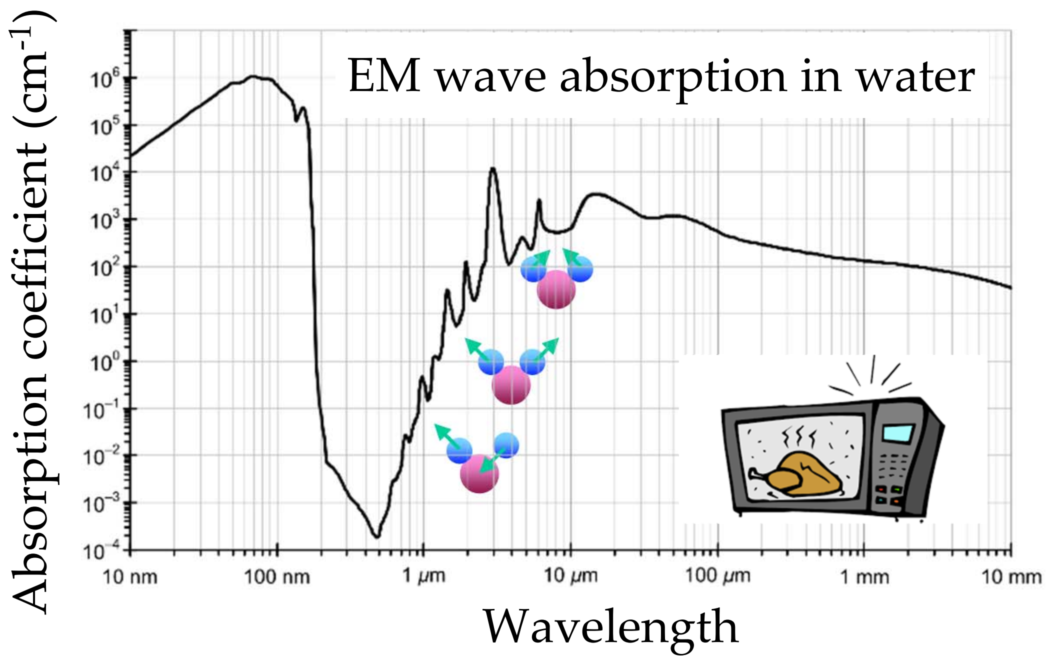

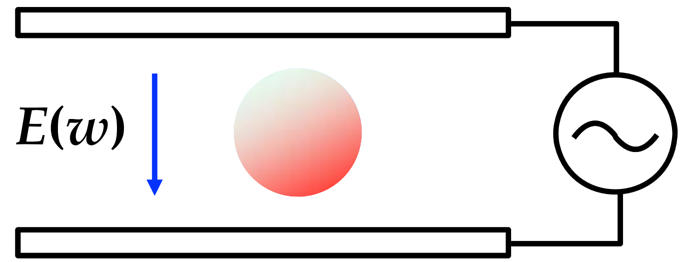

dielectric material
in an oscillating electric field

Photo-absorption by ^{208}Pb

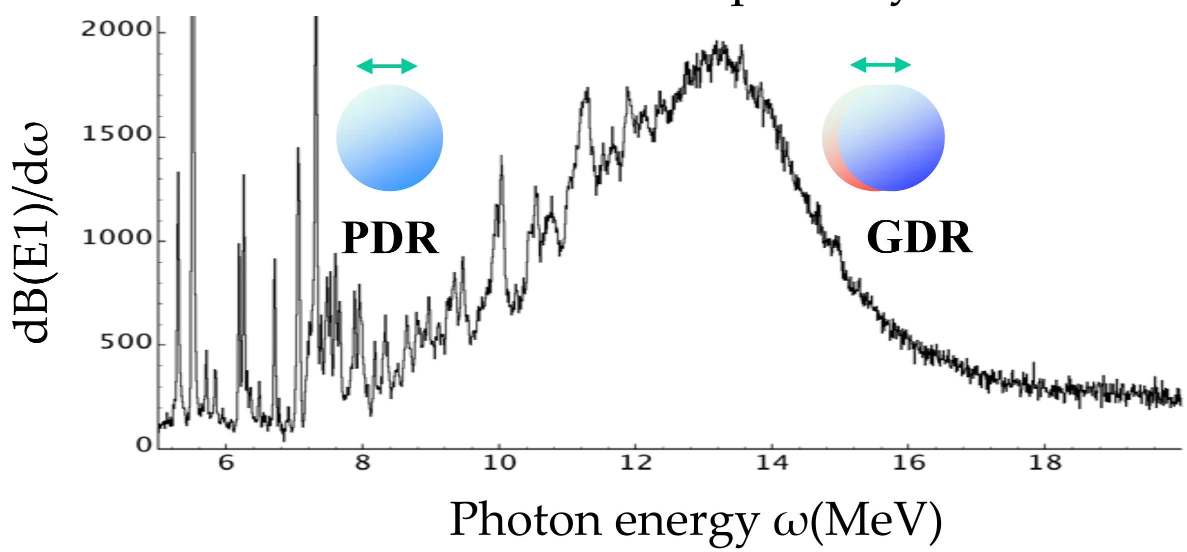

Electric Dipole Response of Nuclei

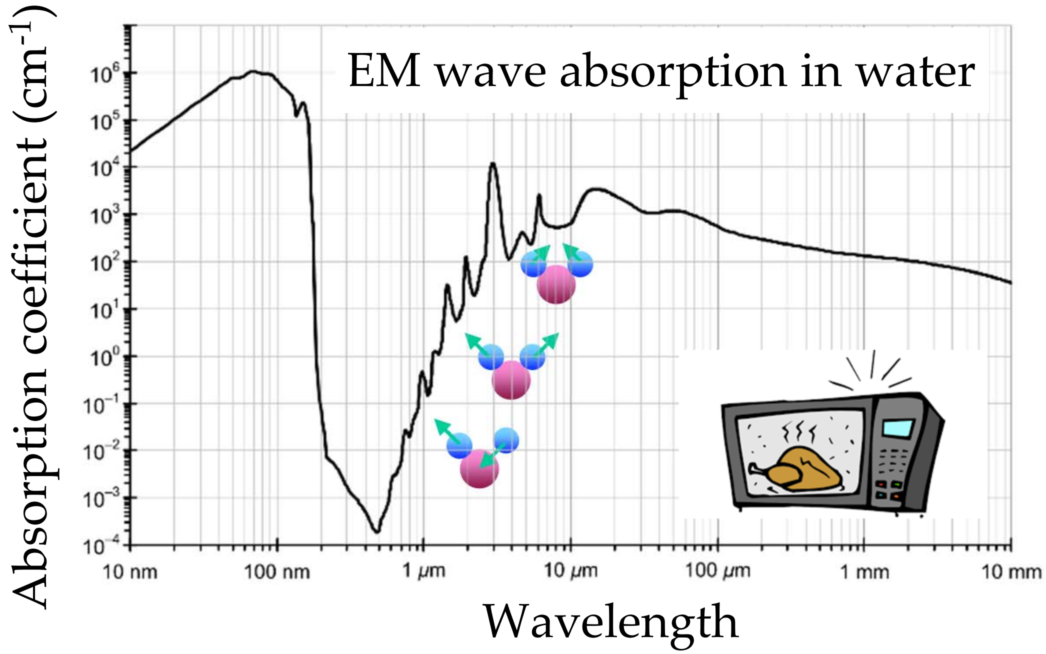

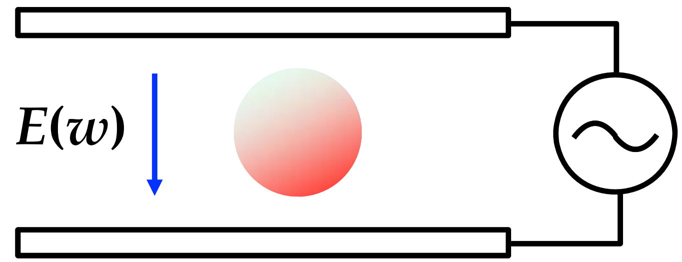

dielectric material
in an oscillating electric field

Photo-absorption by ^{208}Pb

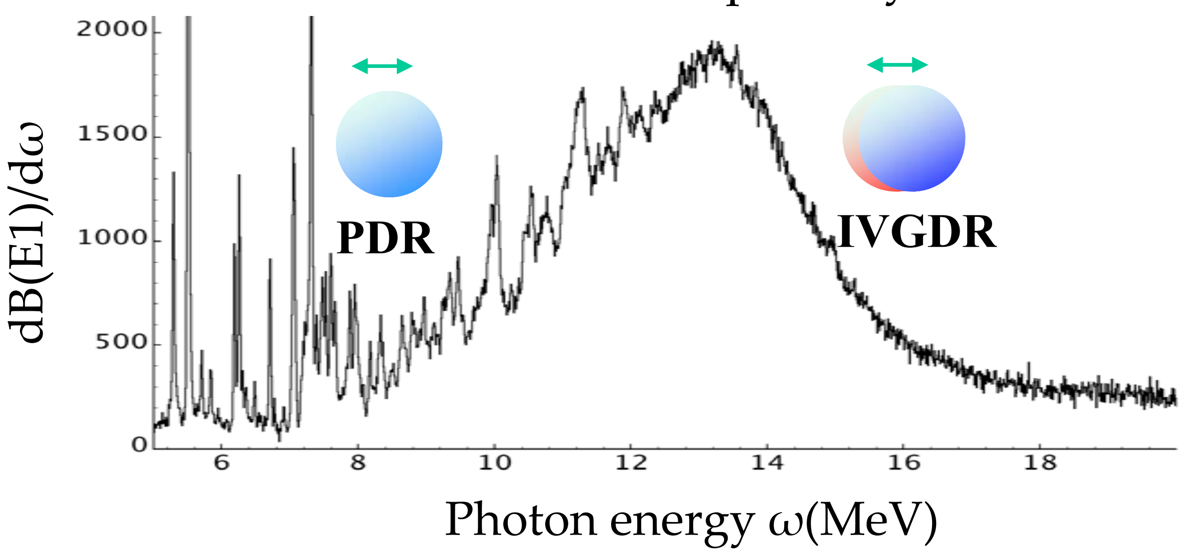

Electric Dipole Response of Nuclei

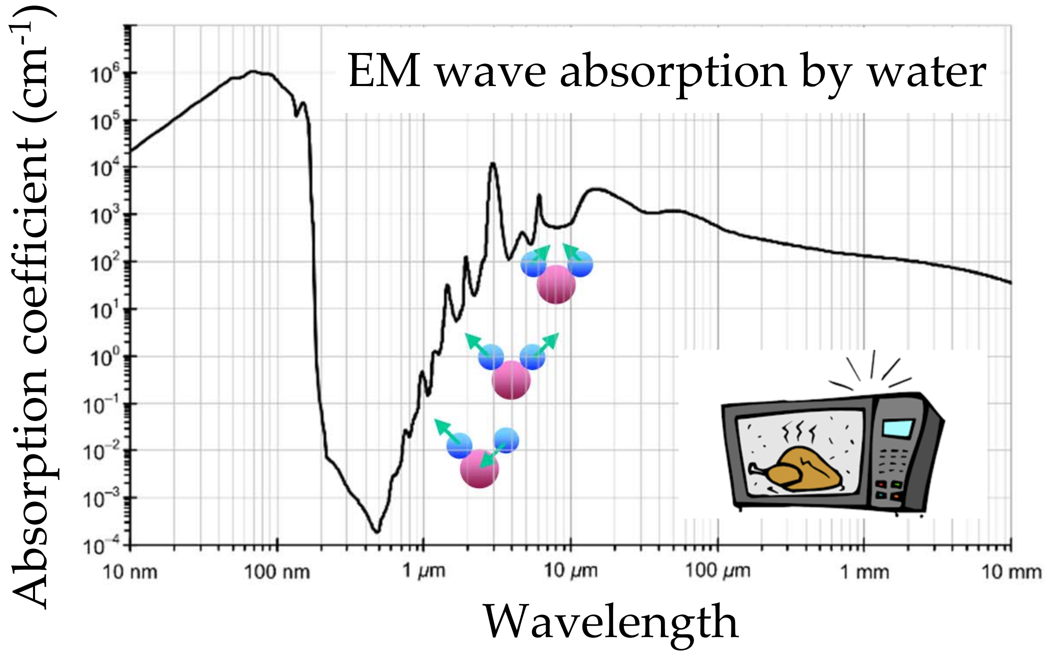

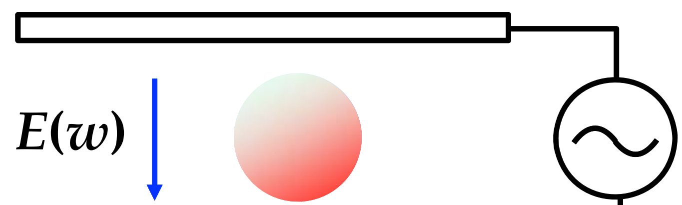

dielectric material
in an oscillating electric field

Photo-absorption by ^{208}Pb

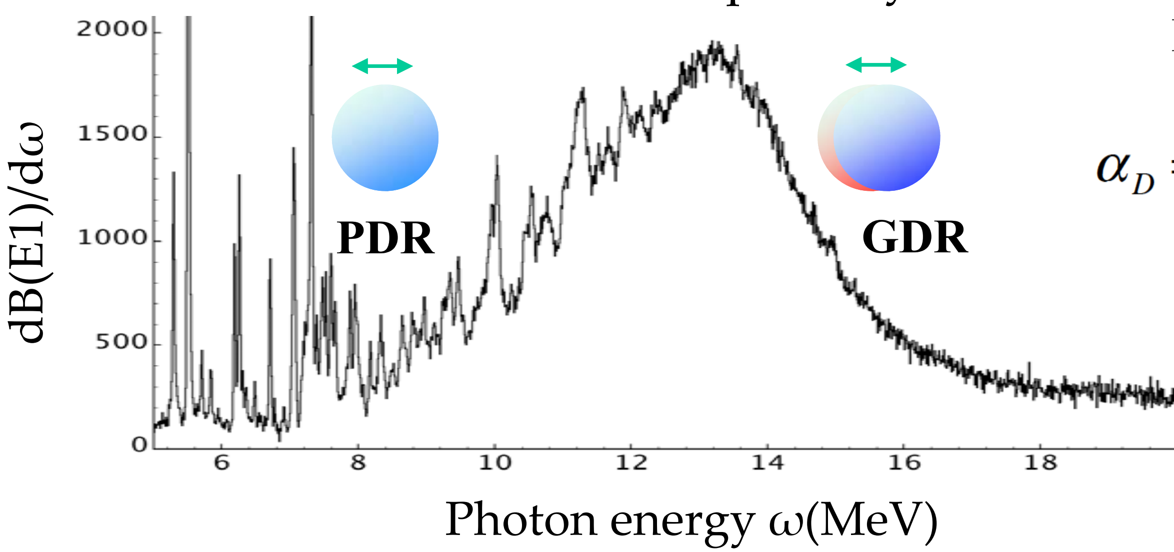

Inversely energy-weighted sum-rule

$$\alpha_D = \frac{\hbar c}{2\pi^2}\int \frac{\sigma_{\rm abs}^{E1}}{\omega^2}d\omega = \frac{8\pi}{9}\int \frac{dB(E1)}{\omega}$$

first order perturbation calc.

A.B. Migdal: 1944

Electric Dipole Response of Nuclei

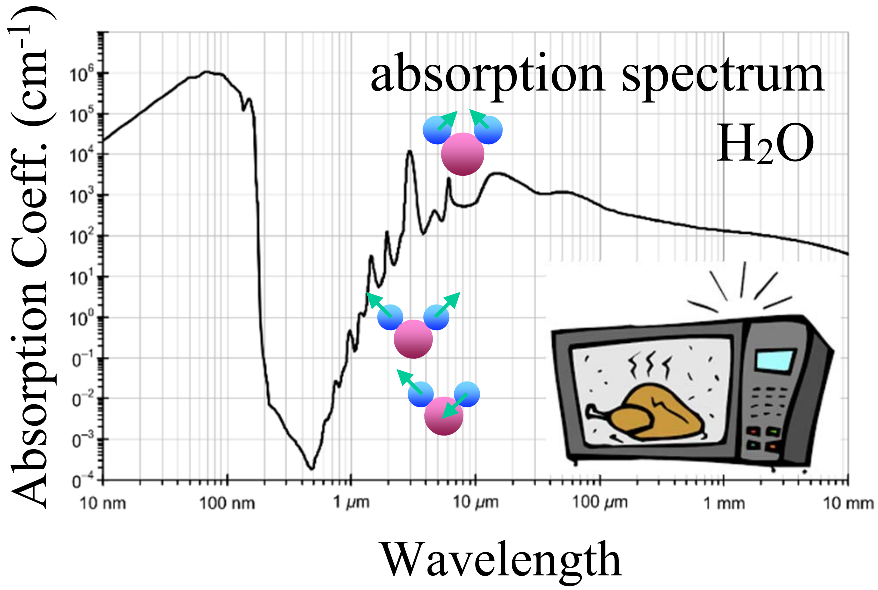

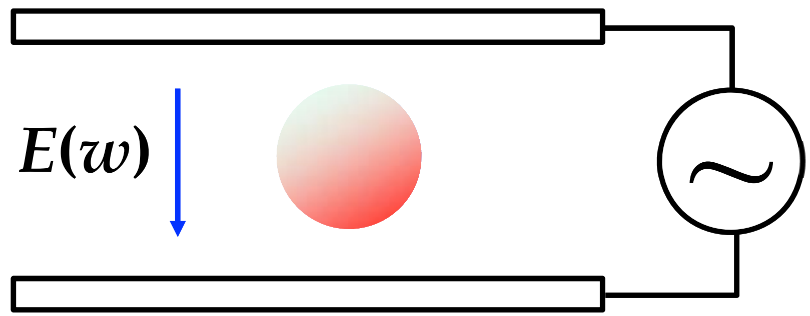

dielectric material
in an oscillating electric field

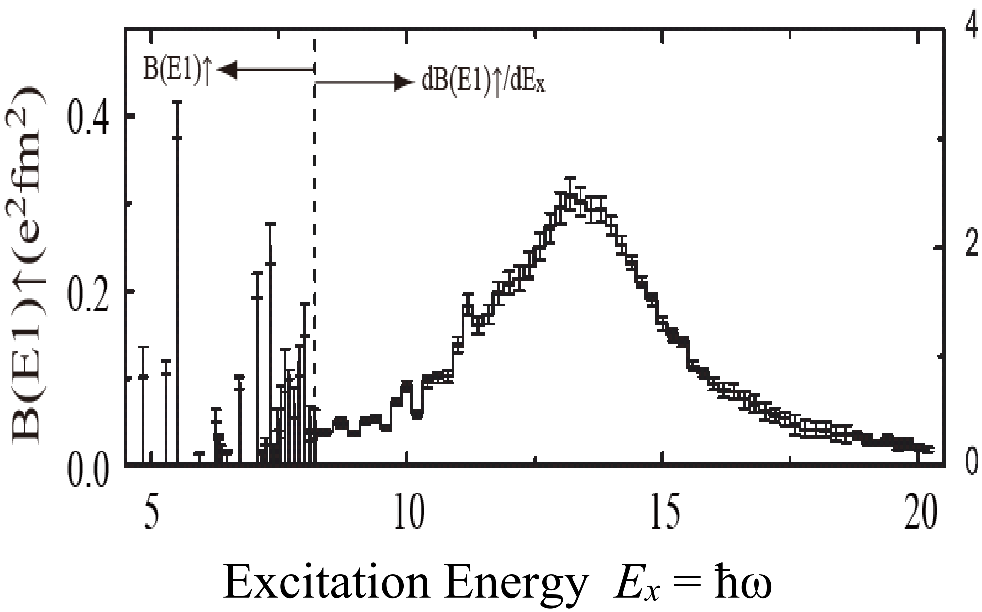

Electric Dipole (E1)
Reduced Transition Probability

$$\frac{dB(E1)}{dE_x} = \frac{9\hbar c}{16\pi^3 e^2}\frac{\sigma_{abs}^{E1}}{E_x}$$

Electric Dipole Response

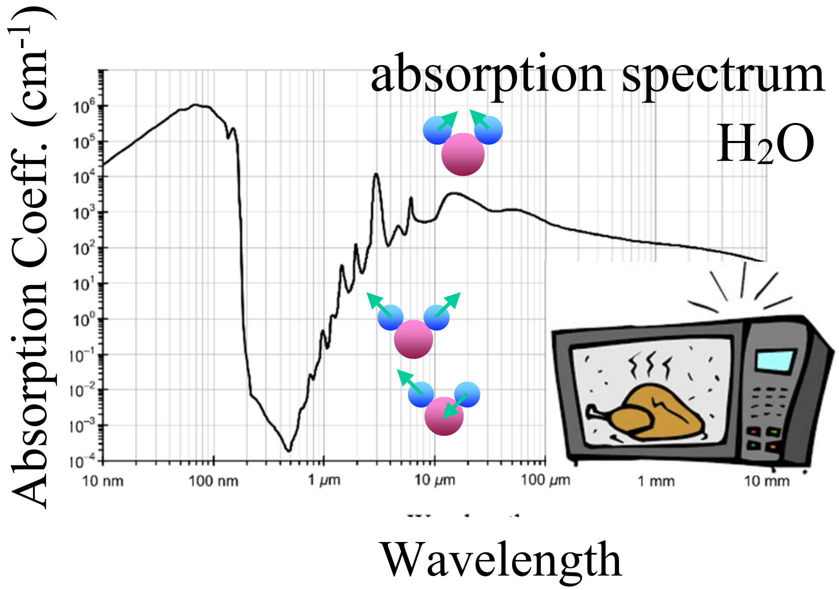

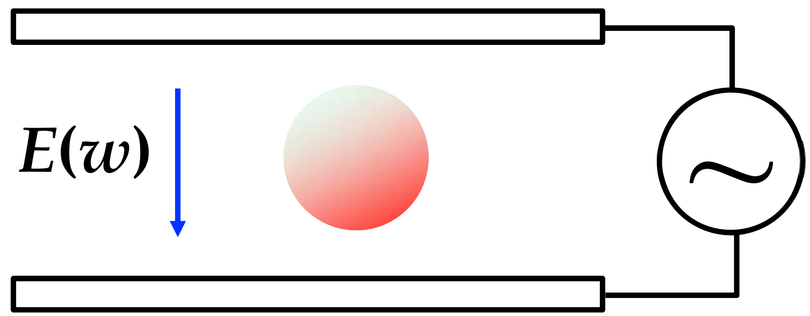

dielectric material
in an oscillating electric field

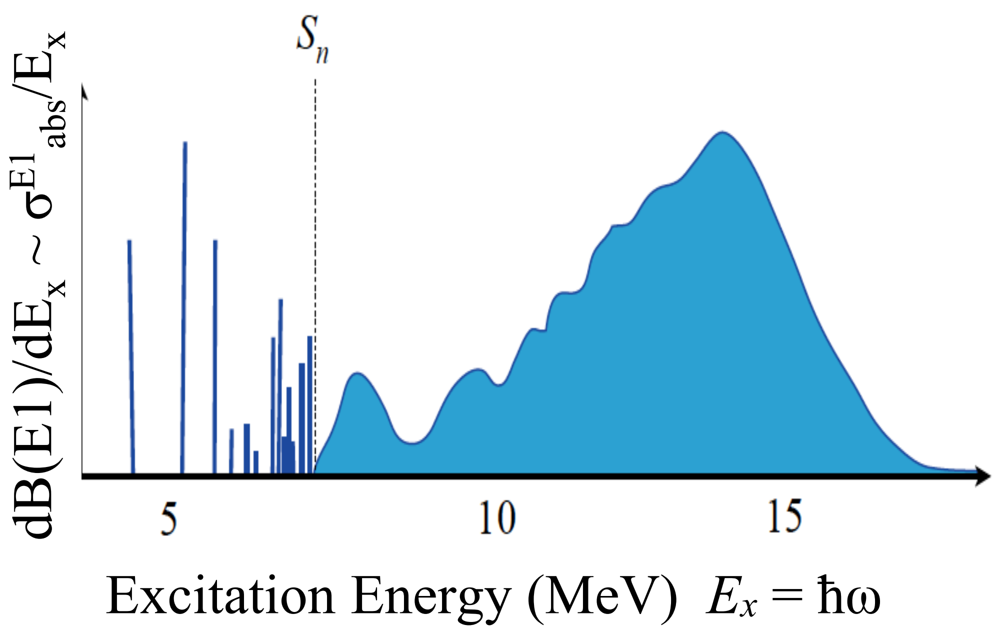

Electric Dipole (E1)
Reduced Transition Probability

$$\frac{dB(E1)}{dE_x} = \frac{9\hbar c}{16\pi^3 e^2} \frac{\sigma_{\mathrm{abs}}^{E1}}{E_x}$$

Static Electric Dipole Polarizability (α_D)

Electric dipole moment

$$p = \alpha_D \times E$$

α_D: **electric dipole polarizability**

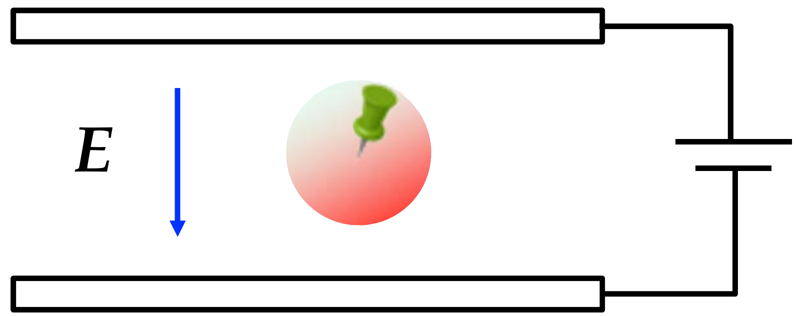

nucleus
in a static electric field
with fixing the c.m. position

Inversely energy-weighted sum-rule of B(E1)

$$\alpha_D = \frac{8\pi e^2}{9} \int \frac{dB(E1)}{E_x}$$

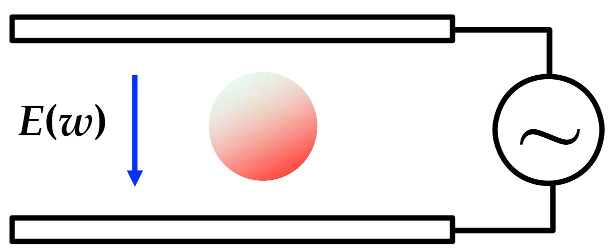

first order perturbation calc. A.B. Migdal: 1944

Electric Dipole Polarizability (α_D)

Electric dipole moment

$$p = \alpha_D \times E$$

***α_D*: electric dipole polarizability**

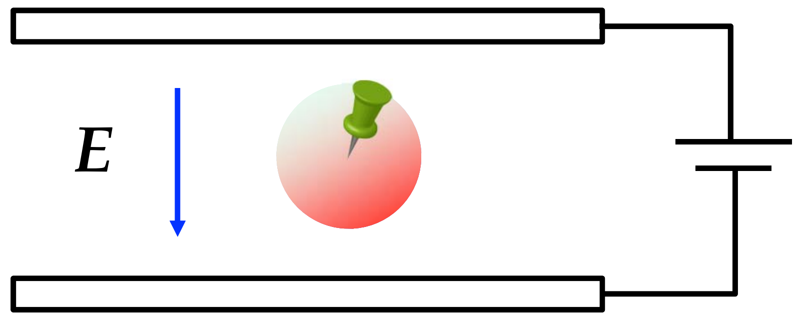

nucleus
in a static electric field
with fixing the c.m. position

Inversely energy-weighted sum-rule of B(E1)

$$\alpha_D = \frac{8\pi e^2}{9} \int \frac{1}{E_x} \frac{dB(E1)}{E_x}$$

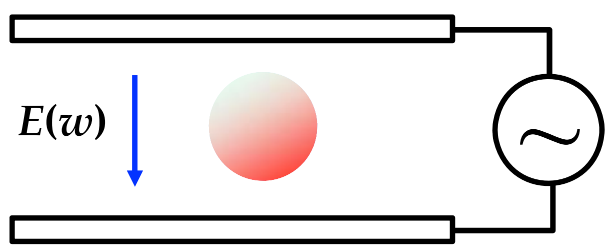

first order perturbation calc. A.B. Migdal: 1944

Electric Dipole Polarizability (α_D)

Electric dipole moment

$$p = \alpha_D \times E$$

***α_D*: electric dipole polarizability**

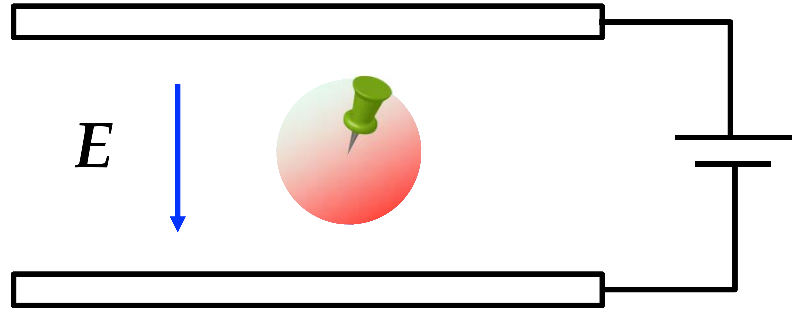

nucleus
in a static electric field
with fixing the c.m. position

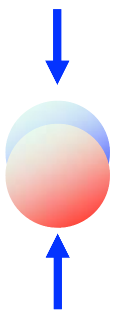

The **restoring force** originates from the **symmetry energy**.

Inversely energy-weighted sum-rule of B(E1)

$$\alpha_D = \frac{8\pi e^2}{9} \int \frac{dB(E1)}{E_x}$$

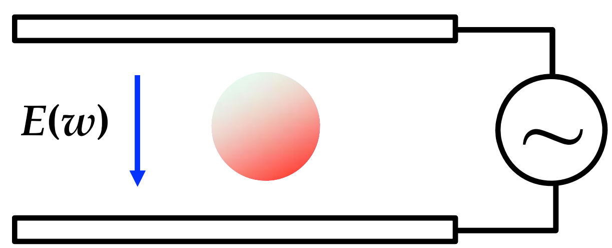

first order perturbation calc. A.B. Migdal: 1944

Static Electric Dipole Polarizability (α_D)

Electric dipole moment

$$p = \alpha_D \times E$$

***α_D*: electric dipole polarizability**

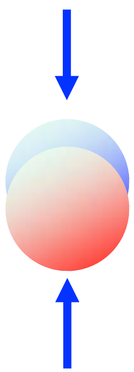

The **restoring force** originates from the **symmetry energy.**

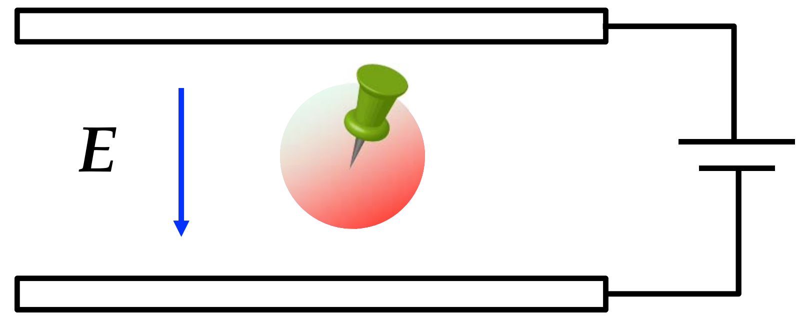

nucleus
in a static electric field
with fixing the c.m. position

Electric dipole polarizability (EDP) is sensitive to the symmetry energy below the nuclear saturation density and to the neutron skin thickness.

Nuclear Equation of State (EOS)

at zero temperature

Nuclear EOS neglecting Coulomb

$$\frac{E}{A}(\rho,\delta)=\frac{E}{A}(\rho,0)+S(\rho)\delta^2+\cdots$$

$$\delta \equiv \frac{\rho_n-\rho_p}{\rho_n+\rho_p}$$ Asymmetry parameter

Symmetry energy

$$S(\rho)=J+\frac{L}{3\rho_0}(\rho-\rho_0)+\ldots$$

Density difference between n and p increases the system energy by the symmetry energy.

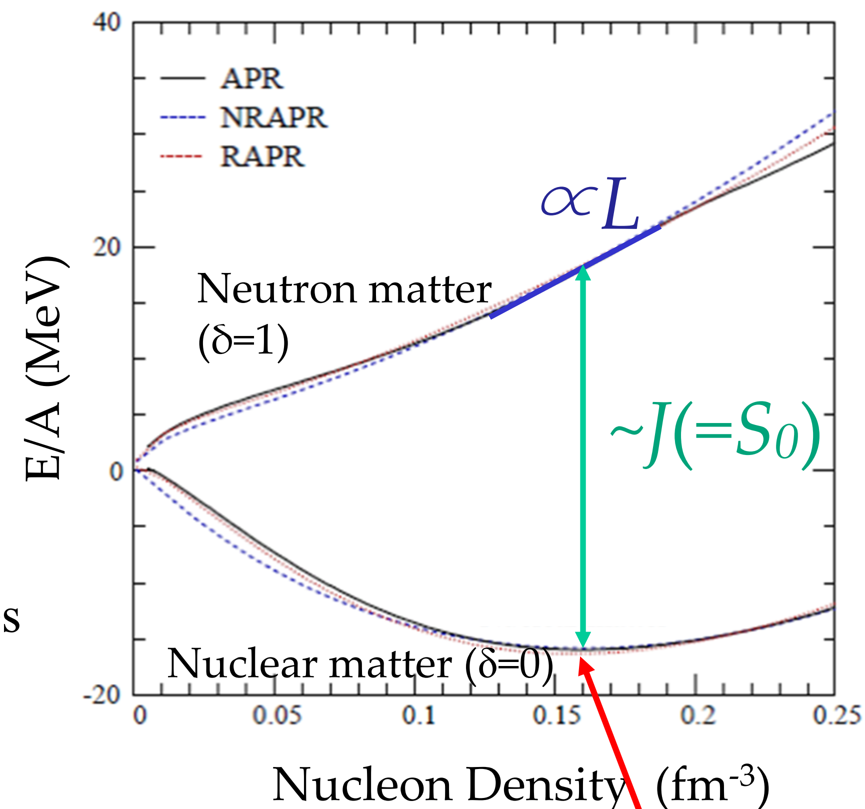

Saturation Density ρ_0

~0.16 fm^{-3}

Electric Dipole Polarizability (α_D) in the correlation of J and L

~L

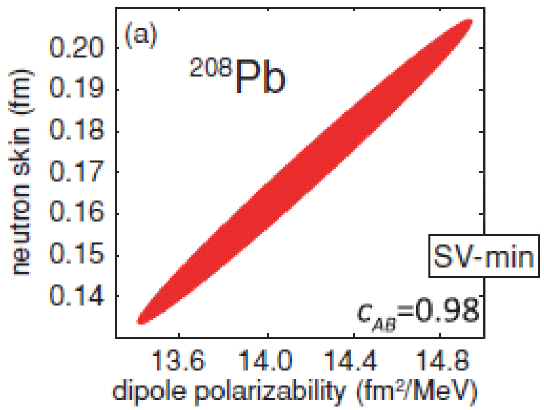

P.-G. Reinhard and W. Nazarewicz, PRC 81, 051303(R) (2010).

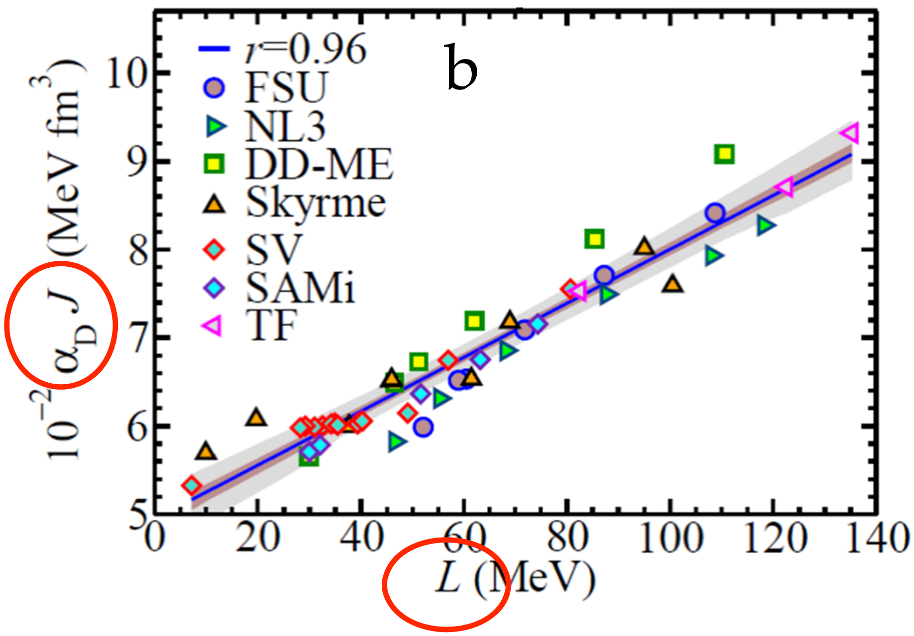

X. Roca-Maza *et al.*, PRC**88**, 024316(2013)

Correlations observed in various interaction sets in the framework of EDF.

$$\alpha_D^{\mathrm{DM}} \approx \frac{\pi e^2}{54}\frac{A\langle r^2\rangle}{J}\left[1+\frac{5}{3}\frac{L}{J}\epsilon_A\right]$$

insights from the droplet model

Precise determination of α_D of ^{208}Pb gives a constraint band in the *J*-*L* plane.

Electric Dipole Polarizability (α_D) in the correlation of *J* and *L*

X. Roca-Maza *et al.*, PRC**88**, 024316(2013)

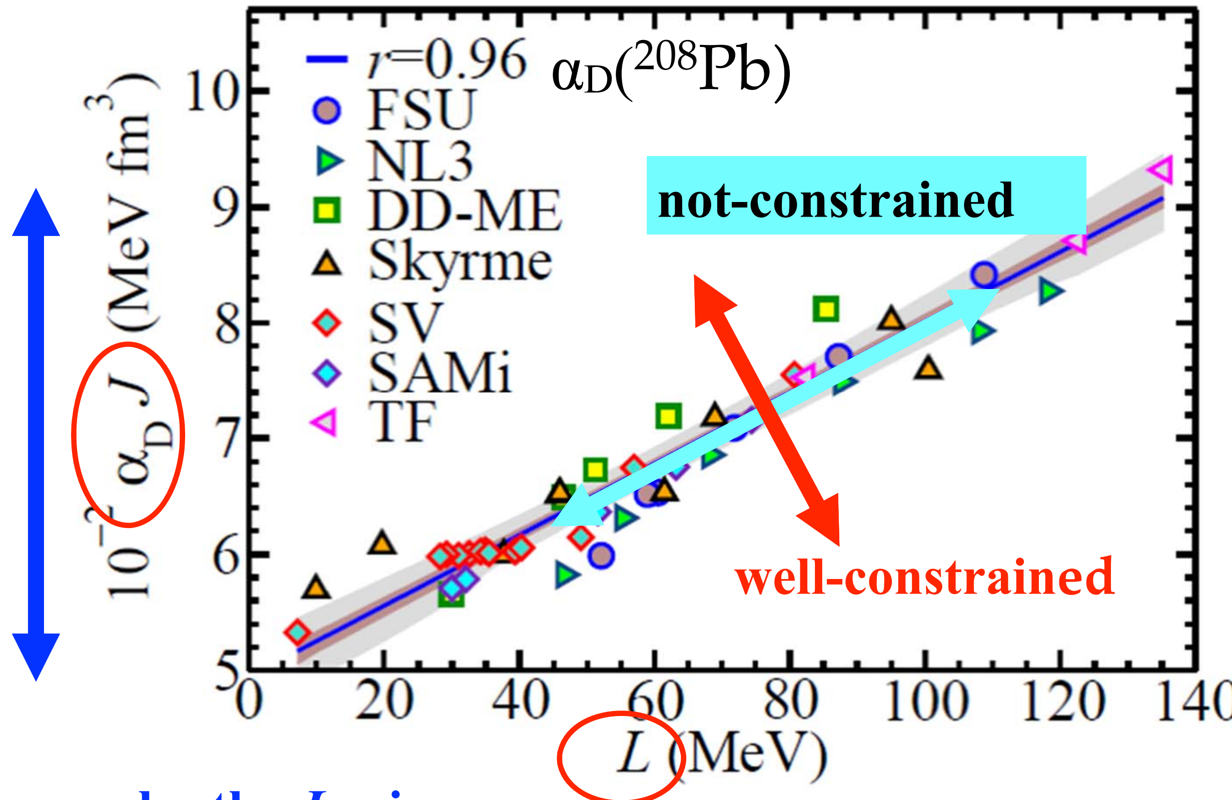

α_D scales the J axis.

The parameters of each set of the effective interactions were determined so as to reproduce basic nuclear properties like nuclear masses and nuclear charge radii of representative nuclei. The parameters are well constrained in the one direction but not in the other direction.

α_D scales the *J* axis

One of the unknowns, aD, has been determined experimentally to extract the constraint band in the *J*-*L* plane.

Electric Dipole Polarizability (α_D) in the correlation of *J* and *L*

X. Roca-Maza *et al.*, PRC**88**, 024316(2013)

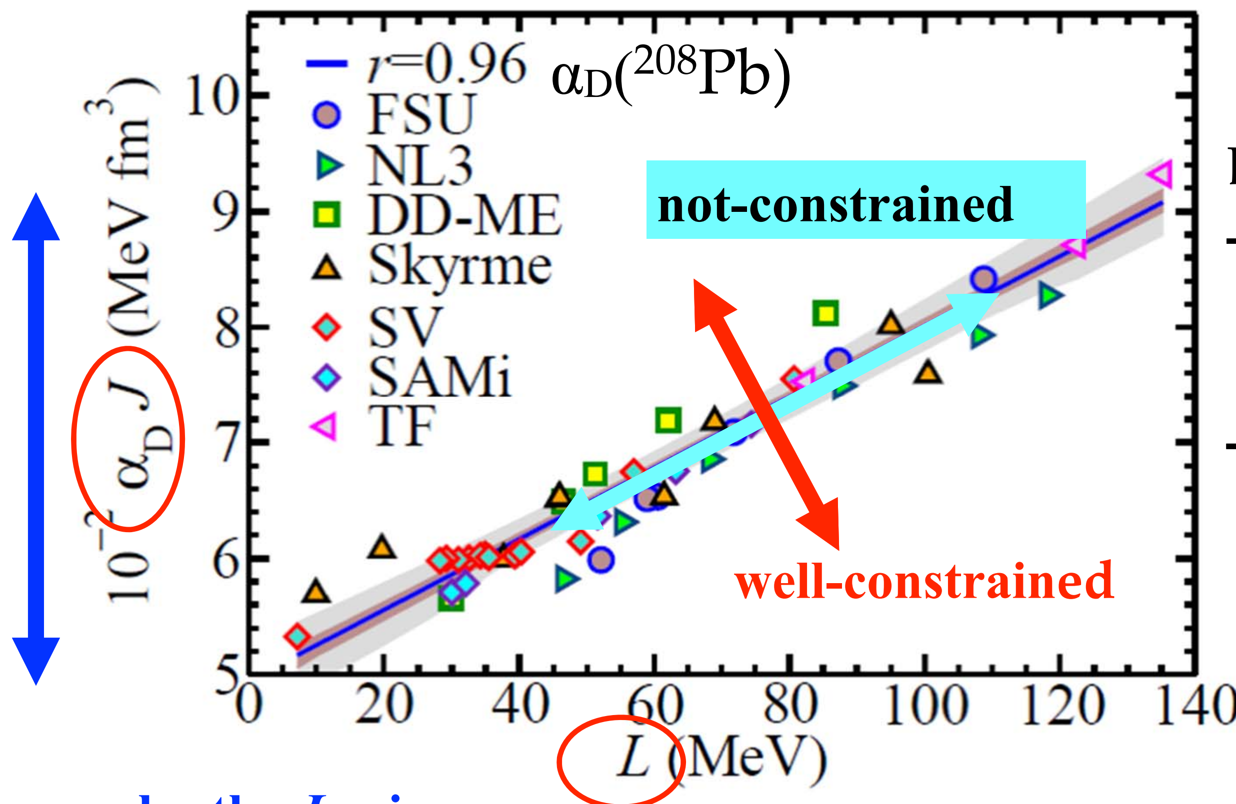

α_D scales the *J* axis

α_D scales the J axis.

Effective Interactions

- → reproduce e.g. nuclear masses and charge radii of representative nuclei
- → constrained in one direction but not in the other

One of the unknowns, aD, has been determined experimentally to extract the constraint band in the *J*-*L* plane.

Electric Dipole Response of Nuclei

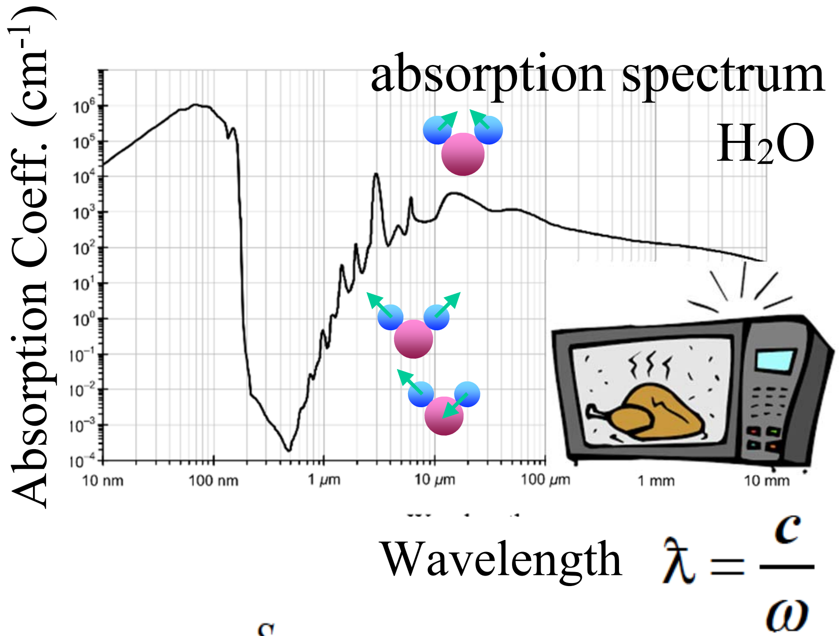

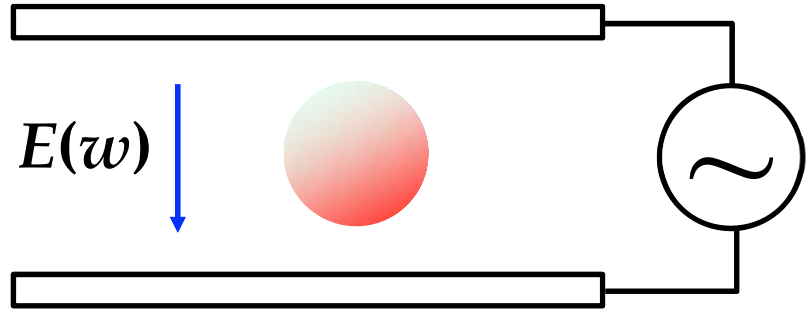

dielectric material
in an oscillating electric field

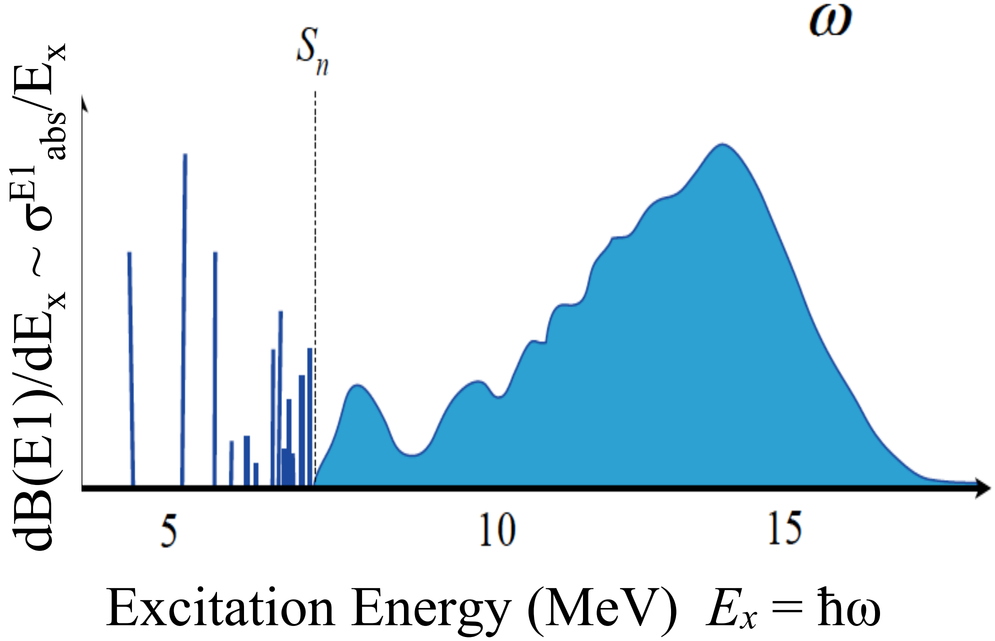

Electric Dipole (E1)
Reduced Transition Probability

$$\frac{dB(E1)}{dE_x} = \frac{9\hbar c}{16\pi^3 e^2}\frac{\sigma^{E1}_{abs}}{E_x}$$

Electric Dipole Polarizability (α_D)

Electric dipole moment

$$p = \alpha_D \times E$$

α_D: electric dipole polarizability

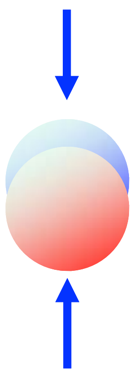

The **restoring force** originates from the **symmetry energy.**

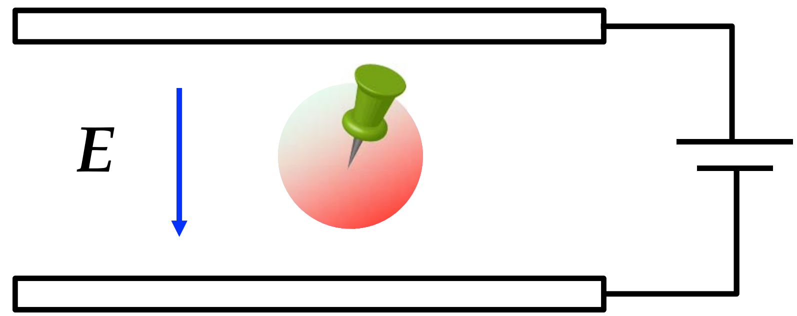

nucleus
in a static electric field
with fixing the c.m. position

Inversely energy-weighted sum-rule of B(E1)

$$\alpha_D = \int \frac{1}{\omega} \frac{dB(E1)}{d\omega} d\omega$$

first order perturbation calc.

A.B. Migdal: 1944

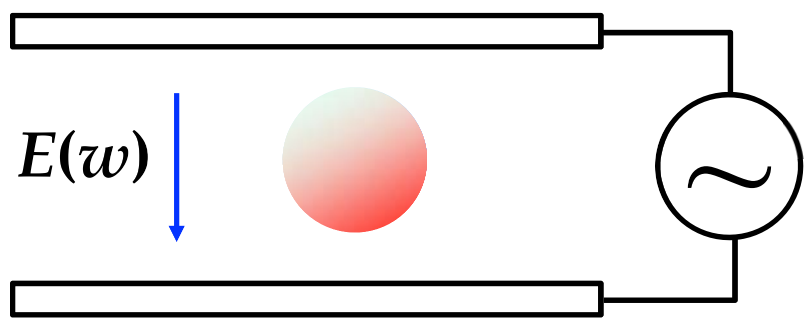

dielectric material
in an oscillating electric field

Electric Dipole Response of Nuclei

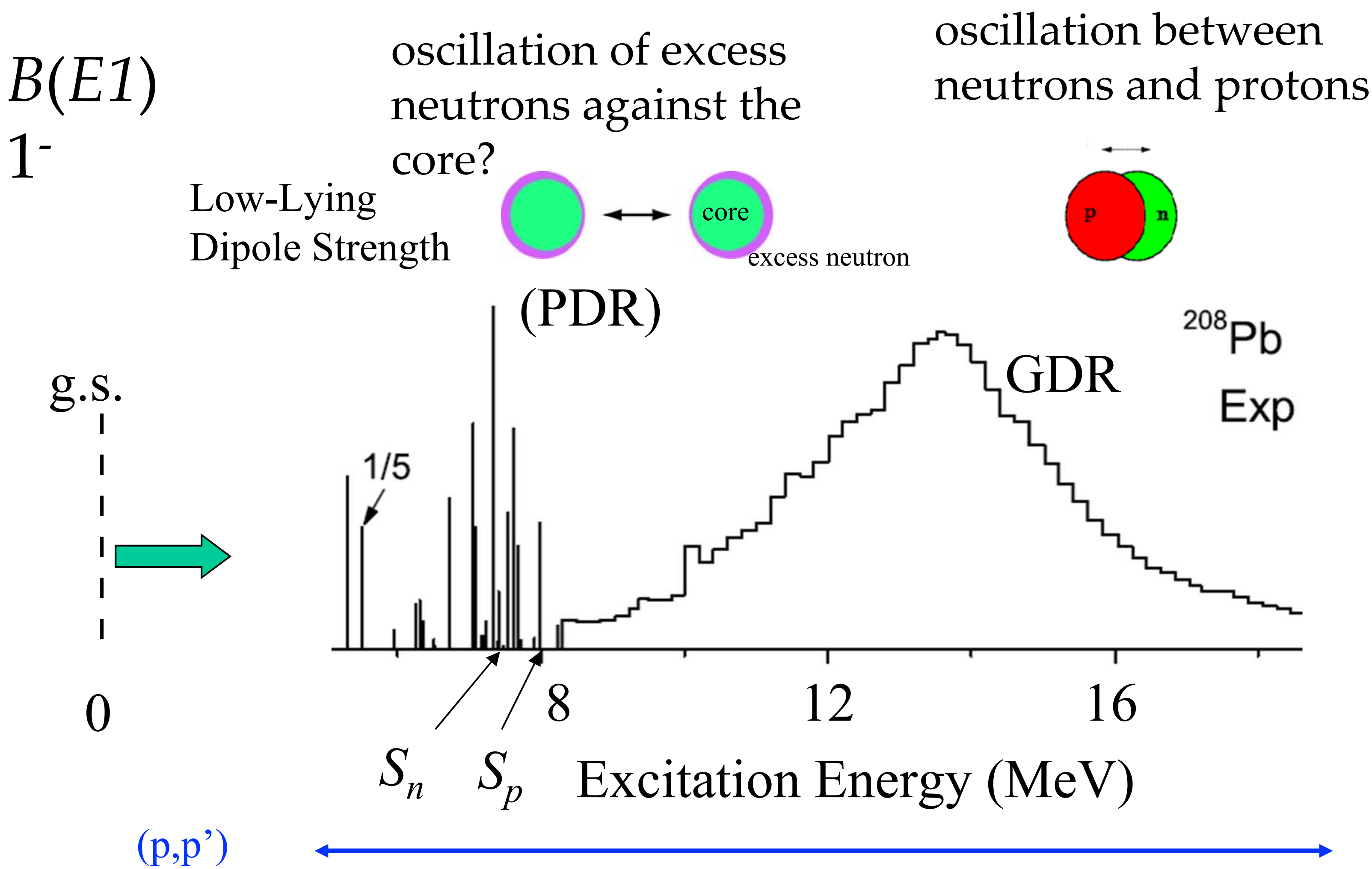

Electric Dipole Response

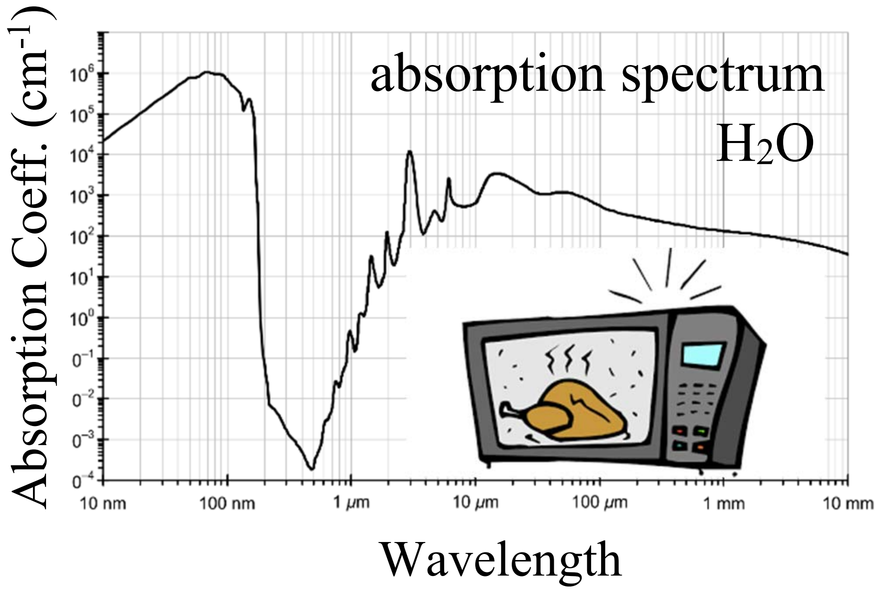

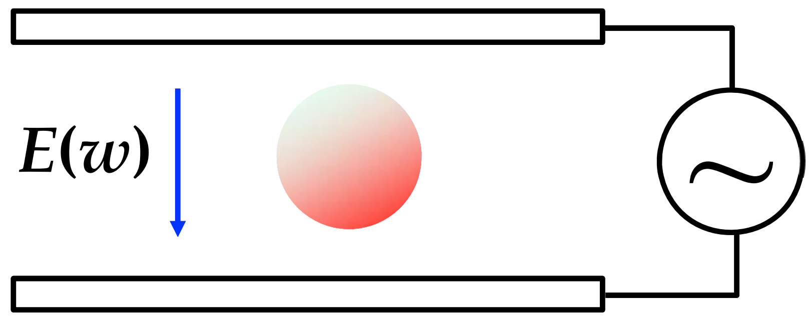

a nucleus
in an oscillating electric field

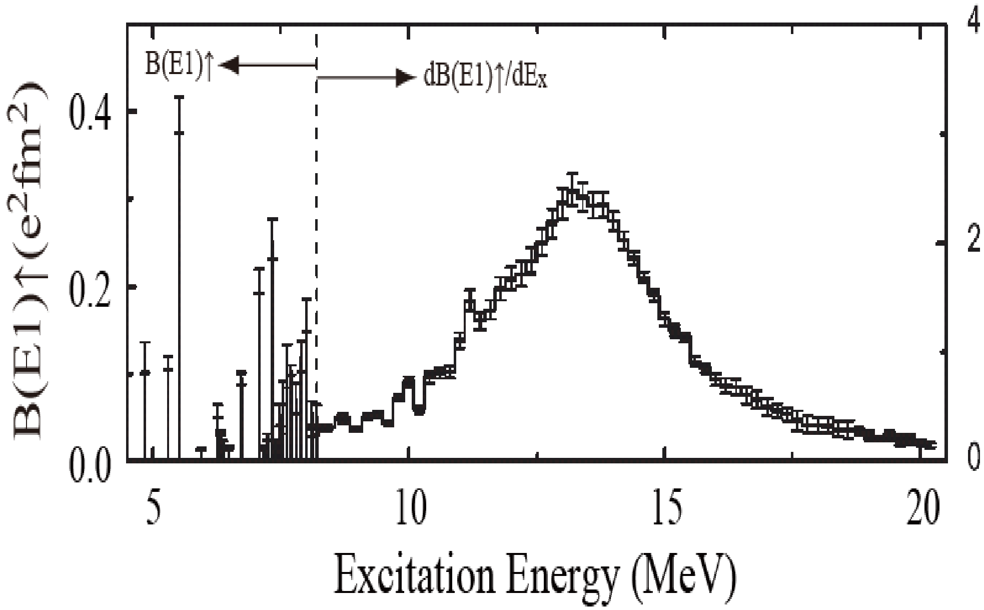

E1 Reduced Transition Probability

$$B(E1) = \frac{9\hbar c}{16\pi^3 e^2} \frac{\sigma_{abs}^{E1}}{\omega}$$

Probing the E1 Response by Proton Scattering

Missing Mass Spectroscopy by Virtual Photon Excitation

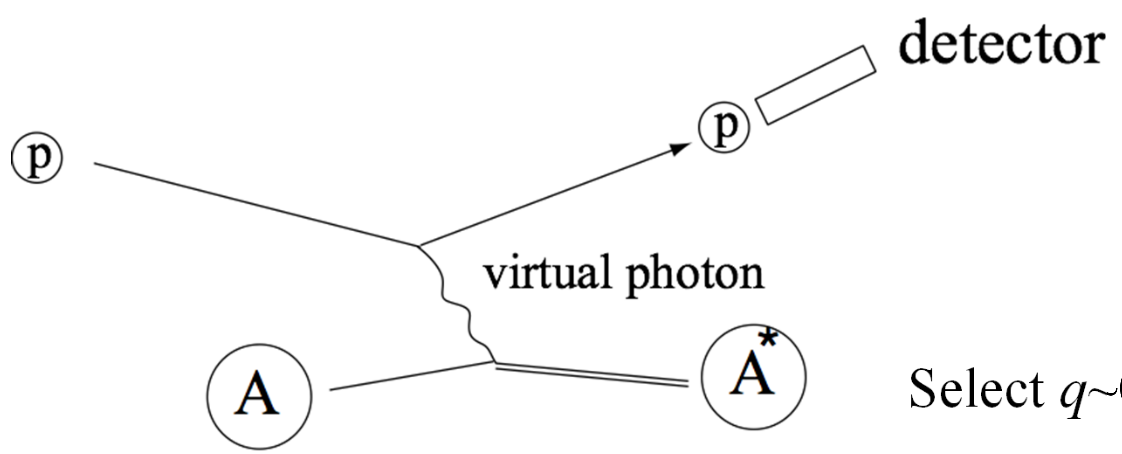

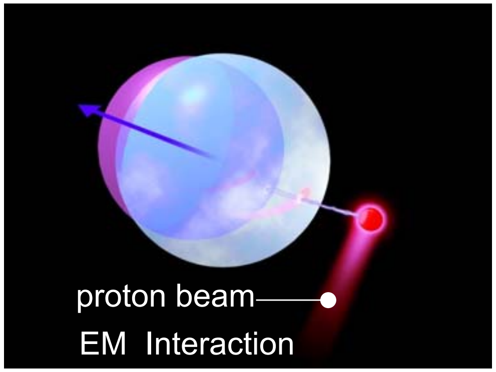

Select q~0 (~0 deg.)

- **Missing mass spectroscopy**:
  Total strength is measured independently from the decaying channels.
- **Multipole decomposition** of the strength in the continuum:
  Includes the contribution of unresolved small states
- **Coulomb excitation**: EM Interaction
  Absolute determination of the transition strength.

Nuclear Equation of State (EOS)

at zero temperature

Nuclear EOS neglecting Coulomb

$$\frac{E}{A}(\rho,\delta)=\frac{E}{A}(\rho,0)+S(\rho)\delta^2+\cdots$$

$$\delta\equiv\frac{\rho_n-\rho_p}{\rho_n+\rho_p}$$ Asymmetry parameter

Symmetry energy

$$S(\rho)=J+\frac{L}{3\rho_0}(\rho-\rho_0)+\ldots$$

⇔ difference between *p*-*n* chemical potentials: how the system energy changes when protons are replaced by the neutrons

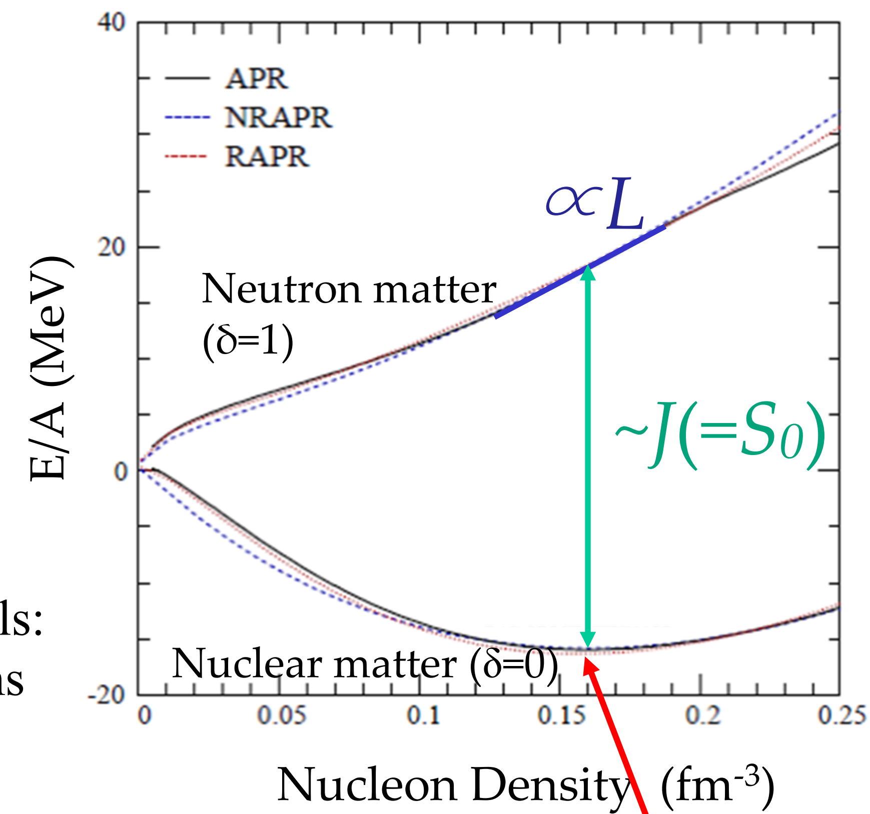

Saturation Density ρ_0

~0.16 fm^{-3}

Nucleus

Neutron Star

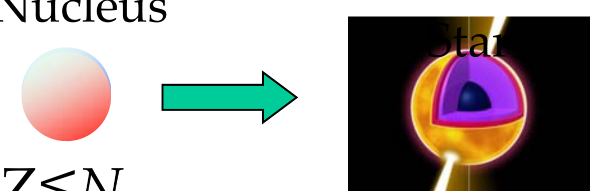

Z≲*N*

Z≪*N*

Nuclear Equation of State (EOS)

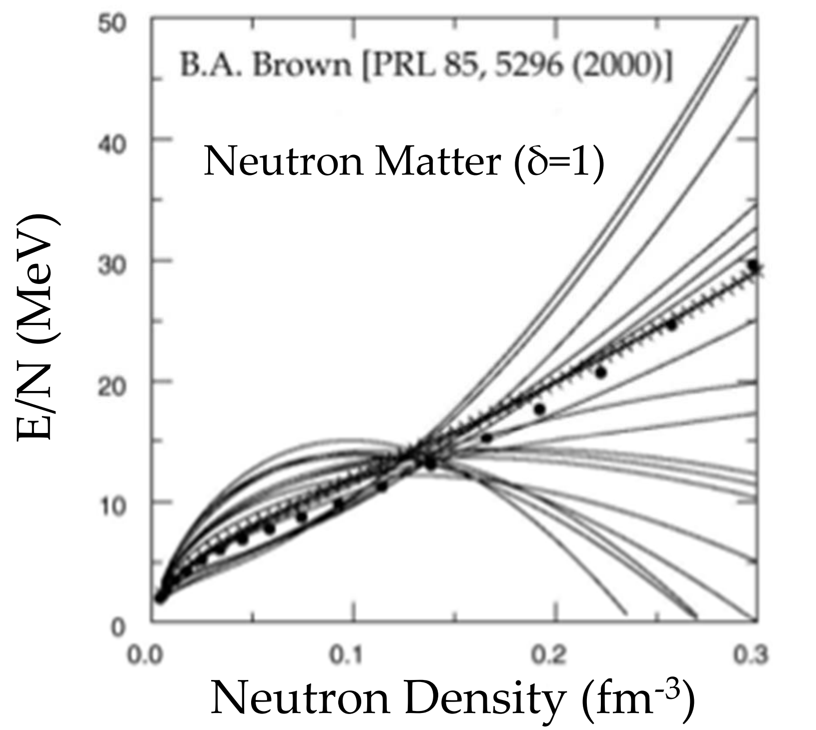

FIG. 2. The neutron EOS for 18 Skyrme parameter sets. The filled circles are the Friedman-Pandharipande (FP) variational calculations and the crosses are SkX. The neutron density is in units of neutron/fm^3.

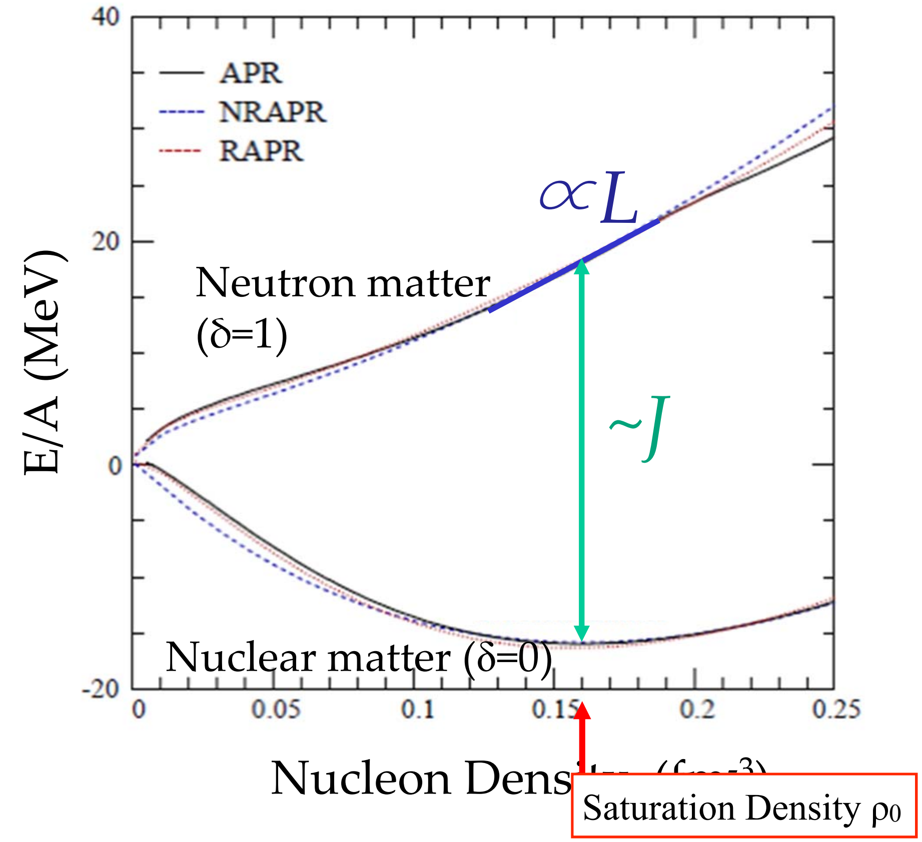

Steiner et al., Phys. Rep. 411 325(2005)

Prediction of the neutron matter EOS is much model dependent.

Neutron Skin and Density Dependence of the Symmetry Energy

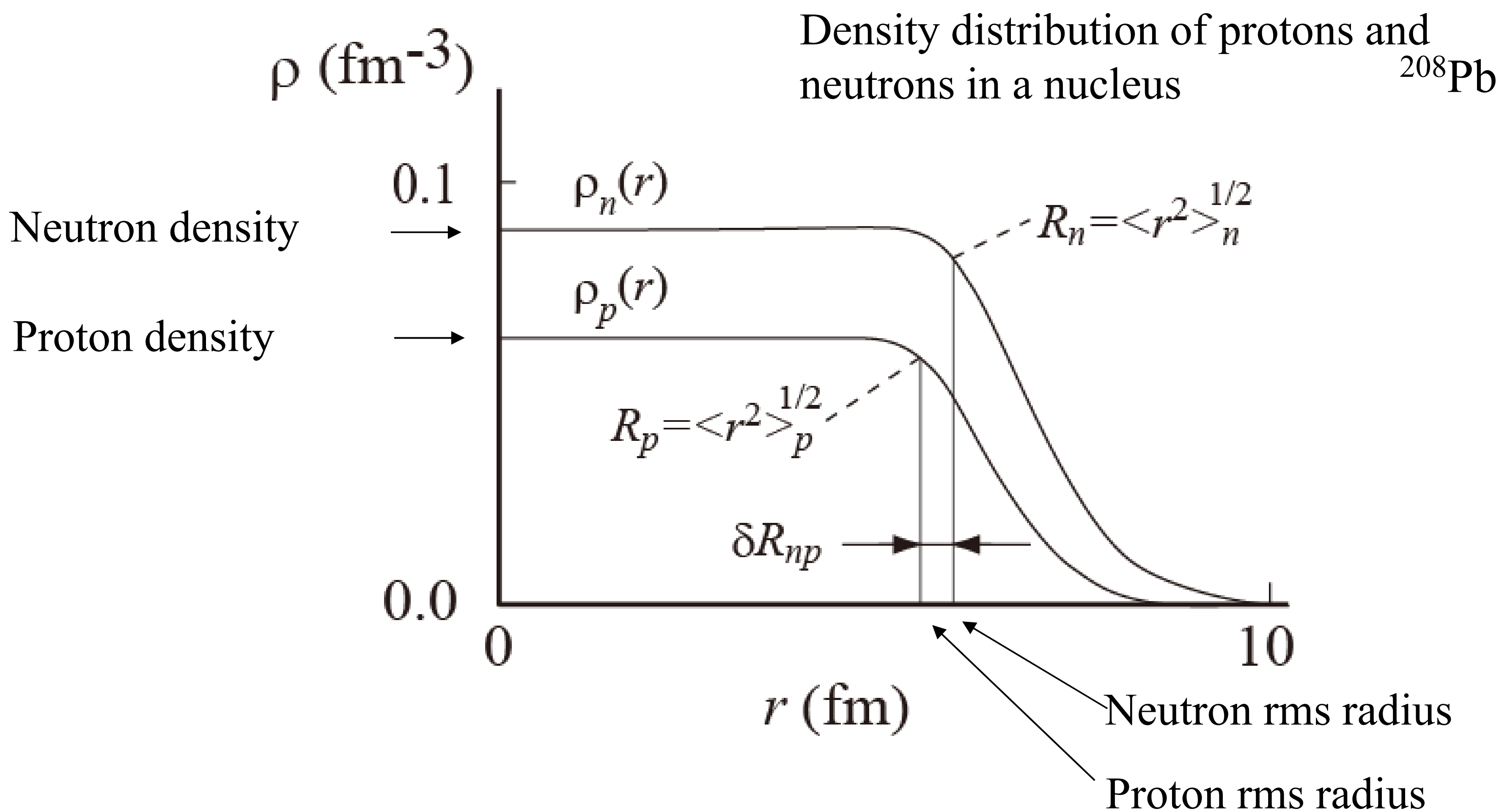

Neutron Skin and Density Dependence of the Symmetry Energy

For larger *L*:

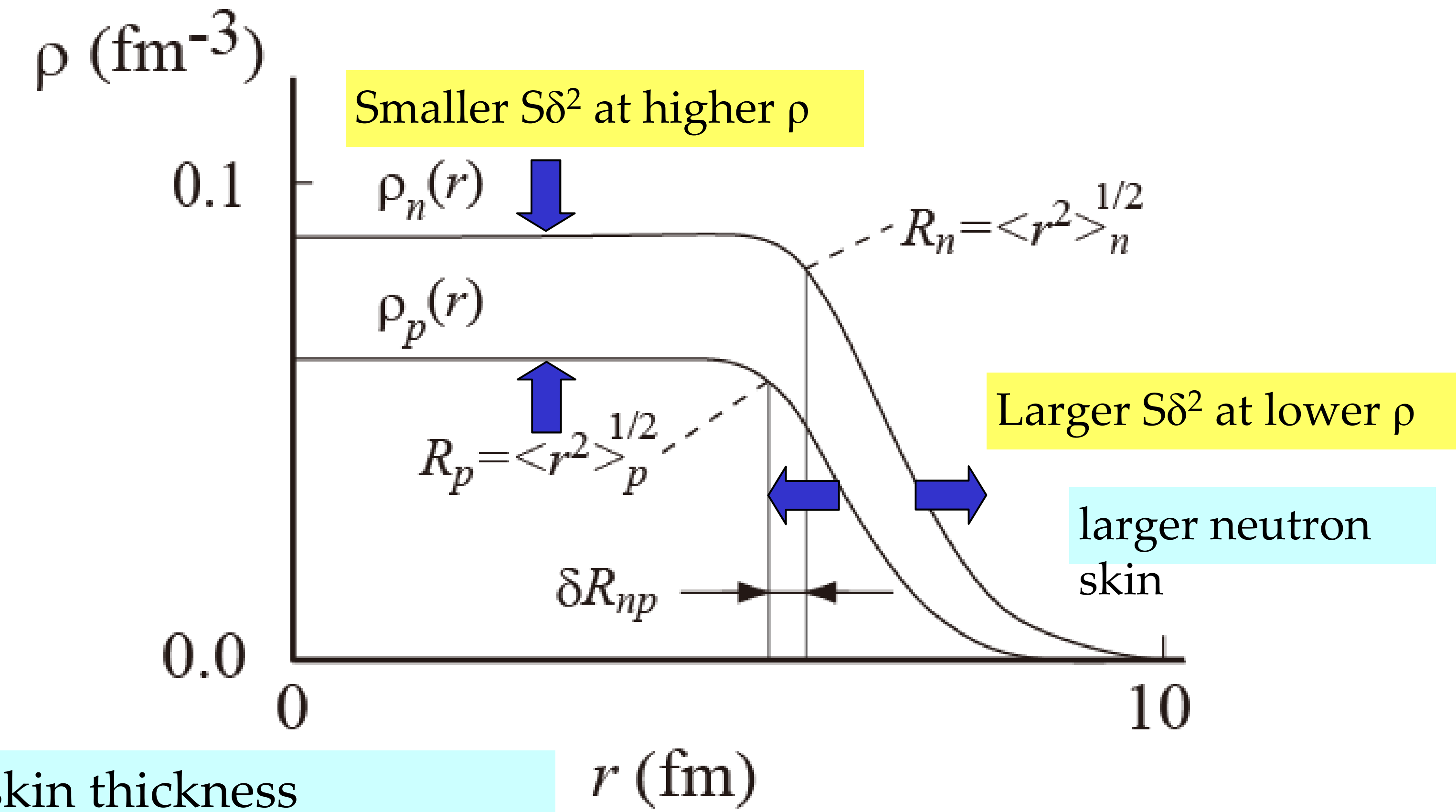

Neutron skin thickness

↕

Density dependence of the symmetry energy ⟸ Energy minimum (equilibrium)

Neutron Skin and Density Dependence of the Symmetry Energy

For smaller *L*:

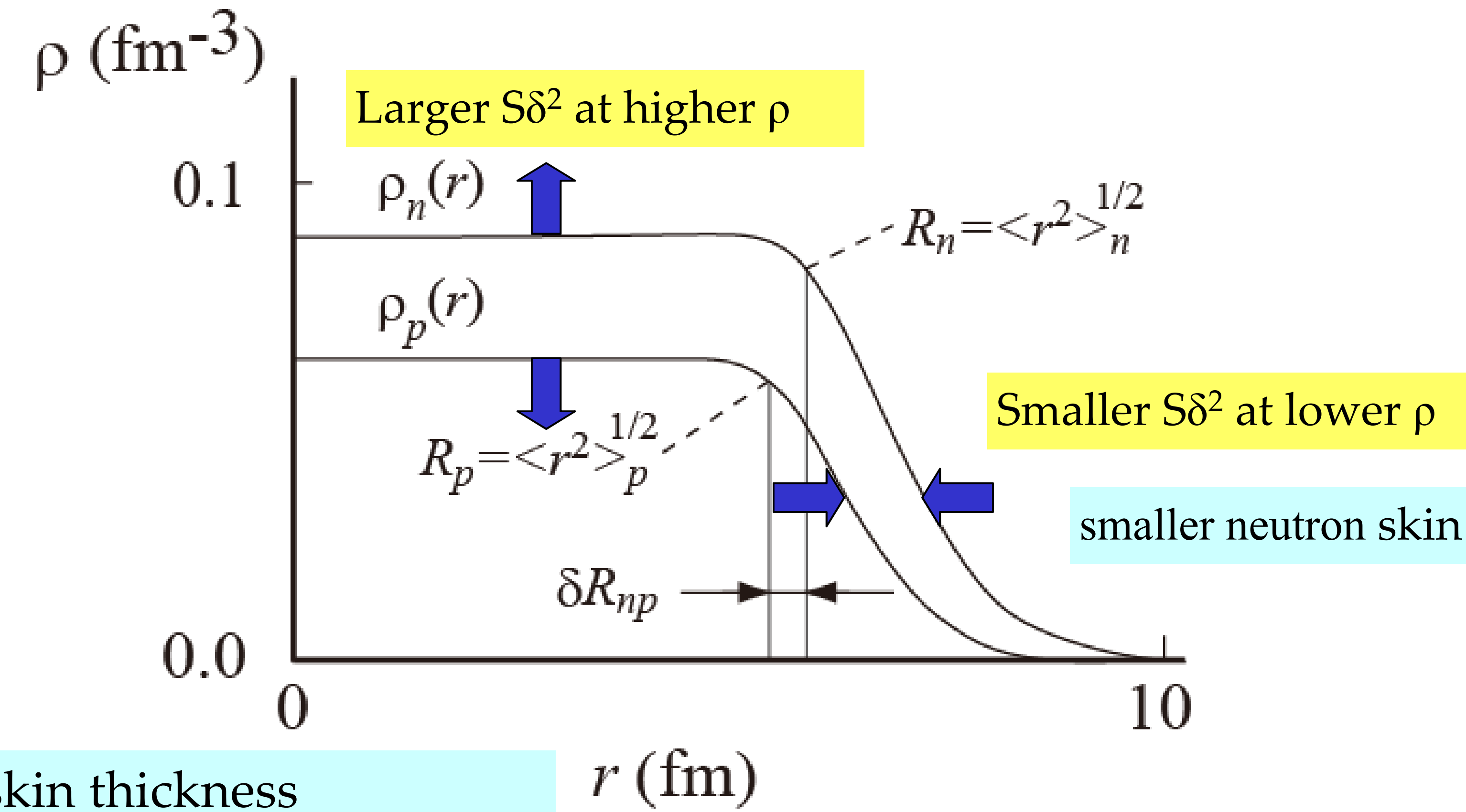

Neutron skin thickness

↕

Density dependence of the symmetry energy ⟸ Energy minimum (equilibrium)

Neutron Skin and Density Dependence of the Symmetry Energy

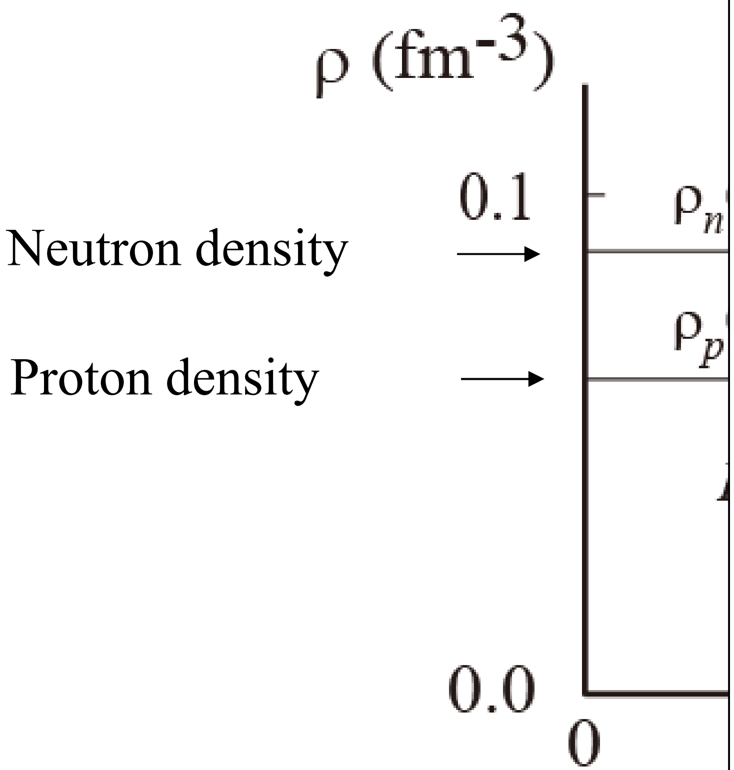

X. Roca-Maza *et al.*, PRL**106**, 252501 (2011)

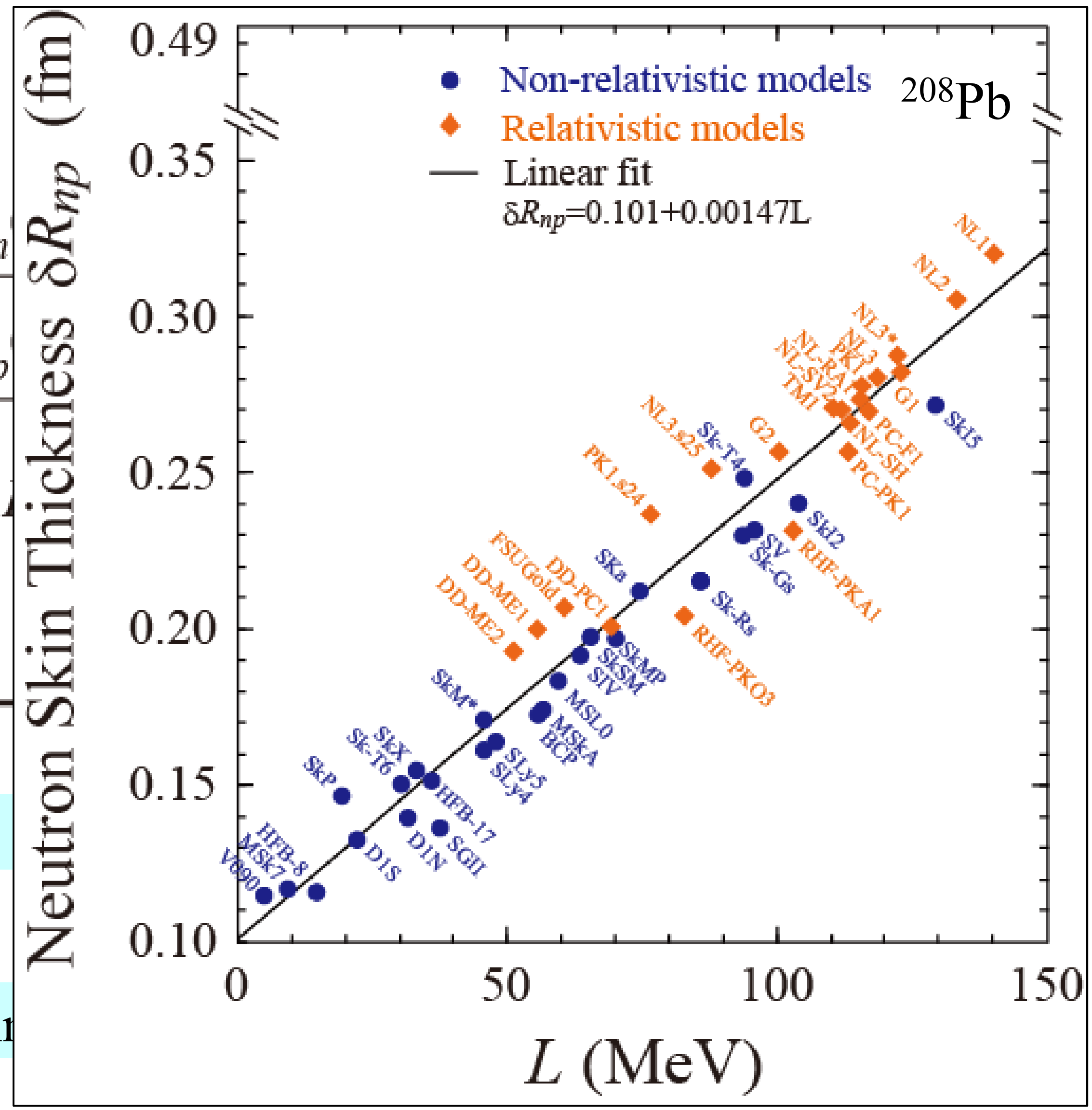

Neutron skin thickness

Density dependence of the symm

Probing the E1 Response by Proton Scattering

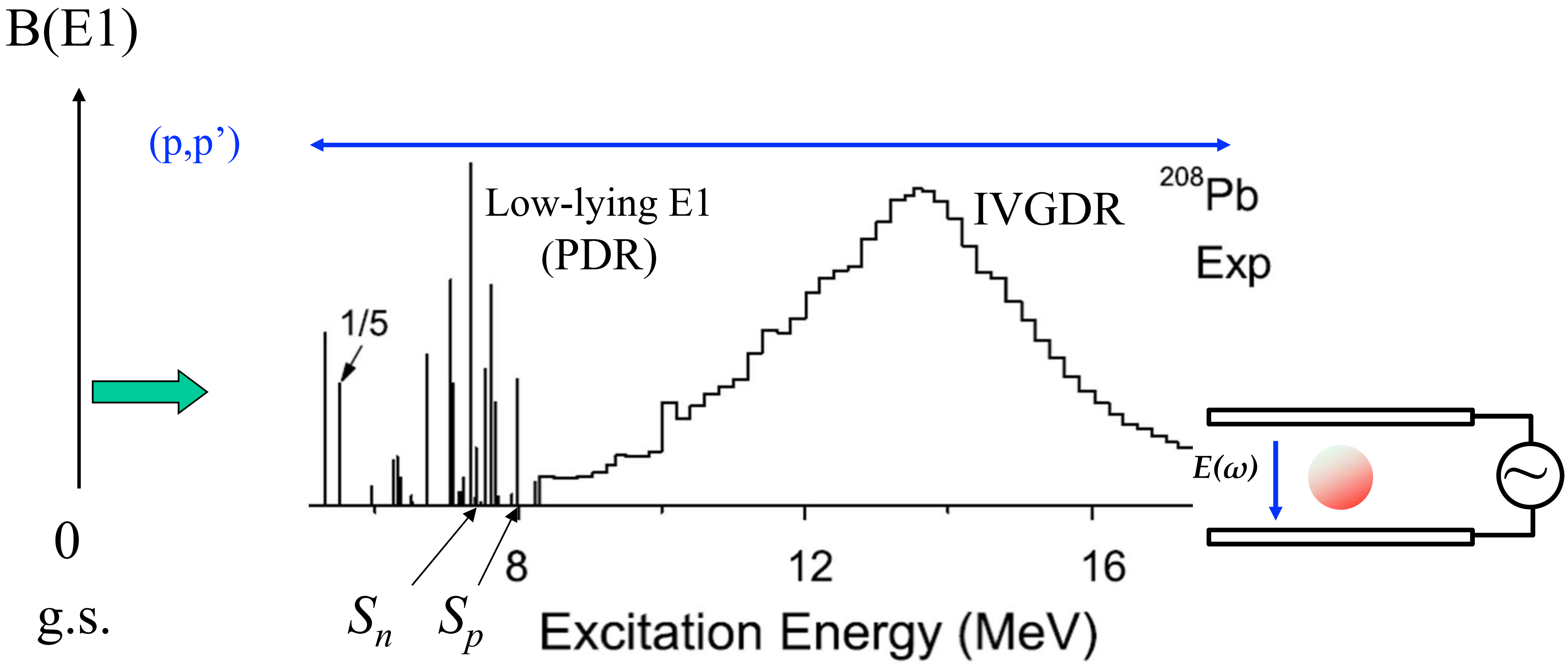

- Single shot measurement across S_n in $E_x = $ 5-22 MeV.
- Uniform detection efficiency (80-90%) and solid angle
- High energy resolution (20-30 keV)
- Polarized beam, polarization detection ⟶ extraction of E1
- Isotopically enriched target with a few mg/cm^2 thickness

Experimental Methods

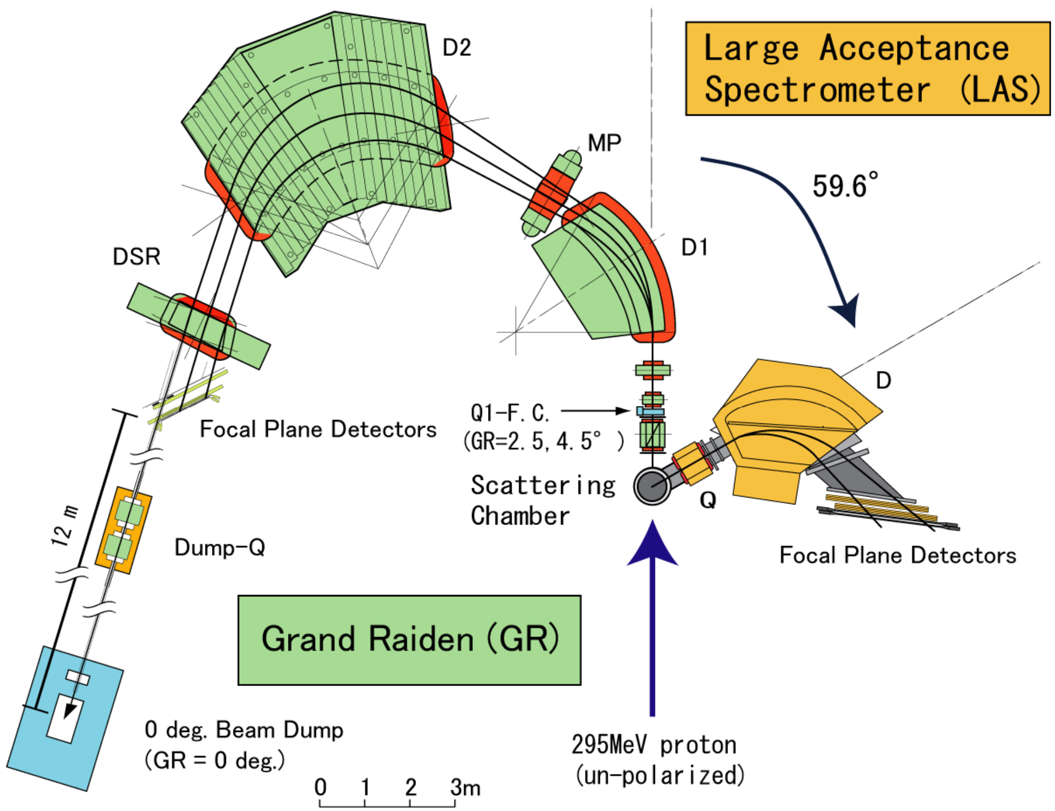


ウラジオストク
Владивосток
吉林
辽宁
北朝鮮
평양
東海
札幌
仙台
Soul
서울
Daejeon
大韓民国
日本
黄海
東京
Tokyo
부산
Busan
名古屋
広島
Osaka
Fukuoka
福岡
東シナ海
Google
200 km

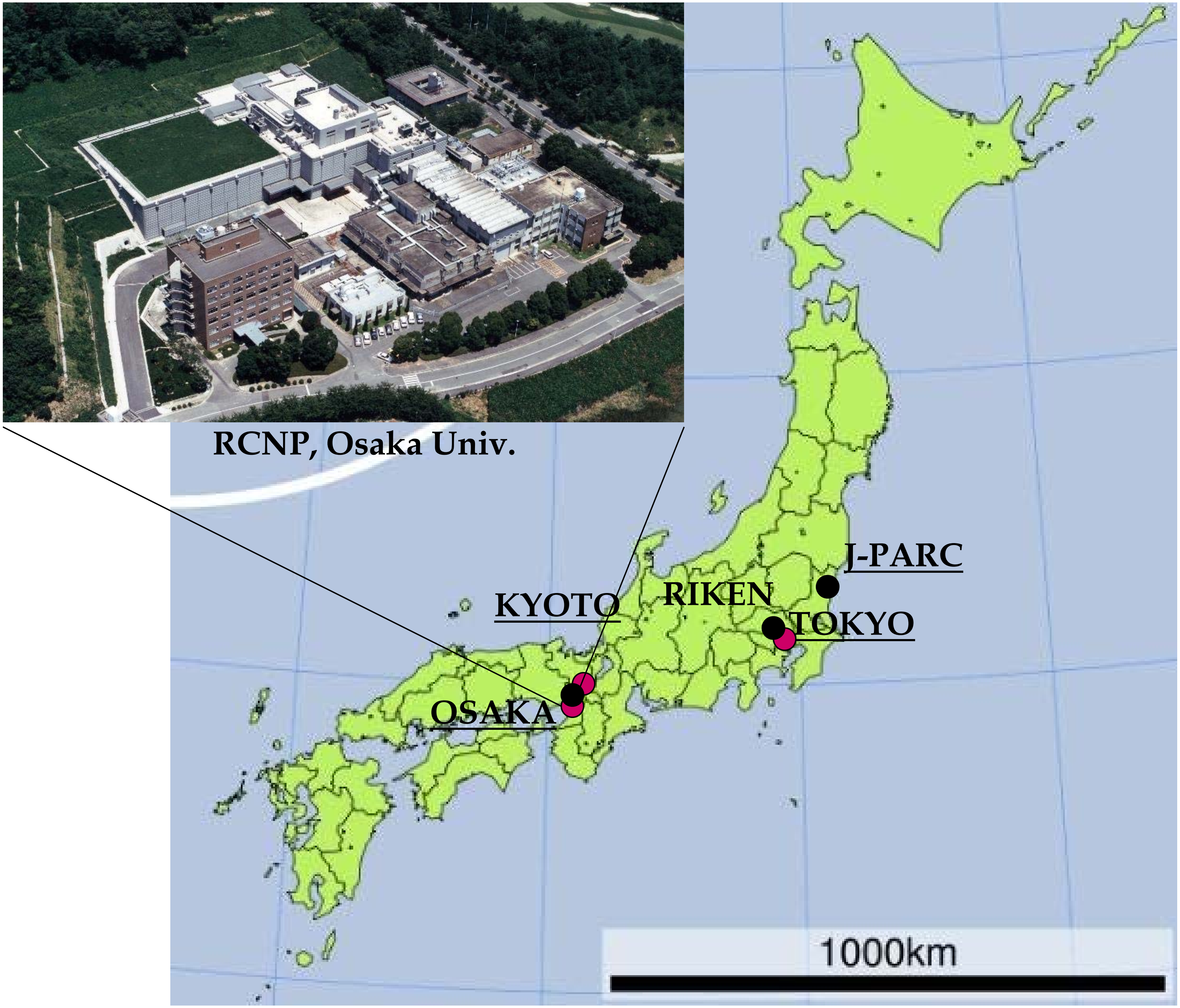
RCNP, Osaka Univ.
J-PARC
KYOTO
RIKEN
TOKYO
OSAKA
1000km


Tokyo
RCNP
OSAKA
~18 neutron stars

Research Center for Nuclear Physics (RCNP), Osaka University

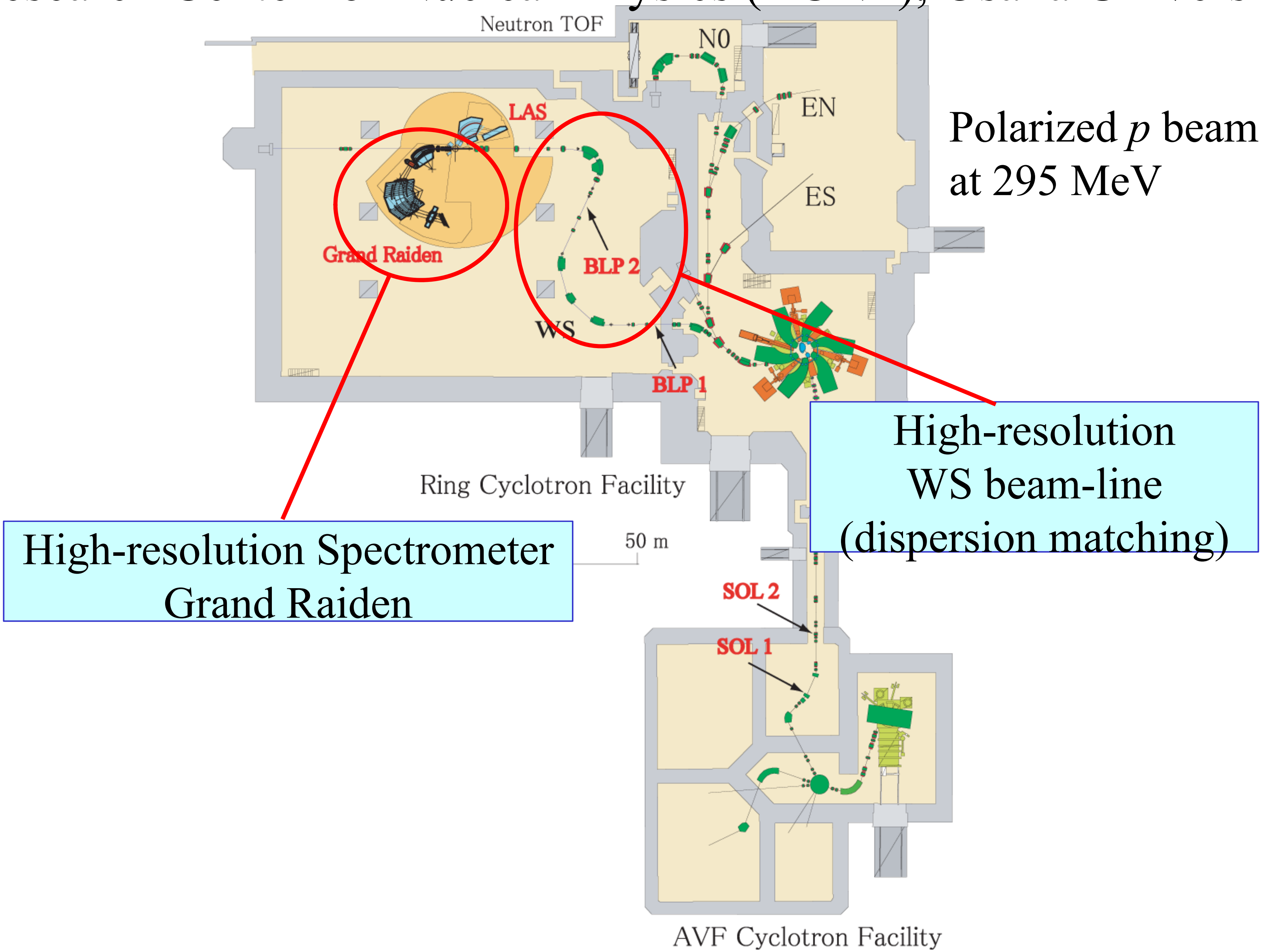

High-Resolution Spectrometer “Grand Raiden”

High resolution of 20-30 keV: dispersion matching.

Proton scattering
at very forward angles
at RCNP, Osaka Univ.

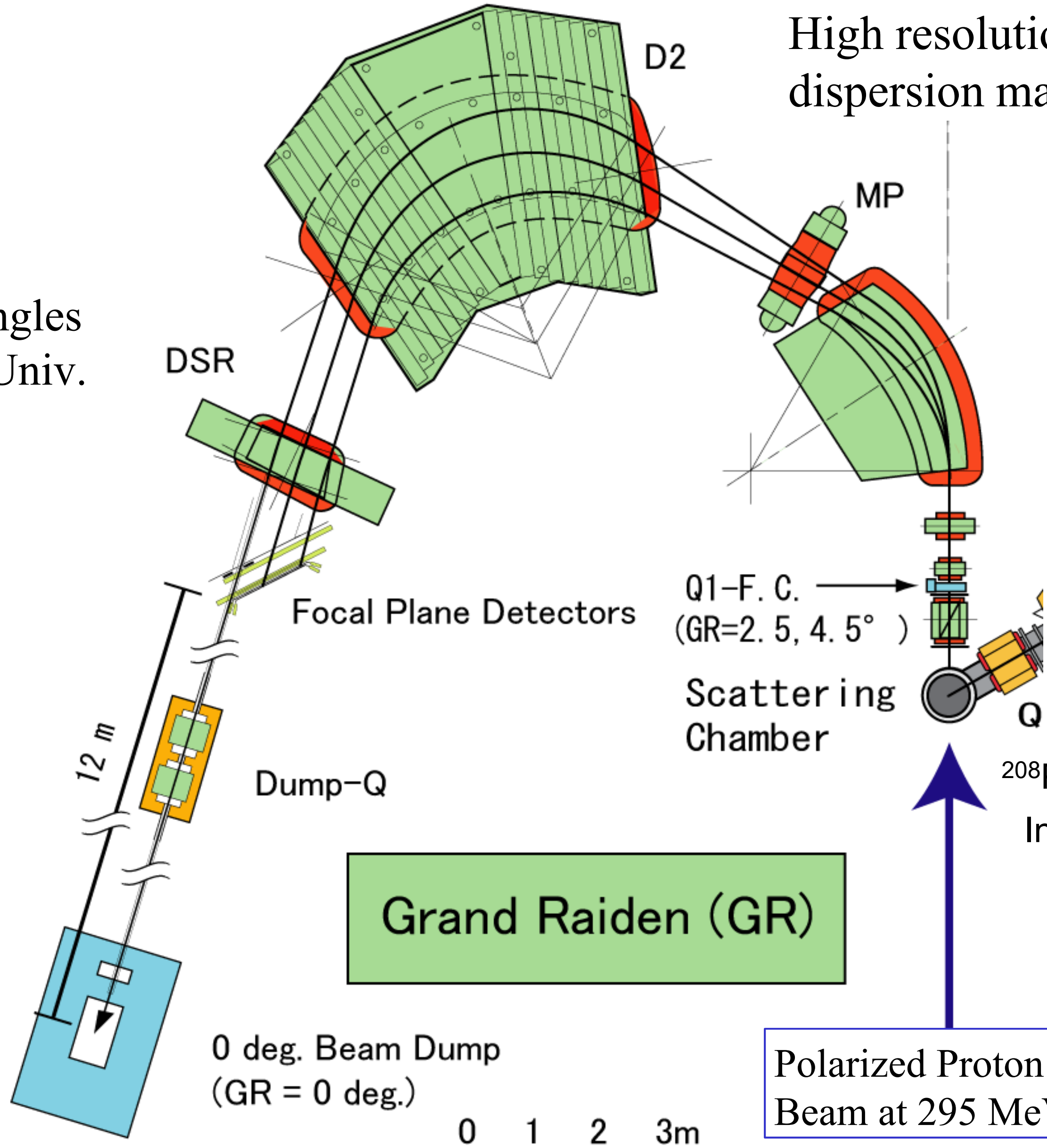

^{208}Pb target: 5.2 mg/cm^2
Intensity : 1-8 nA

AT et al., NIMA605, 326 (2009)

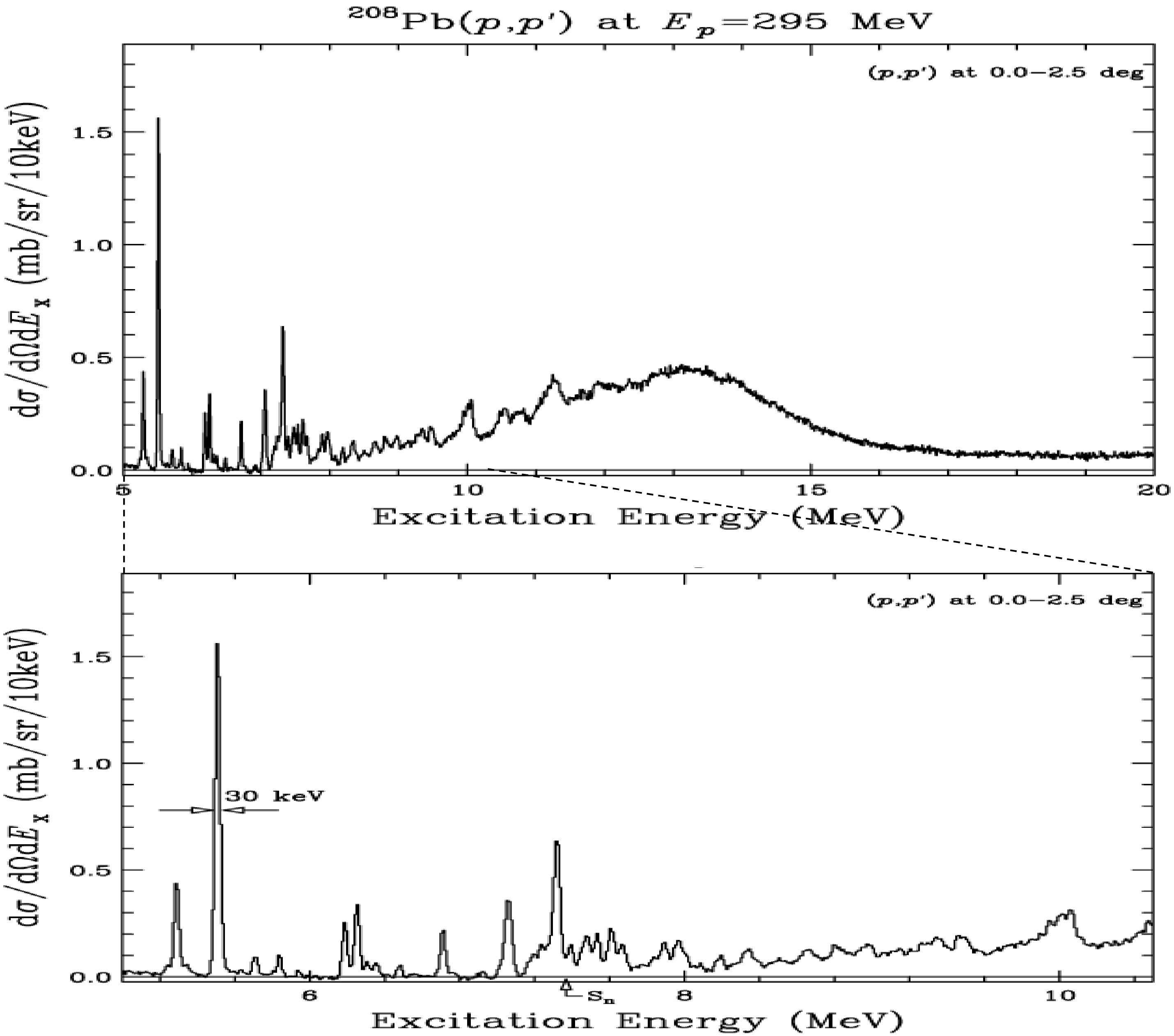
^{208}Pb(p,p') at E_p=295 MeV
(p,p') at 0.0–2.5 deg
dσ/dΩdE_x (mb/sr/10keV)
0.0
0.5
1.0
1.5
5
10
15
20
Excitation Energy (MeV)
(p,p') at 0.0–2.5 deg
dσ/dΩdE_x (mb/sr/10keV)
30 keV
S_n
6
8
10
Excitation Energy (MeV)

B(E1): continuum and GDR region

Method 1: Multipole Decomposition

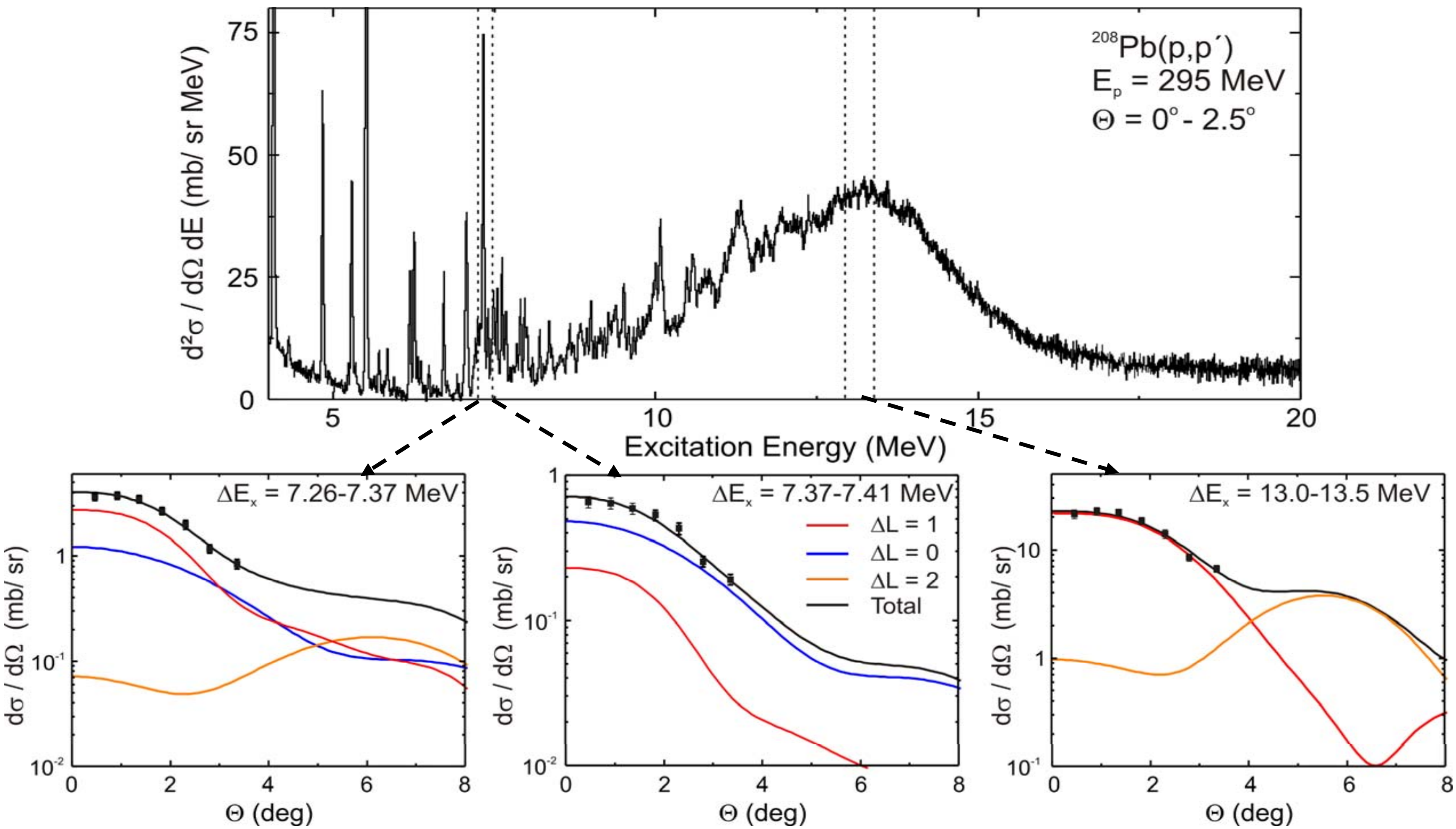

- Neglect of data for Θ>4: (p,p´) response too complex
- Included E1/M1/E2 or E1/M1/E3 (little difference)

Grazing Angle = 3.0 deg

B(E1): continuum and GDR region

Method 2: Decomposition by Spin Observables

- Polarization observables at 0° ➡ spinflip / non-spinflip separation
  model-independent
  T. Suzuki, PTP 103 (2000) 859

E1 / spin-M1 decomposition

$$\text{Total Spin Transfer } \Sigma \equiv \frac{3-(2D_{SS}+D_{LL})}{4} = \begin{cases} 1 \text{ for } \Delta S = 1 & \text{spin-M1} \\ 0 \text{ for } \Delta S = 0 & \text{E1} \end{cases}$$

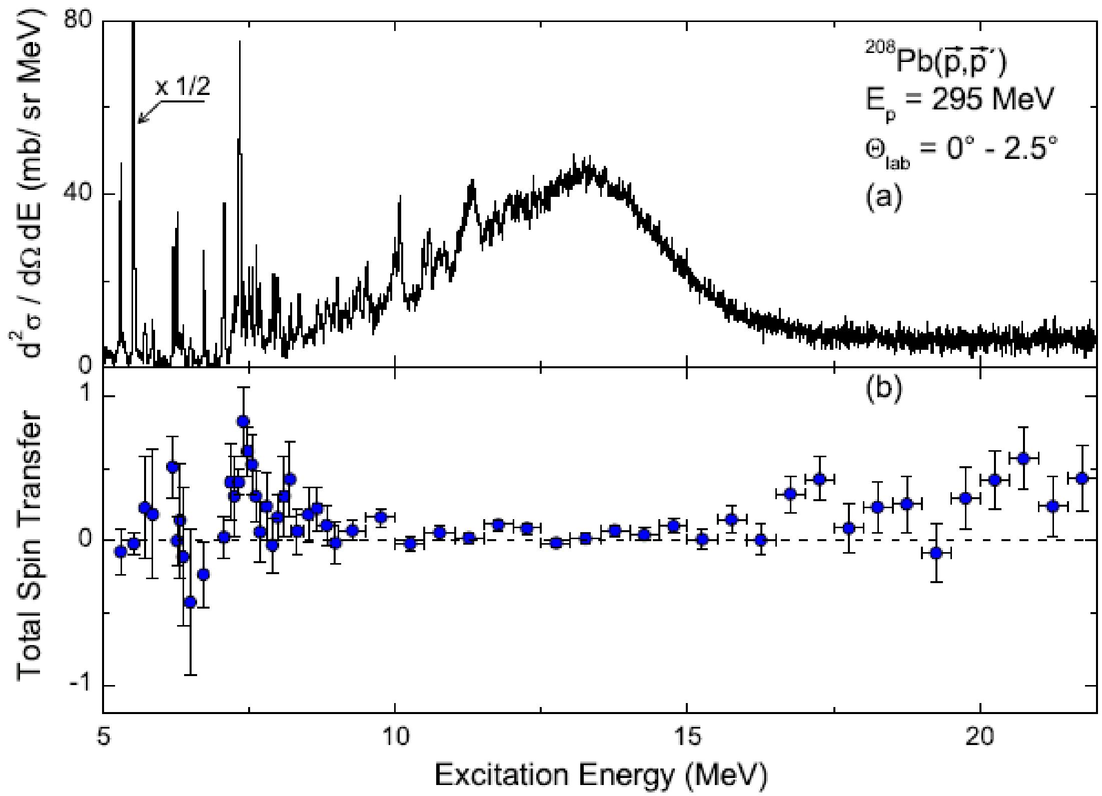

Comparison with (γ,γ’) and (γ,xn)

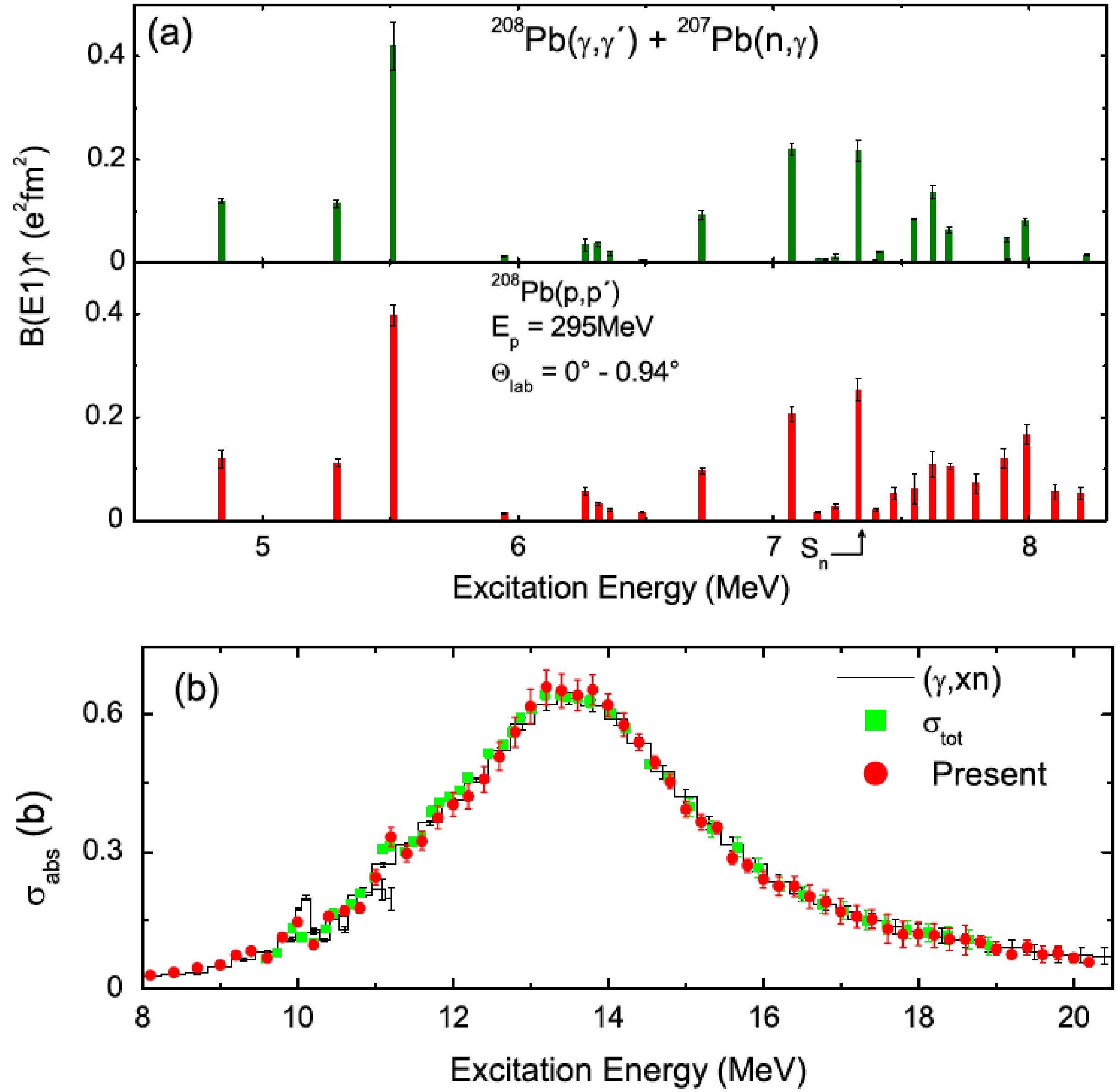

low-lying discrete states

GDR region

Setup for E282&E316

Comparison between the two methods

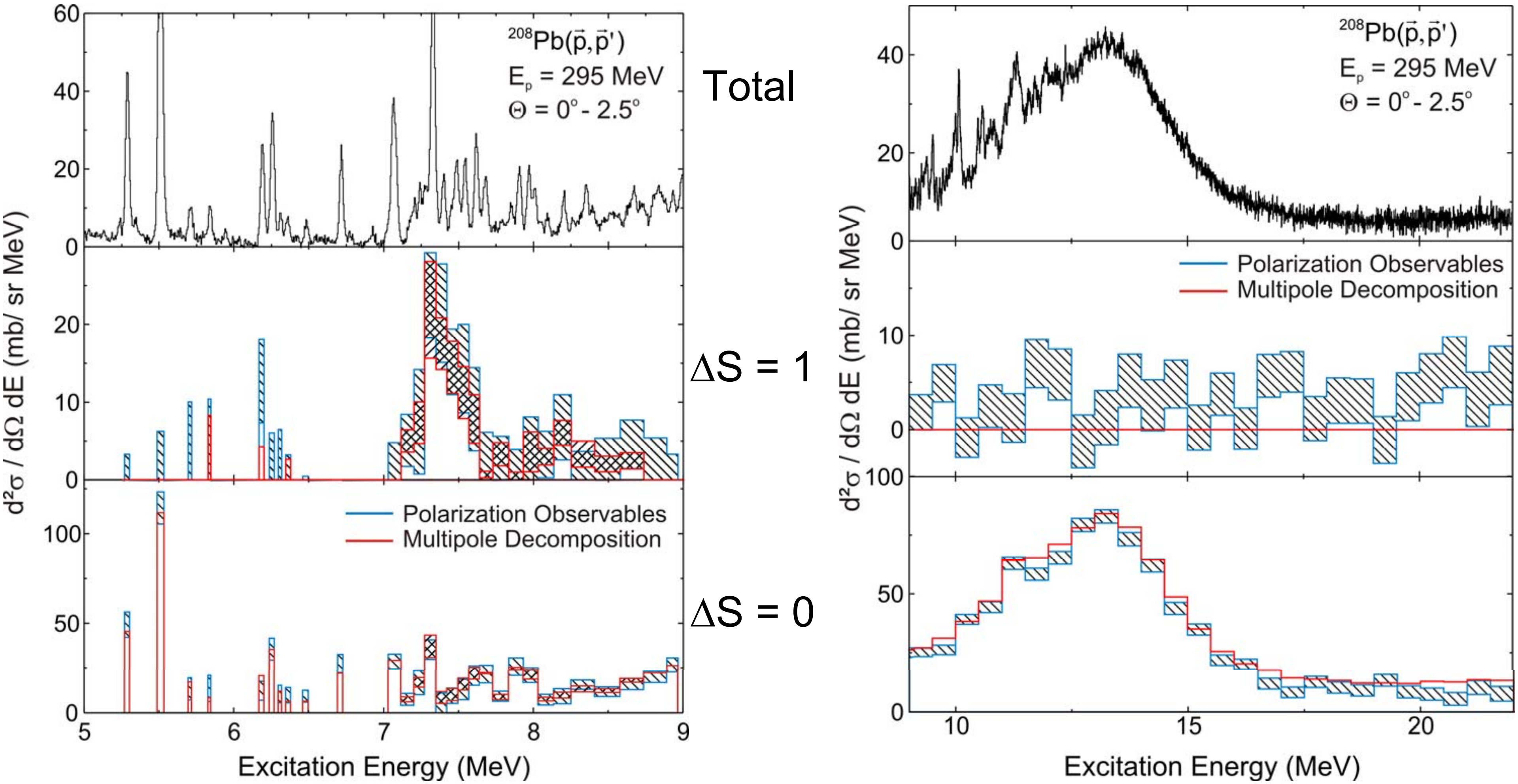

E1 Response of ^{208}Pb and α_D

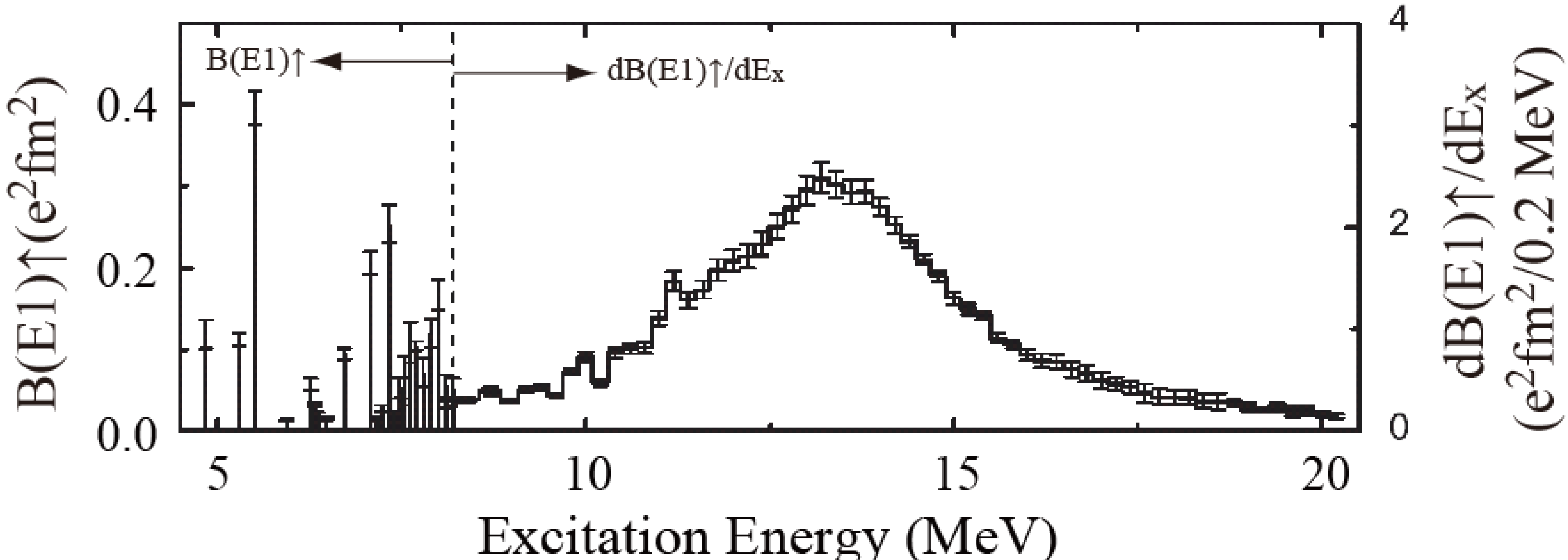

E_x	0 – 10	10 – 20	20 – 130 MeV
α_D	2.7	16.2	1.2 fm^3

total 20.1±0.6 fm^3

combined data

The dipole polarizability of ^{208}Pb has been precisely determined.

AT et al., PRL107, 062502(2011)

Electric Dipole Polarizability: ^{208}Pb, ^{120}Sn

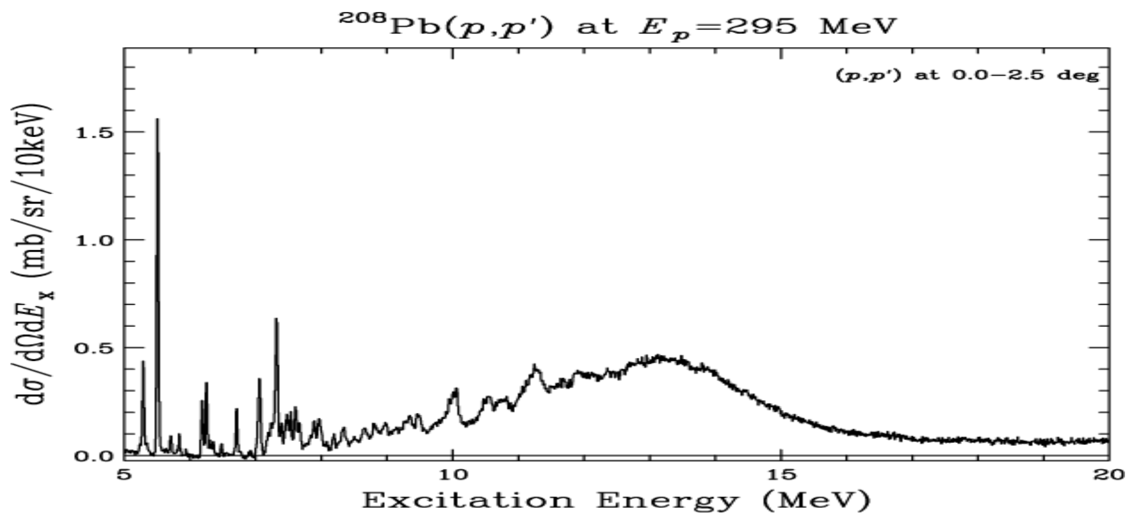

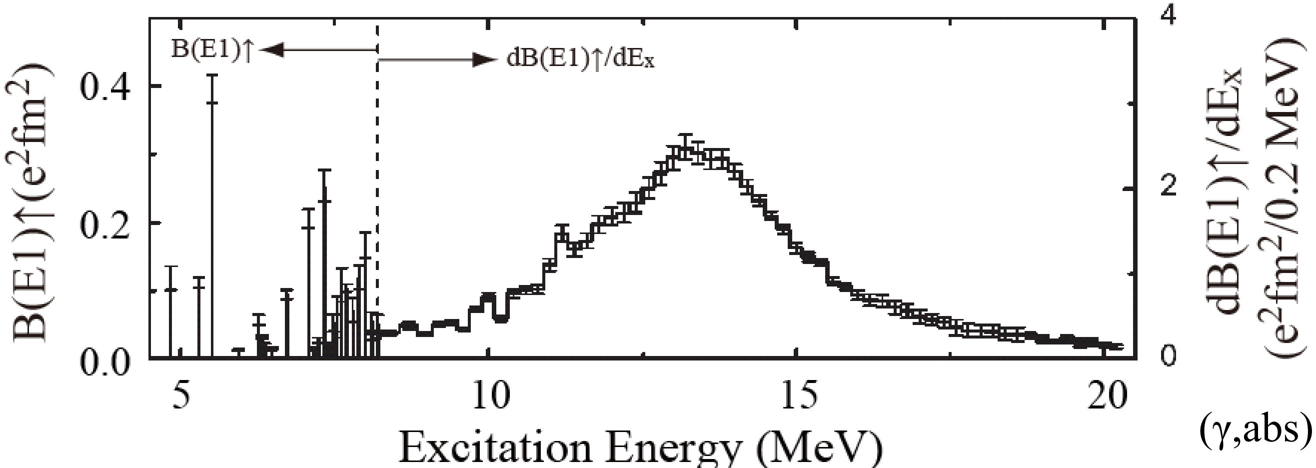

(γ,abs) at Mainz

E_x	0	10	20	130 MeV
α_D	2.7	16.2		1.2 fm³

total 20.1±0.6 fm³

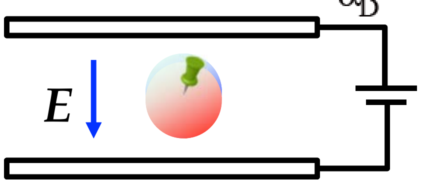

AT et al., PRL107, 062502(2011)

Electric Dipole Polarizability: ^{208}Pb, ^{120}Sn

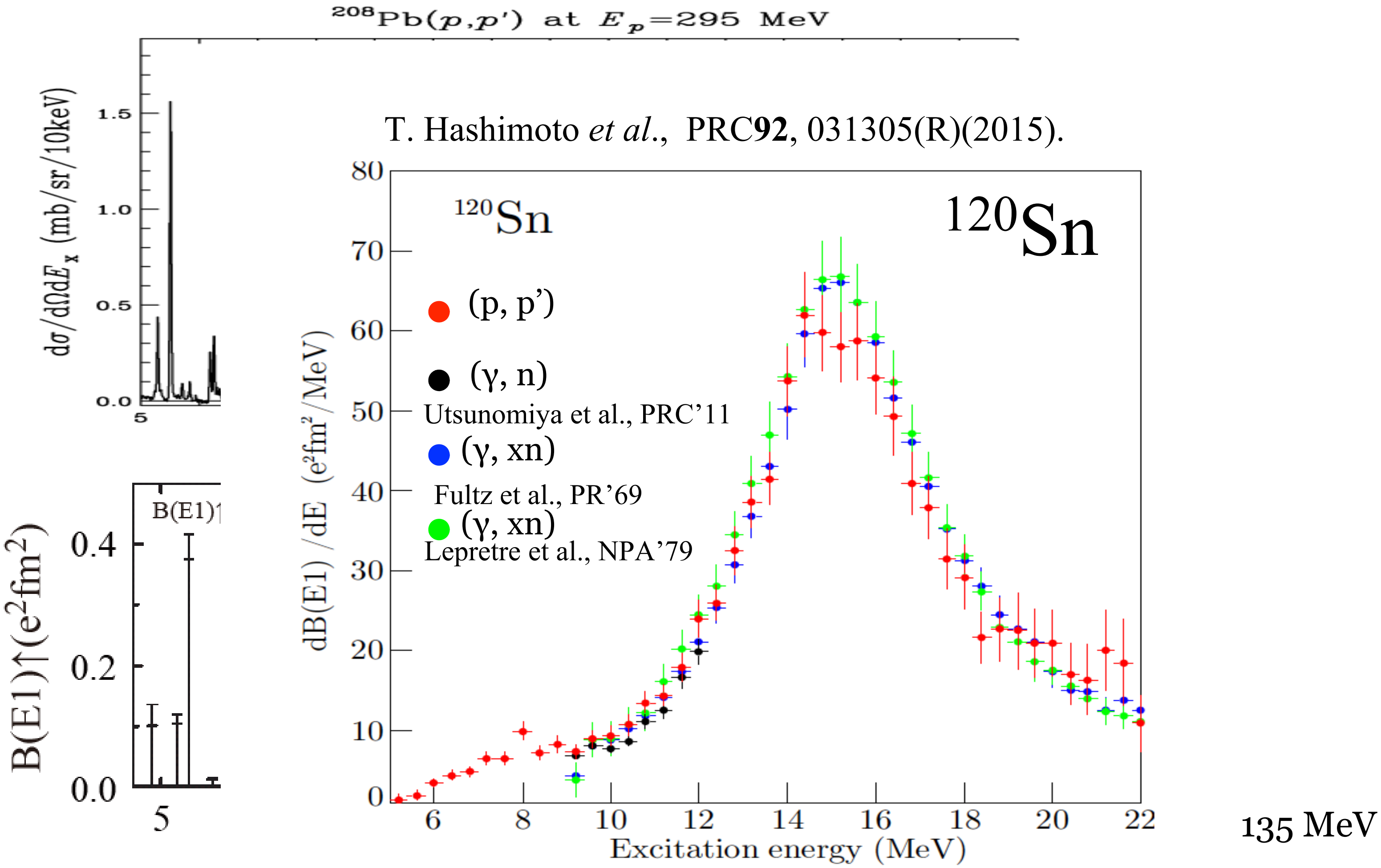

E_x 0

1.12 ± 0.07 | 7.00 ± 0.29 | 0.82 ± 0.12

Total: $\alpha_D = 8.93 \pm 0.36\ fm^3$

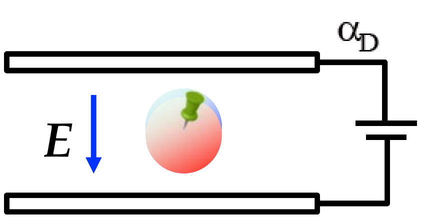

Electric Dipole Polarizability of ^{48}Ca

where the EDF and ab-initio calculations meet each other

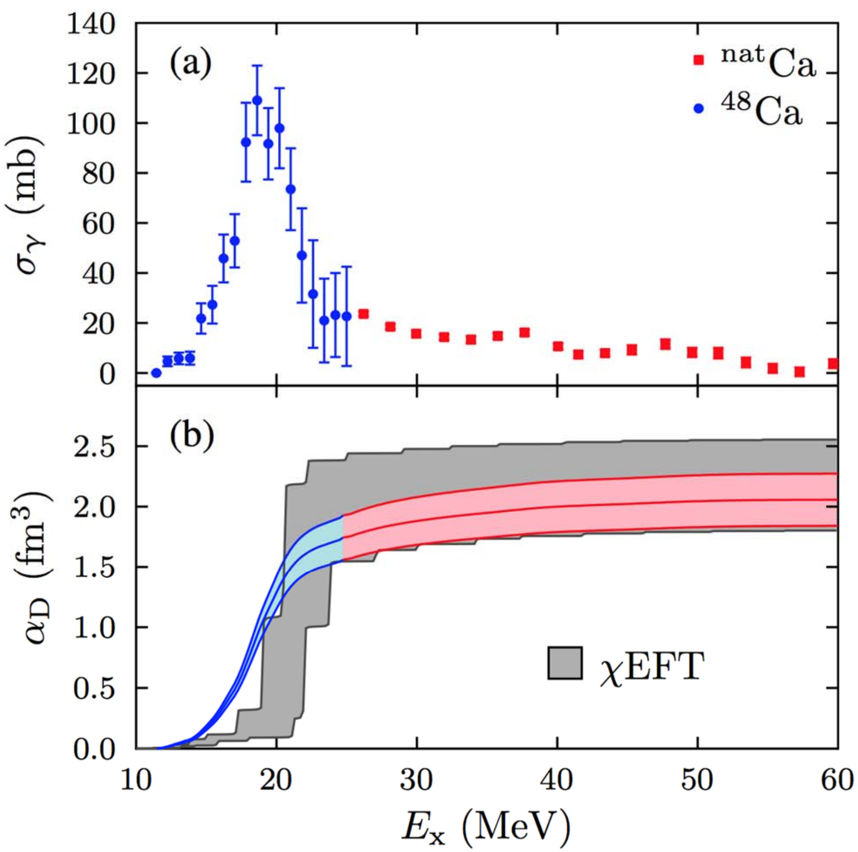

J. Birkhan et al., PRL118, 252501(2017)

Theory: Darmstadt-Tennessee-TRIUMF

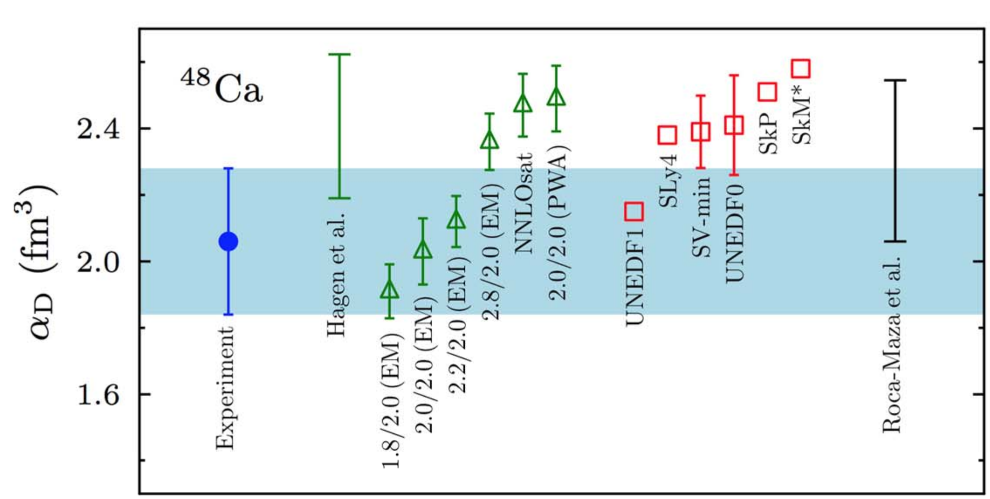

A dedicated new measurement is planned in 2020 for smaller exp. uncertainty.

Relative Contribution of the Electric Dipole Responses to α_D

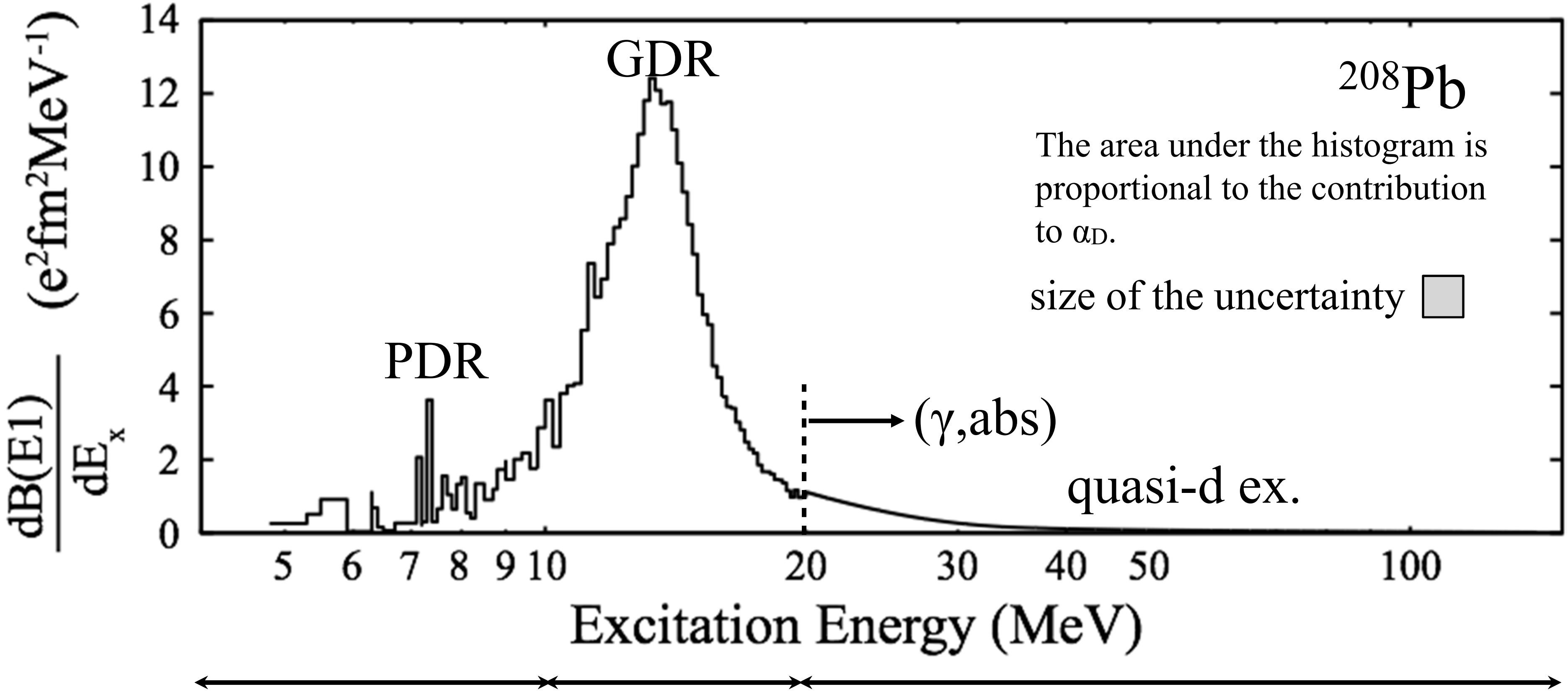

α_D 2.7 16.2 1.2 fm^3

total 20.1 ± 0.6 fm^3

Electric Dipole Polarizability

Clear definition

Unambiguous in the integration ra

⟷ Pygmy Dipole Strength

Inversely energy weighted sum-rule

More sensitive to the low-energy st

Good convergence in the excitation

⟷ energy-weighted (TRK) s

Sum-rule for all the transitions

= Ground state property

⟷ easier comparison with th

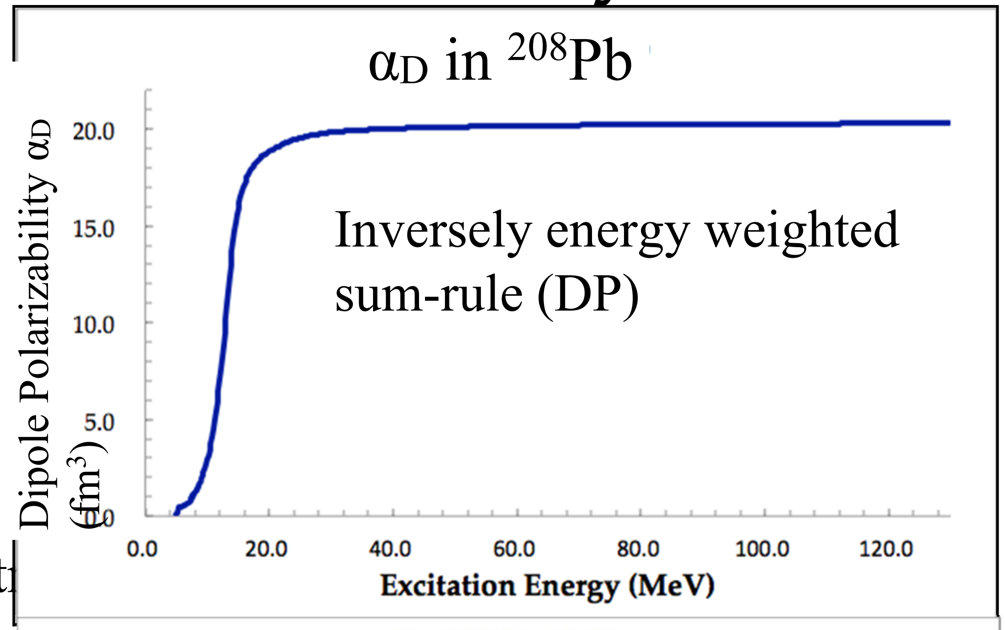

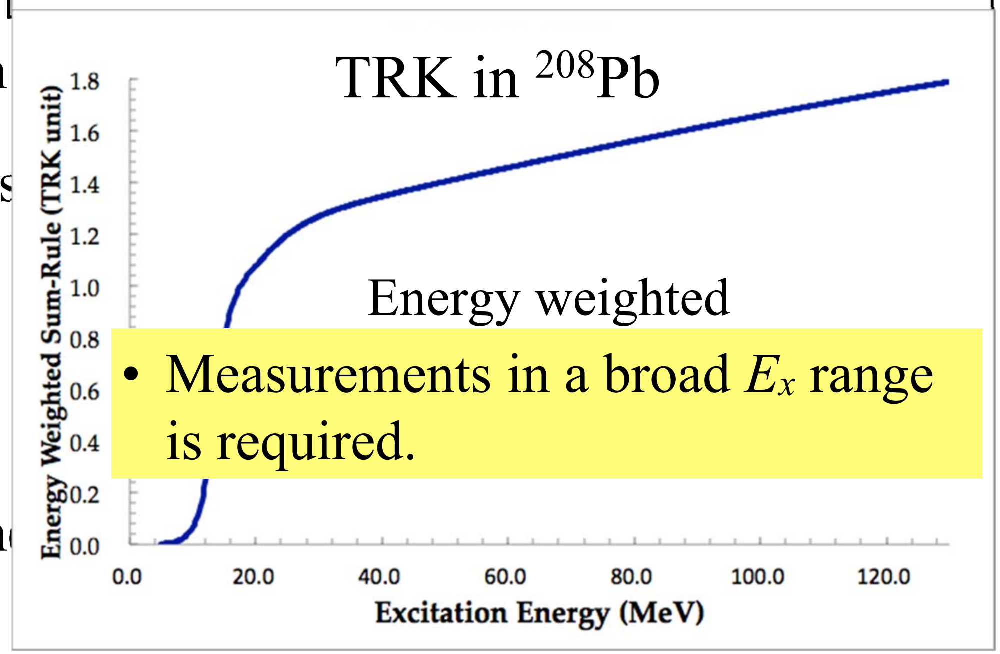

Electric Dipole Polarizability

Clear definition

Unambiguous in the integration ra

⟷ Pygmy Dipole Strength

Inversely energy weighted sum-rule

More sensitive to the low-energy st

Good convergence in the excitation

⟷ energy-weighted (TRK) s

Sum-rule for all the transitions

= Ground state property

⟷ easier comparison with th

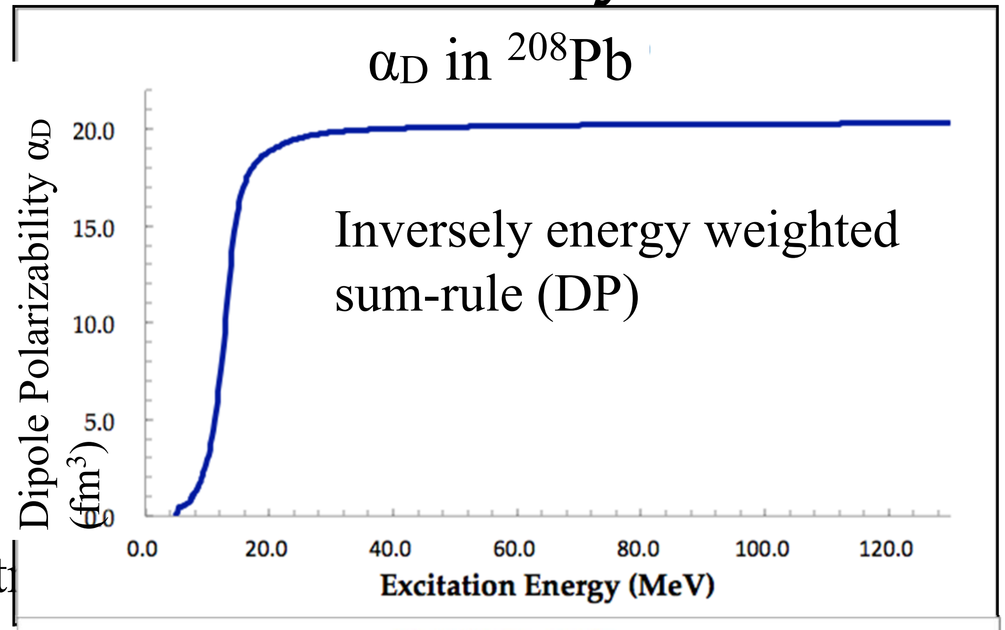

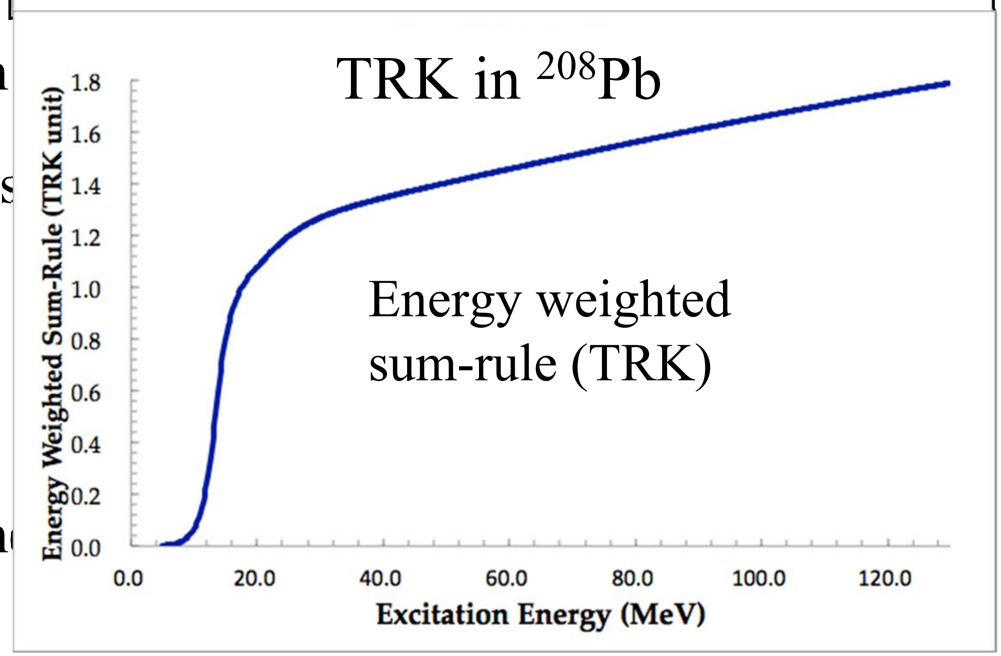

Electric Dipole Polarizability (α_D) in the correlation of *J* and *L*

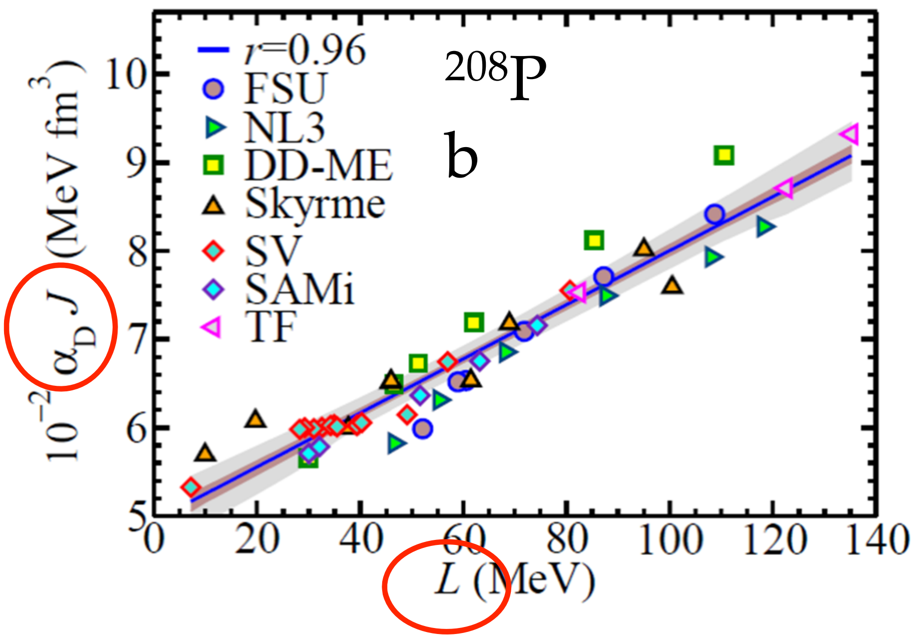

X. Roca-Maza *et al.*, PRC**88**, 024316(2013)

Correlations observed in various interaction sets in the framework of EDF.

$$\alpha_D^{\mathrm{DM}} \approx \frac{\pi e^2}{54} \frac{A\langle r^2 \rangle}{J} \left[1 + \frac{5}{3} \frac{L}{J} \epsilon_A \right]$$

insights from the droplet model

Precise determination of α_D of ^{208}Pb gives a constraint band in the *J*-*L* plane.

Constraints on *J* and *L*

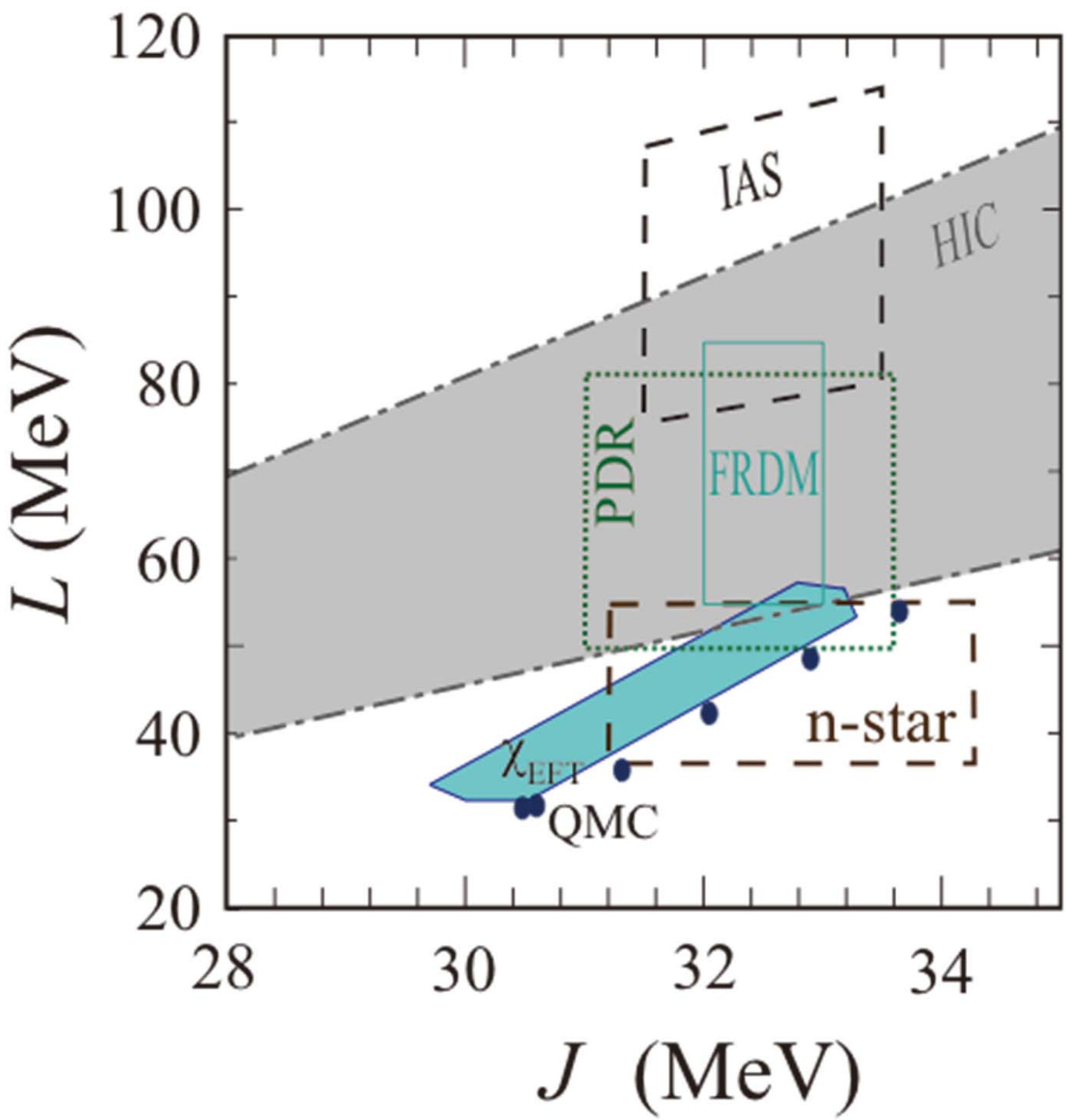

Tsang PRC2012

HIC: Heavy Ion Collision Analysis
Tsang PRL2009

IAS: Isobaric Analog State Energy
Danielewicz&Lee NPA2009

PDR: Pygmy Dipole Resonance in ^{132}Sn, ^{68}Ni, Carbone PRC2010

FRDM: Finite Range Droplet Model
Moeller PRL2012

n-star: Quiescent Low-Mass X-ray Binaries, Stainer PRL2012

χ_{EFT}: Chiral Effective Field Theory, Tews PRL2013

QMC: Quantum Monte-Carlo Calc.
Gandolfi, EPJA50, 10(2014).

Constraints on J and L

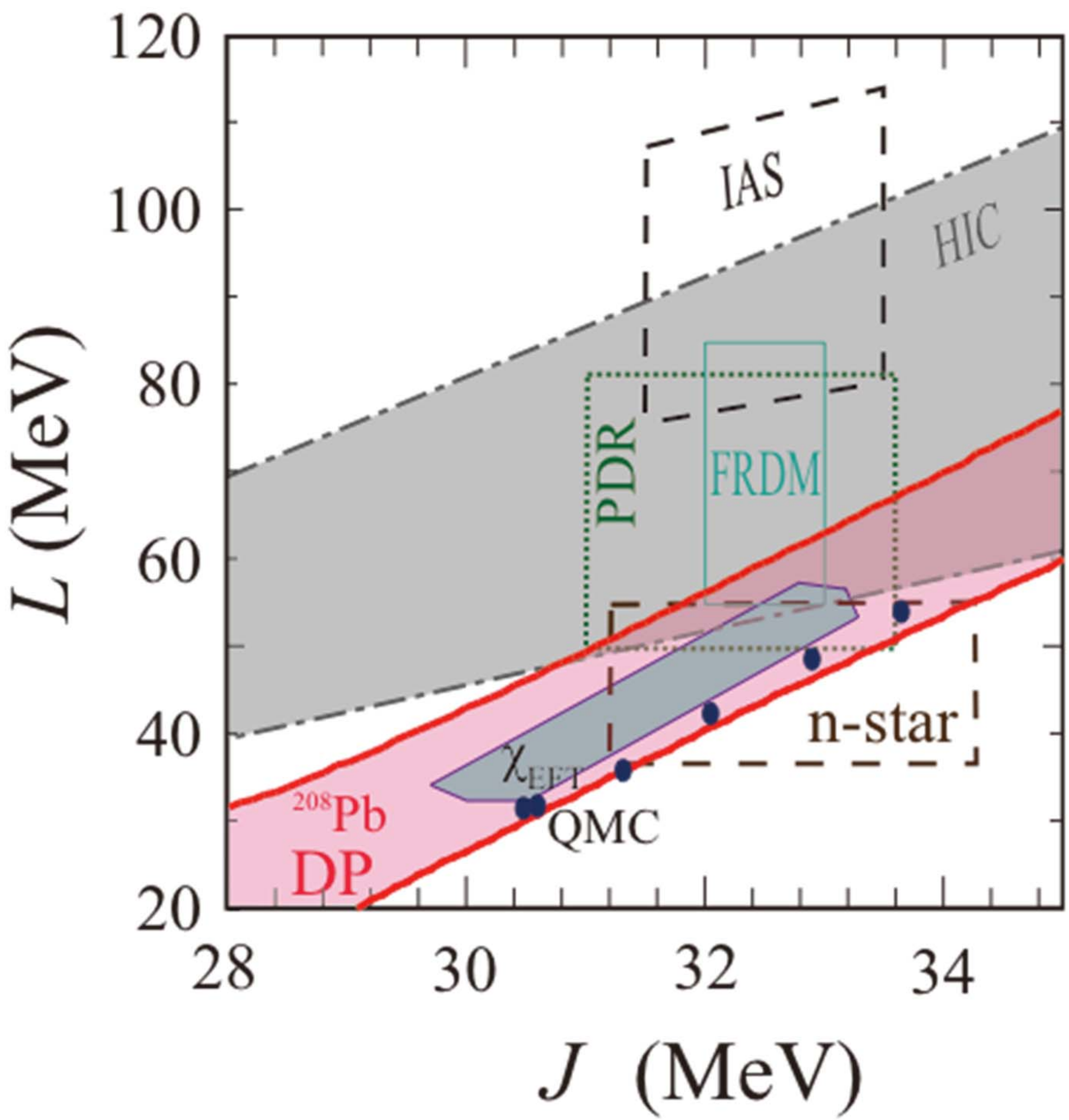

Tsang PRC2012

HIC: Heavy Ion Collision Analysis
Tsang PRL2009

IAS: Isobaric Analog State Energy
Danielewicz&Lee NPA2009

PDR: Pygmy Dipole Resonance in ^{132}Sn, ^{68}Ni, Carbone PRC2010

FRDM: Finite Range Droplet Model
Moller PRL2012

n-star: Quiescent Low-Mass X-ray Binaries, Stainer PRL2012

χ_{EFT}: Chiral Effective Field Theory, Tews PRL2013

QMC: Quantum Monte-Carlo Calc.
Gandolfi, EPJA50, 10(2014).

DP: Dipole Polarizability ^{208}Pb
AT PRL2011&EPJA2014

Constraints on *J* and *L* for experiments and models

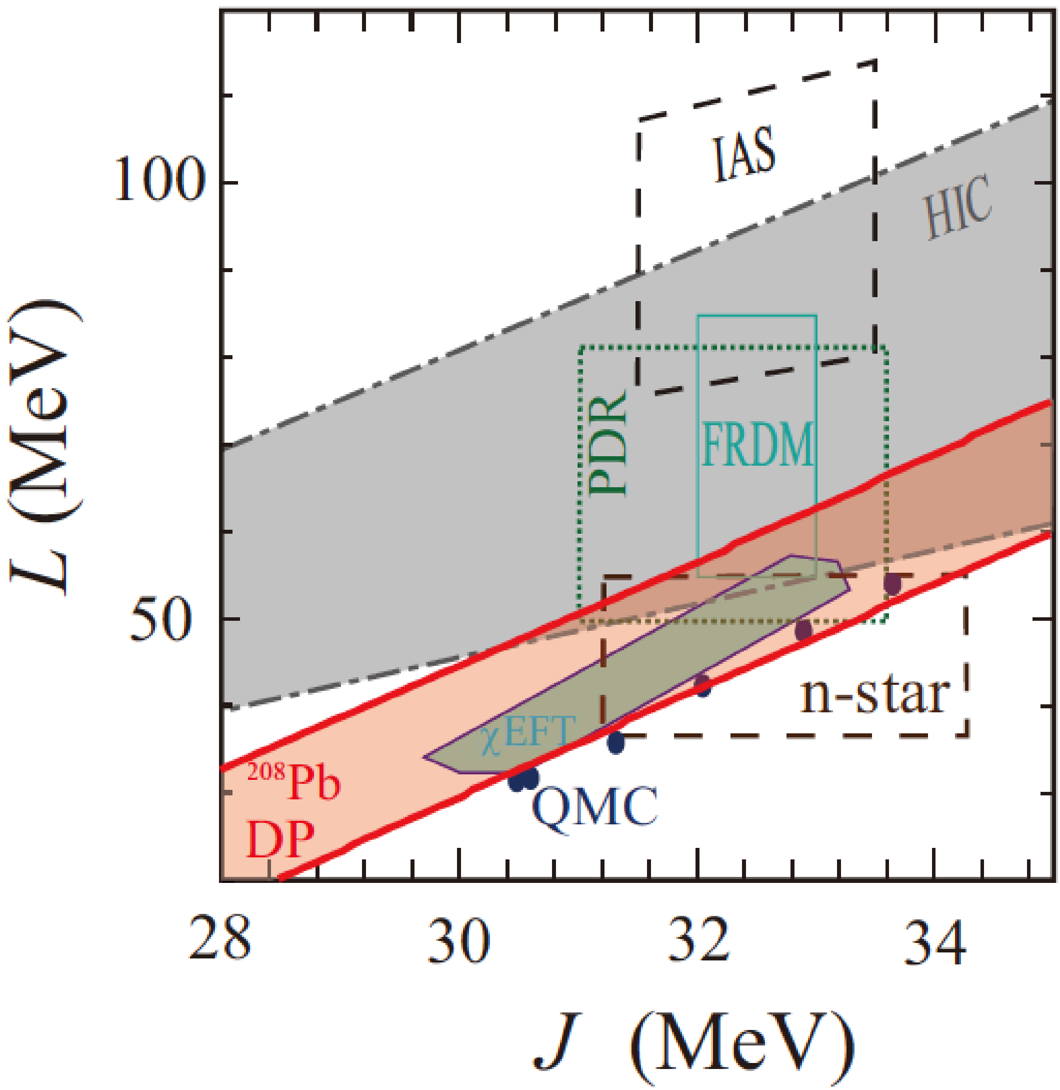

AT et al., EPJA**50**, 28 (2014).

M.B. Tsang *et al.*, PRC**86**, 015803 (2012)

C.J. Horowitz et al., JPG41, 093001 (2014)

DP: Dipole Polarizability
HIC: Heavy Ion Collision
PDR: Pygmy Dipole Resonance
IAS: Isobaric Analogue State
FRDM: Finite Range Droplet Model (nuclear mass analysis)
n-star: Neutron Star Observation
χEFT: Chiral Effective Field Theory

QMC: S. Gandolfi, EPJA50, 10(2014).

I. Tews et al., PRL110, 032504 (2013)

Quasi-Deuteron Excitation Contribution

Photon absorption by a virtual deuteron in the nucleus

needs to be subtracted for comparison with EDF calculations.

^{208}Pb

$\alpha_D(^{208}\mathrm{Pb})$: $20.1 \pm 0.6\ \mathrm{fm}^3$

quasi-*d*: $0.51 \pm 0.15\ \mathrm{fm}^3$

w/o quasi-*d*: $19.6 \pm 0.6\ \mathrm{fm}^3$

^{120}Sn

$\alpha_D(^{120}\mathrm{Sn})$: $8.93 \pm 0.36\ \mathrm{fm}^3$

quasi-*d*: $0.34 \pm 0.08\ \mathrm{fm}^3$

w/o quasi-*d*: $8.59 \pm 0.37\ \mathrm{fm}^3$

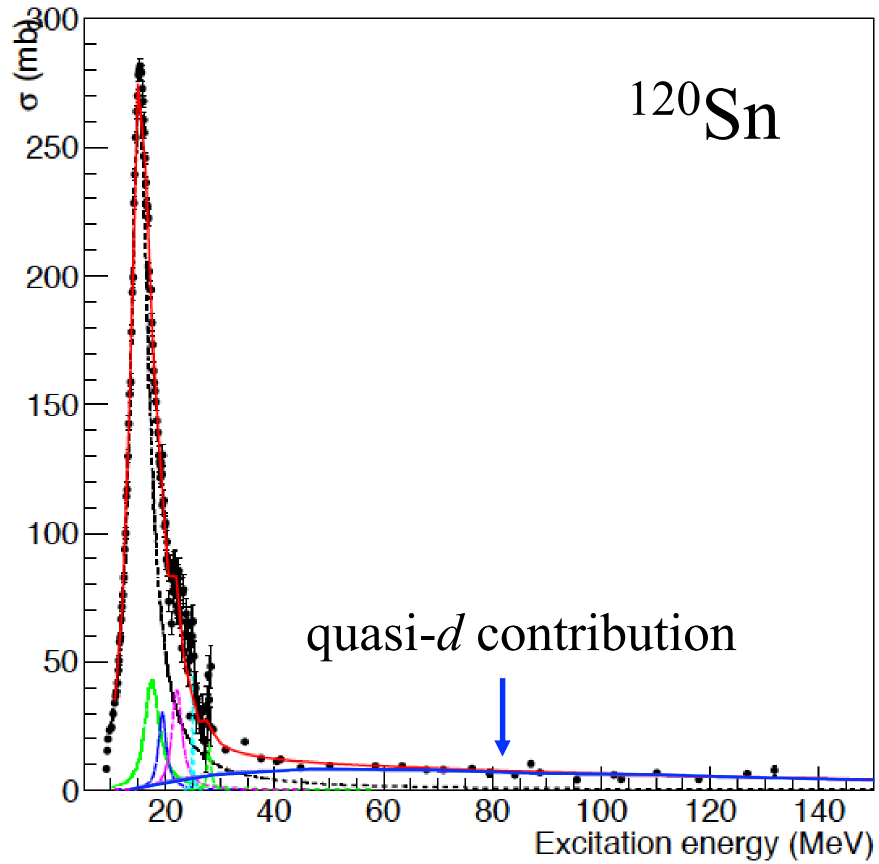

Constraints on *J*-*L* from the EDP data

X. Roca-Maza et al., PRC92, 064304(2015)

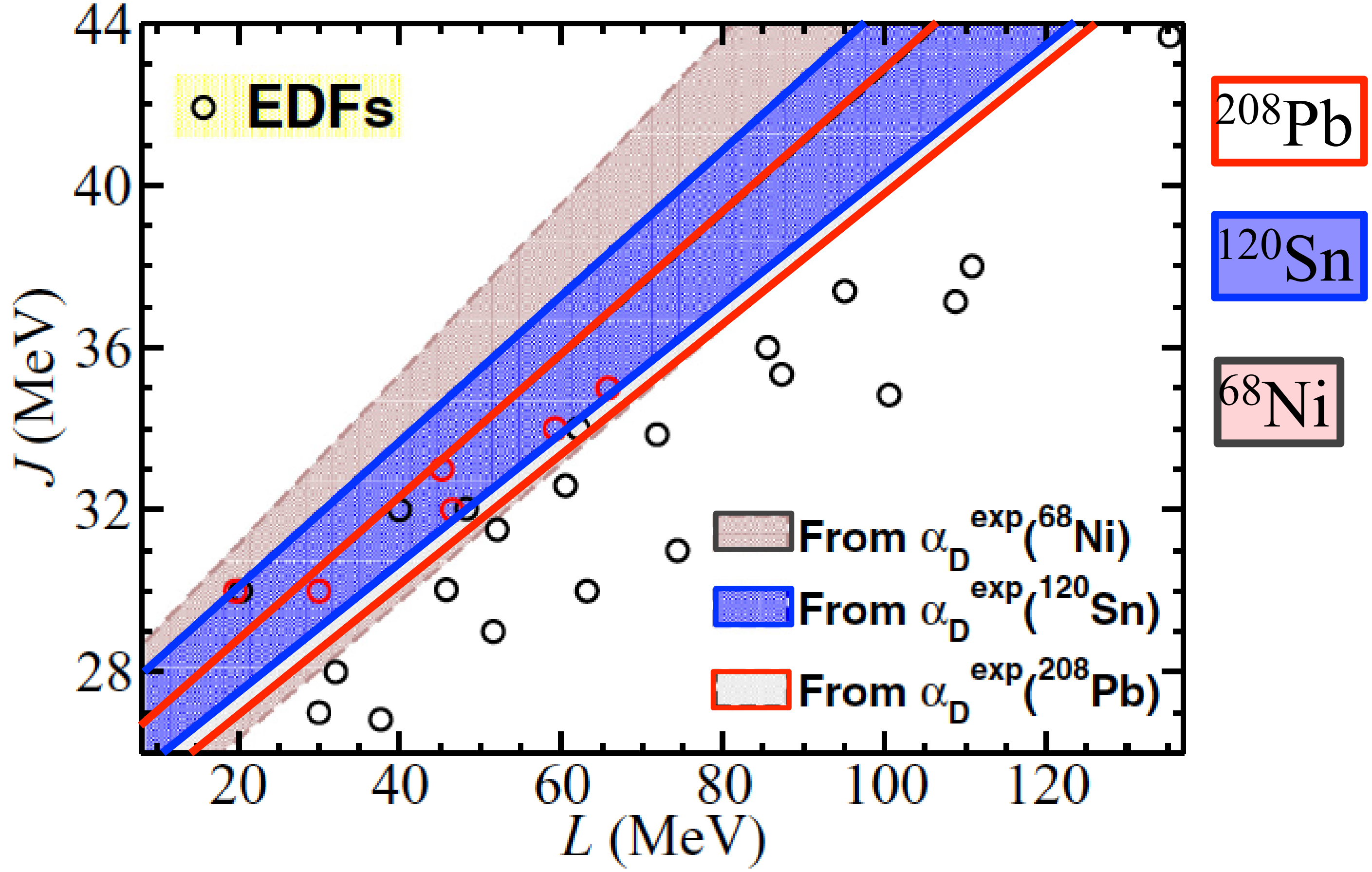

RCNP ^{208}Pb: AT *et al.*, PRL**107**, 062502 (2011).

RCNP ^{120}Sn: T. Hashimoto *et al.*, PRC**92**, 031305(R)(2015).

GSI ^{68}Ni: D.M. Rossi *et al.*, PRL**111**, 242503 (2013).

Constraints on *J*-*L* from the EDP data

X. Roca-Maza et al., PRC92, 064304(2015)

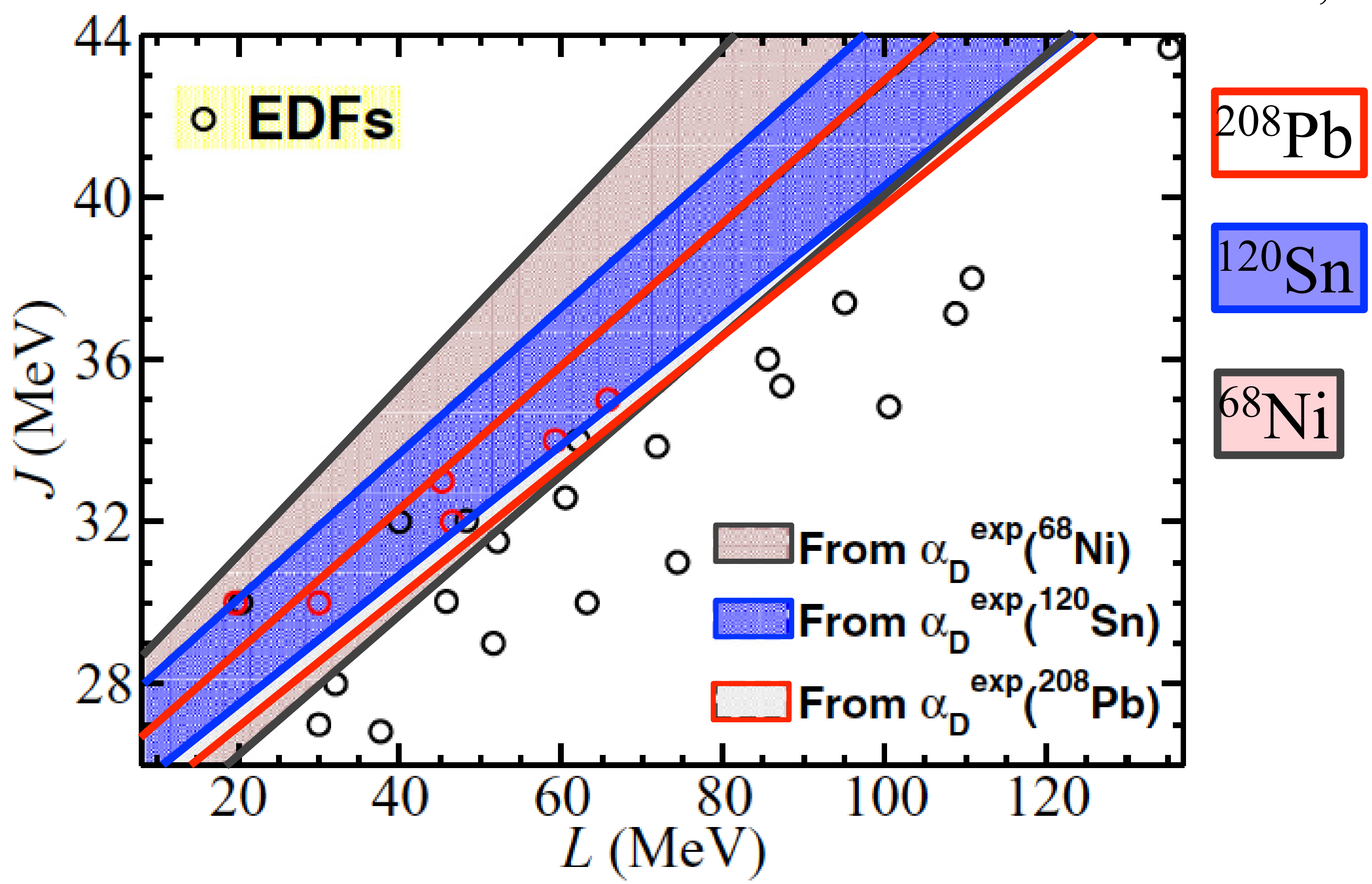

RCNP ^{208}Pb: AT *et al.*, PRL**107**, 062502 (2011).

RCNP ^{120}Sn: T. Hashimoto *et al.*, PRC**92**, 031305(R)(2015).

GSI ^{68}Ni: D.M. Rossi *et al.*, PRL**111**, 242503 (2013).

Neutron Skin Thickness of ^{208}Pb

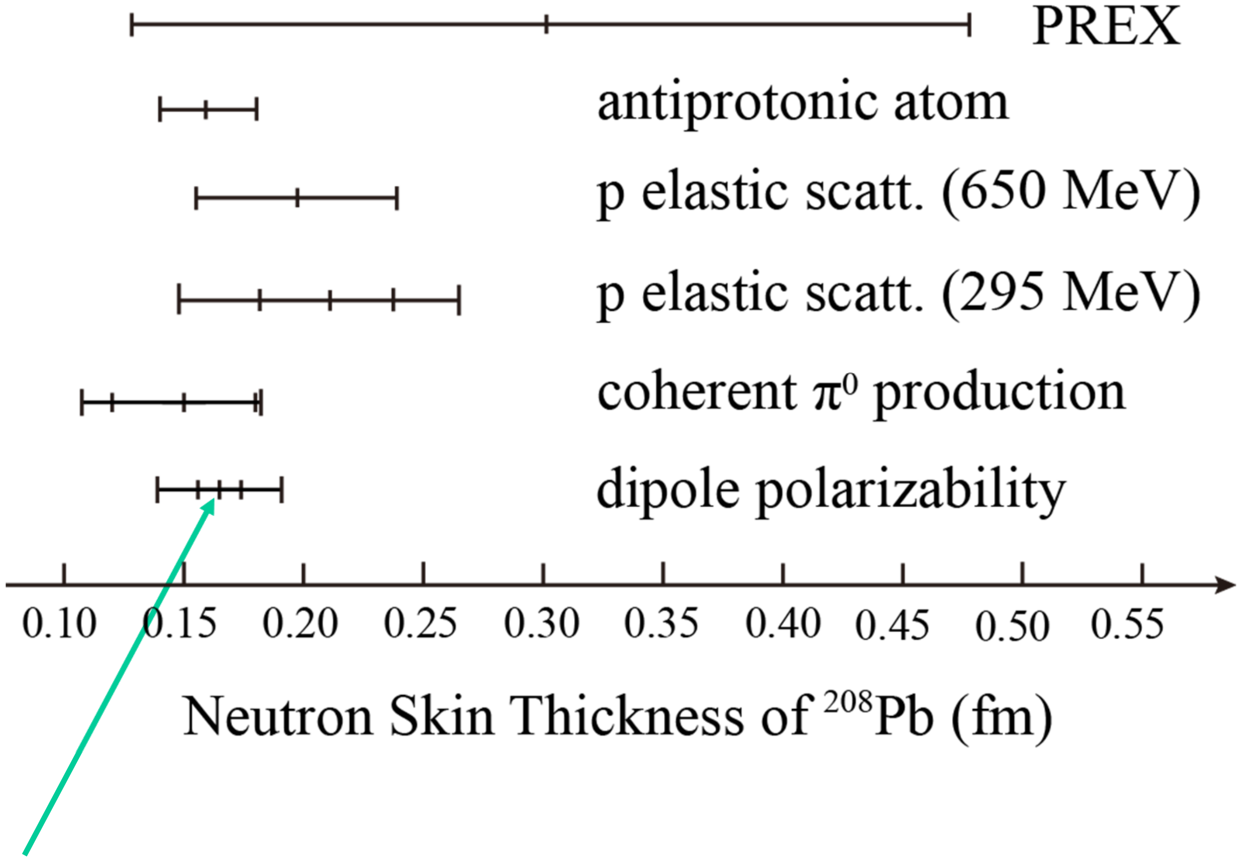

$\Delta R_{np} = 0.165 \pm (0.009)_{\rm expt} \pm (0.013)_{\rm theor} \pm (0.021)_{\rm est}$ fm

for the estimated J=31 ± $(2)_{\rm est}$

X. Roca-Maza *et al.*, PRC**88**, 024316(2013)

Constraints on *J*-*L* from the EDP data

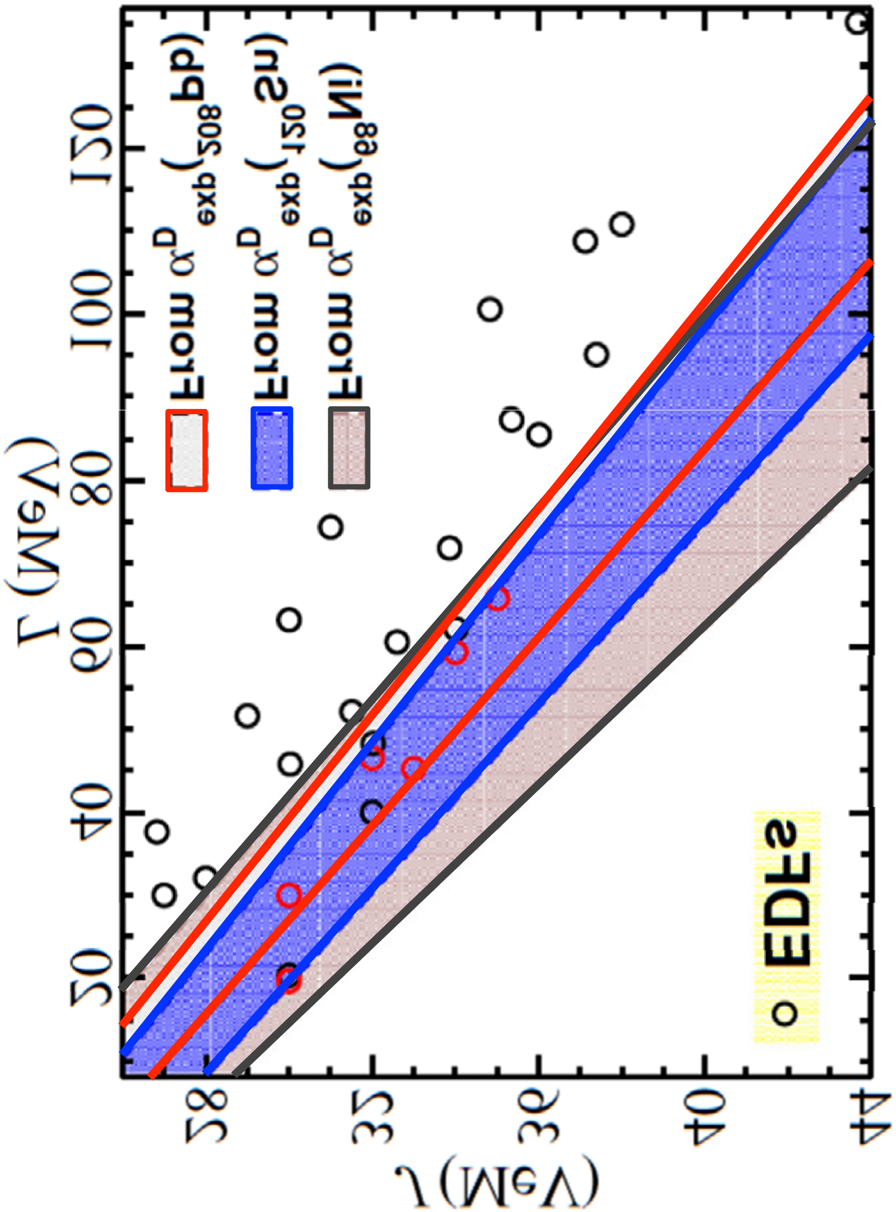

X. Roca-Maza et al., PRC92, 064304(2015)

^{208}Pb

^{120}Sn

^{68}Ni

RCNP ^{208}Pb: AT *et al.*, PRL**107**, 062502 (2011).

RCNP ^{120}Sn: T. Hashimoto *et al.*, PRC**92**, 031305(R)(2015).

GSI ^{68}Ni: D.M. Rossi *et al.*, PRL**111**, 242503 (2013).

These α_D data give essentially one constraint on the symmetry energy in the *J*-*L* plane.

Constraints on J and L

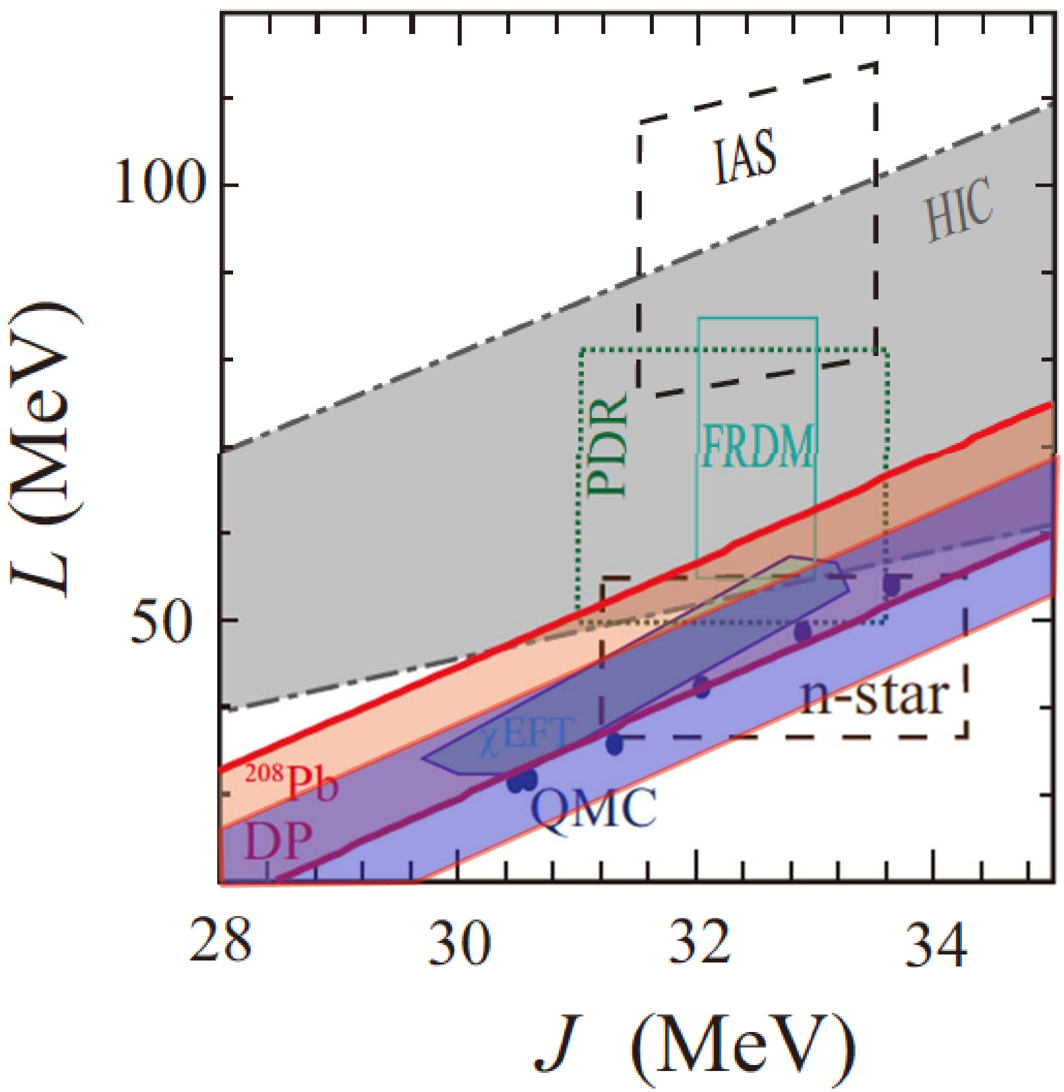

AT et al., EPJA**50**, 28 (2014).

M.B. Tsang *et al.*, PRC**86**, 015803 (2012)

C.J. Horowitz et al., JPG41, 093001 (2014)

DP: Dipole Polarizability
HIC: Heavy Ion Collision
PDR: Pygmy Dipole Resonance
IAS: Isobaric Analogue State
FRDM: Finite Range Droplet Model (nuclear mass analysis)
n-star: Neutron Star Observation
χEFT: Chiral Effective Field Theory

QMC: S. Gandolfi, EPJA50, 10(2014).
I. Tews et al., PRL110, 032504 (2013)

After Subtraction of the quasi-*d* contribution.

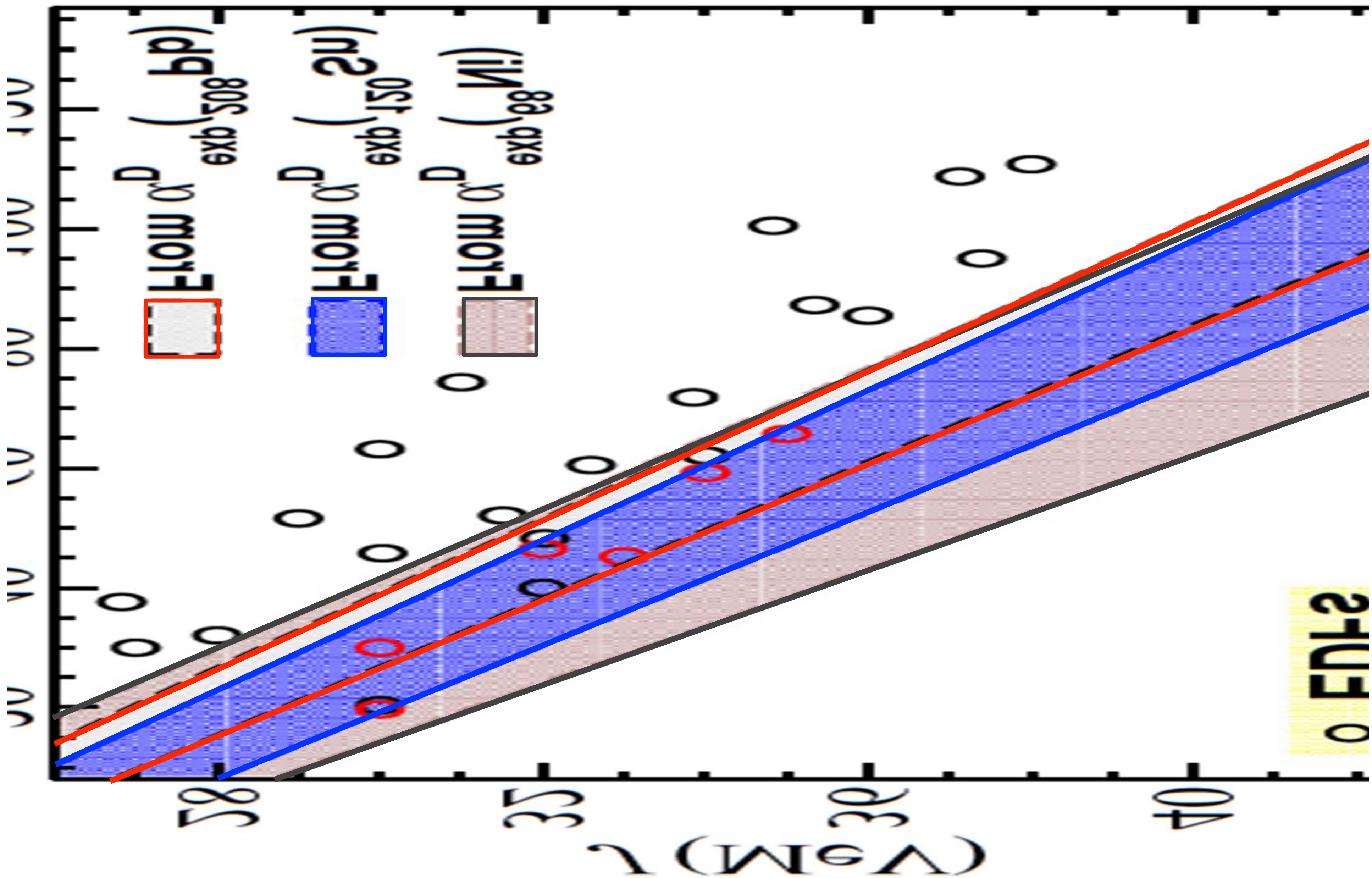
From $\alpha^D_{exp}(^{208}Pb)$
From $\alpha^D_{exp}(^{120}Sn)$
From $\alpha^D_{exp}(^{68}Ni)$
EDFs
J (MeV)
35
36
40

Constraints on *J* and *L*

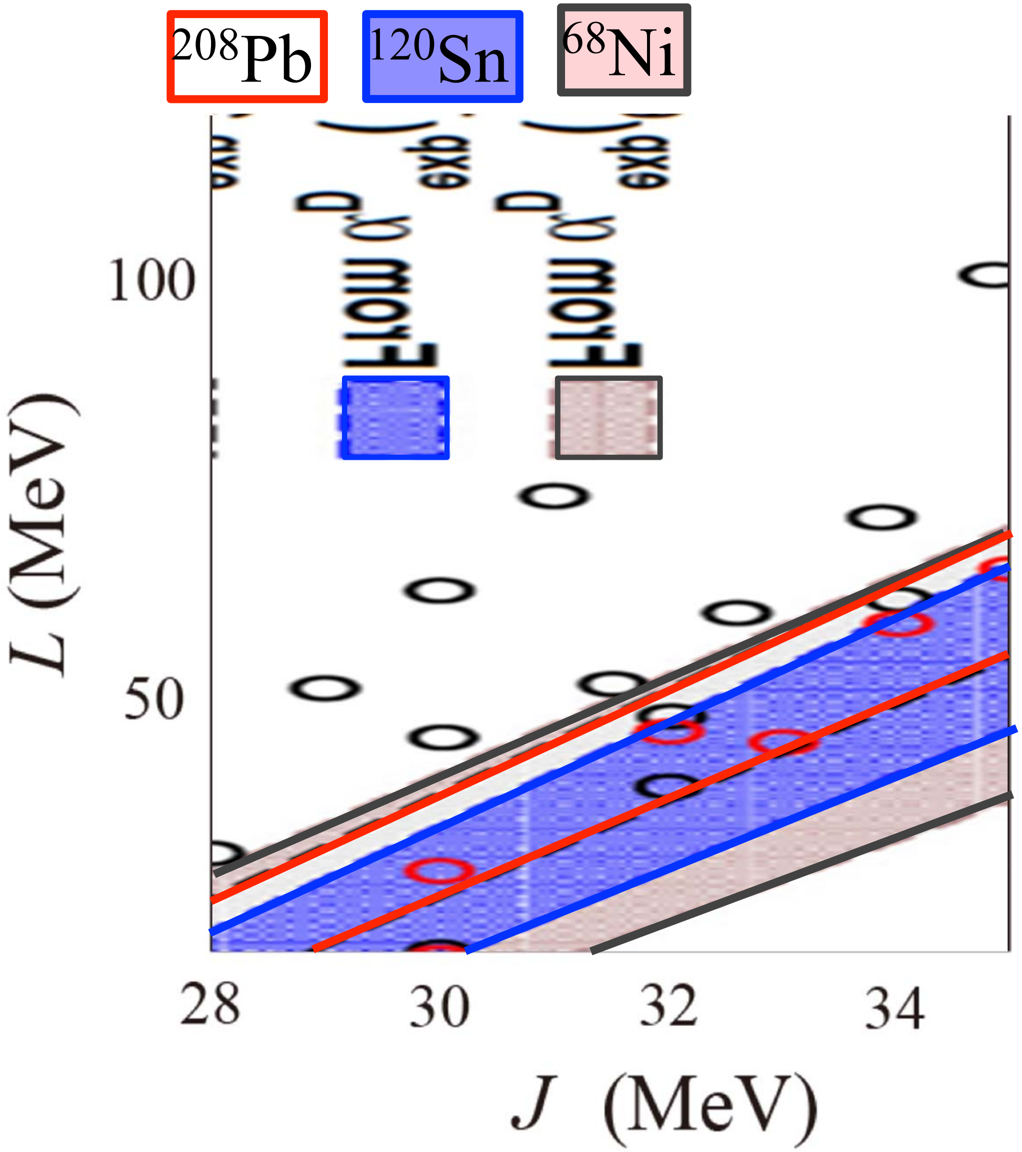

AT et al., EPJA**50**, 28 (2014).

M.B. Tsang *et al.*, PRC**86**, 015803 (2012)

C.J. Horowitz et al., JPG41, 093001 (2014)

DP: Dipole Polarizability
HIC: Heavy Ion Collision
PDR: Pygmy Dipole Resonance
IAS: Isobaric Analogue State
FRDM: Finite Range Droplet Model (nuclear mass analysis)
n-star: Neutron Star Observation
χEFT: Chiral Effective Field Theory

QMC: S. Gandolfi, EPJA50, 10(2014).
I. Tews et al., PRL110, 032504 (2013)

After Subtraction of the quasi-*d* contribution.

Constraints on *J* and *L*

^{208}Pb ^{120}Sn ^{68}Ni

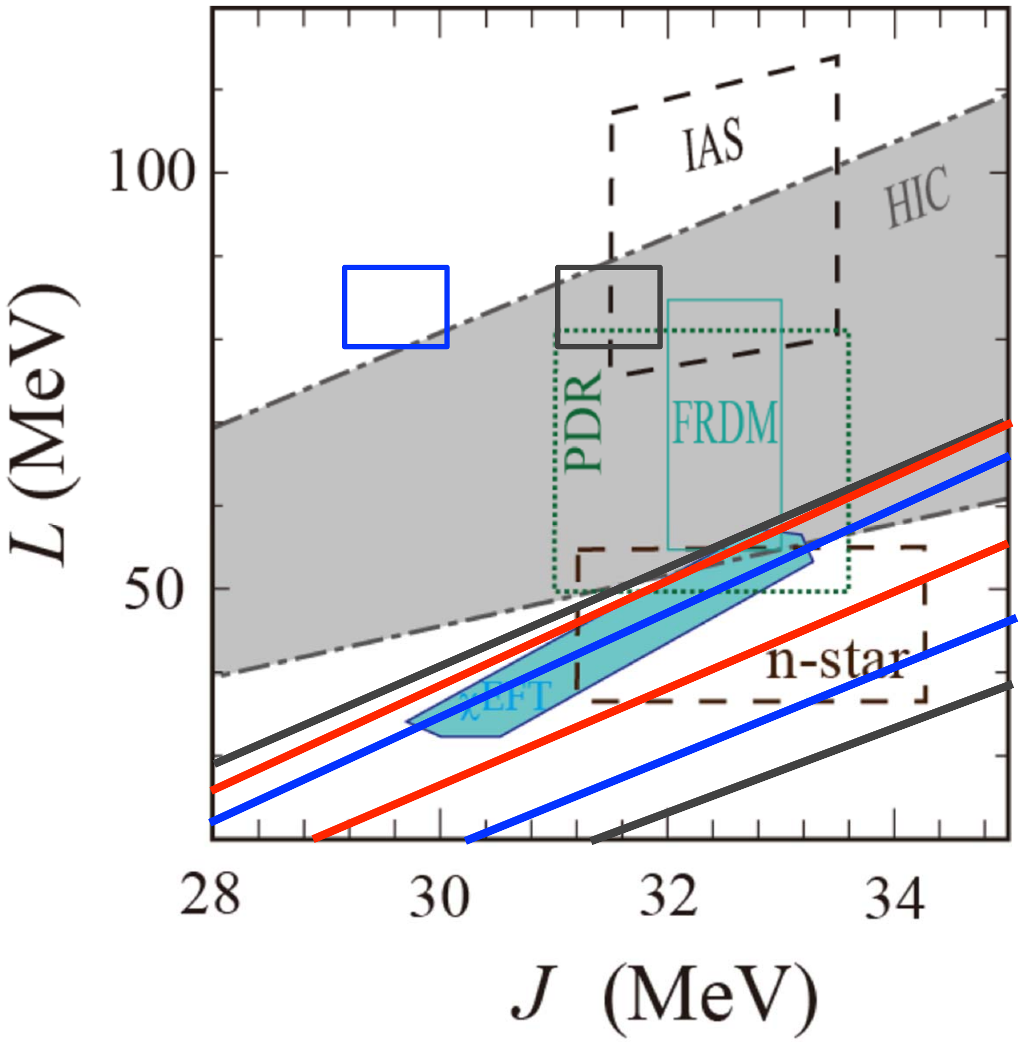

AT et al., EPJA**50**, 28 (2014).

M.B. Tsang *et al.*, PRC**86**, 015803 (2012)

C.J. Horowitz et al., JPG41, 093001 (2014)

DP: Dipole Polarizability
HIC: Heavy Ion Collision
PDR: Pygmy Dipole Resonance
IAS: Isobaric Analogue State
FRDM: Finite Range Droplet Model (nuclear mass analysis)
n-star: Neutron Star Observation
χEFT: Chiral Effective Field Theory

QMC: S. Gandolfi, EPJA50, 10(2014).
I. Tews et al., PRL110, 032504 (2013)

After Subtraction of the quasi-*d* contribution.

Constraints on J and L

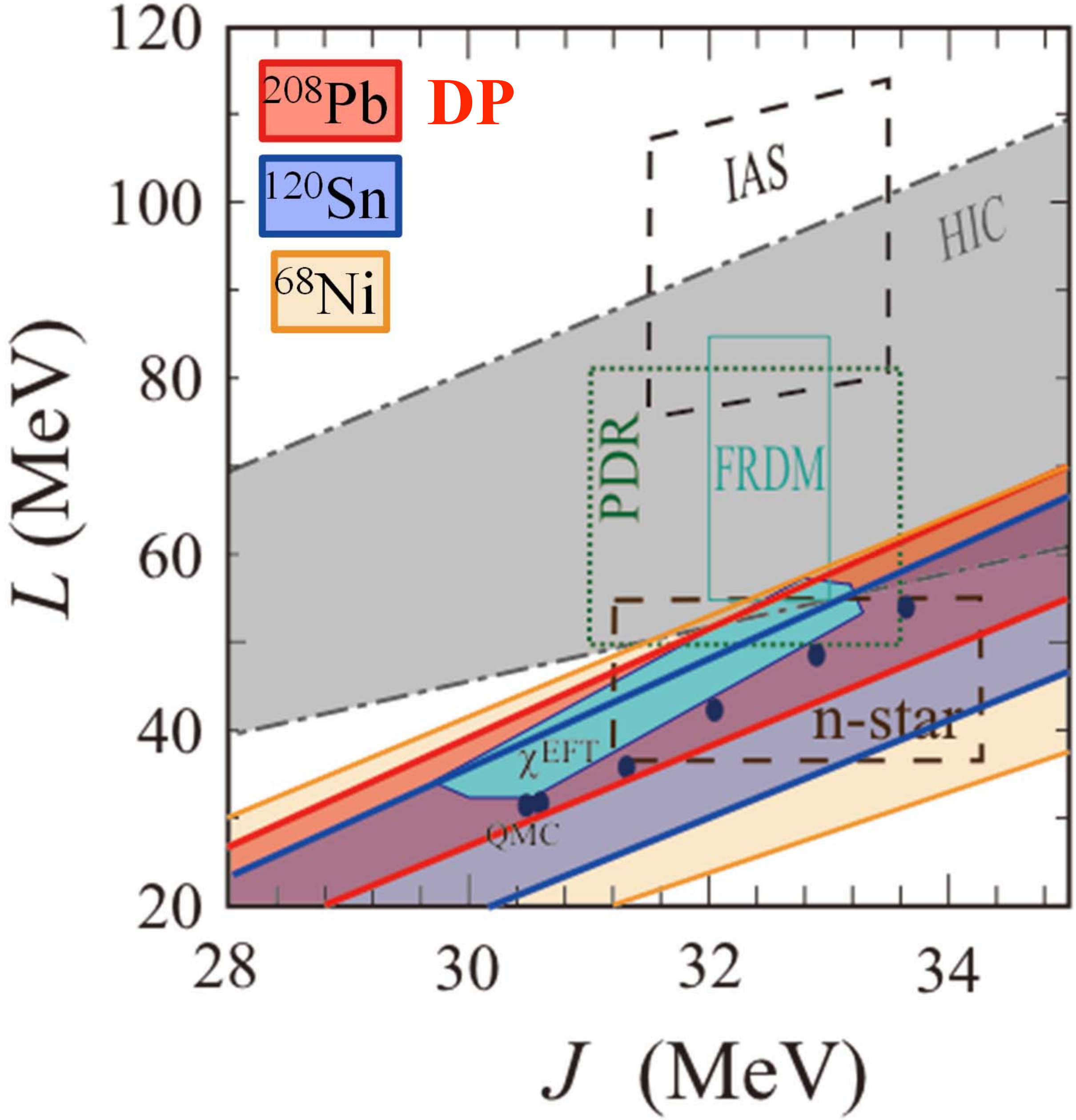

Tsang PRC2012

HIC: Heavy Ion Collision Analysis
Tsang PRL2009

IAS: Isobaric Analog State Energy
Danielewicz&Lee NPA2009

PDR: Pygmy Dipole Resonance in ^{132}Sn, ^{68}Ni, Carbone PRC2010

FRDM: Finite Range Droplet Model
Moller PRL2012

n-star: Quiescent Low-Mass X-ray Binaries, Stainer PRL2012

χEFT: Chiral Effective Field Theory, Tews PRL2013

QMC: Quantum Monte-Carlo Calc.
Gandolfi, EPJA50, 10(2014).

DP: Dipole Polarizability
^{208}Pb AT PRL2011
^{120}Sn Hashimoto PRC2015
^{68}Ni Rossi PRL2013

Constraints on *J* and *L*

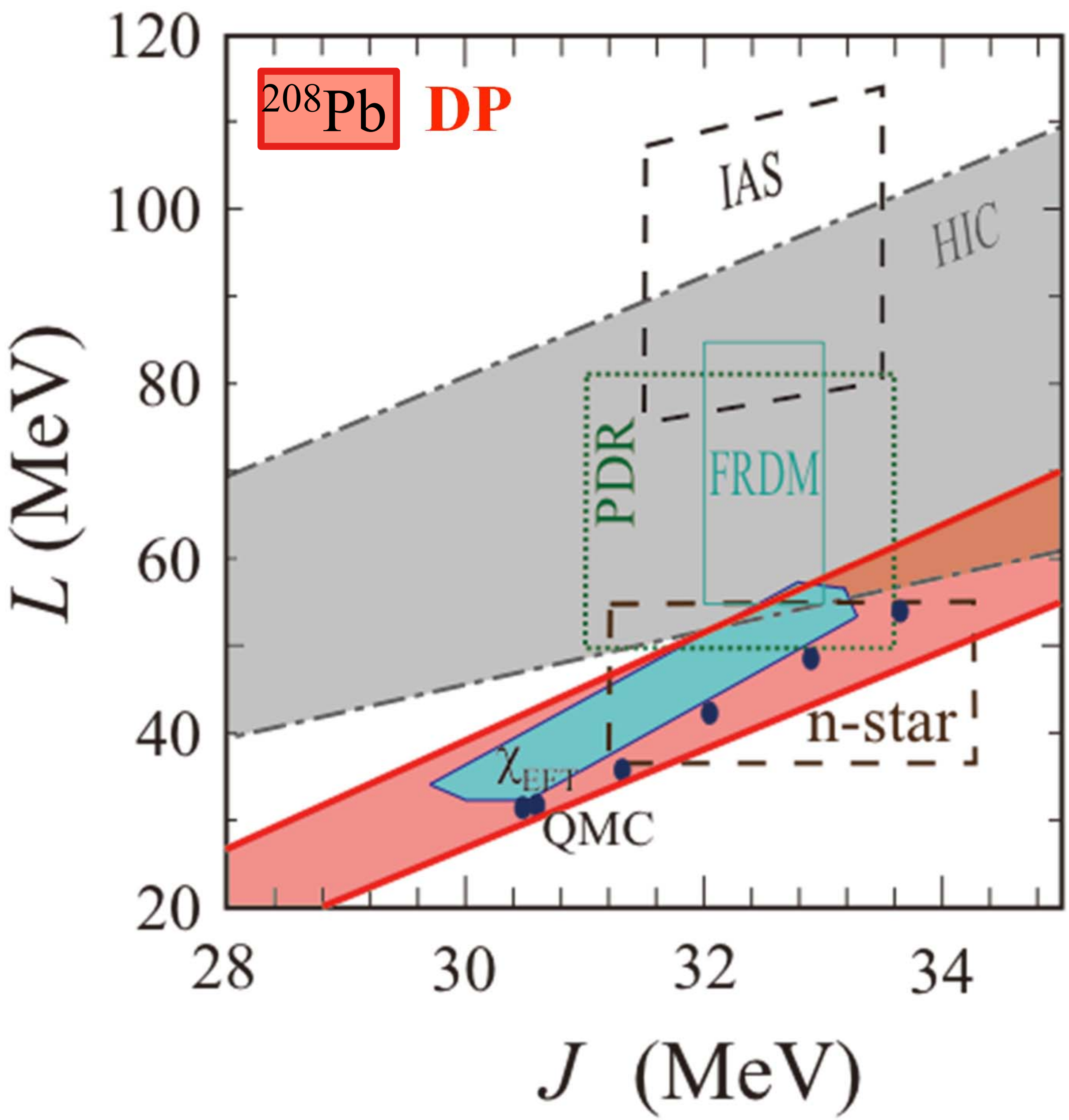

Tsang PRC2012

HIC: Heavy Ion Collision Analysis
Tsang PRL2009

IAS: Isobaric Analog State Energy
Danielewicz&Lee NPA2009

PDR: Pygmy Dipole Resonance in
^{132}Sn, ^{68}Ni, Carbone PRC2010

FRDM: Finite Range Droplet Model
Moller PRL2012

n-star: Quiescent Low-Mass X-ray
Binaries, Stainer PRL2012

χ_{EFT}: Chiral Effective Field Theory,
Tews PRL2013

QMC: Quantum Monte-Carlo Calc.
Gandolfi, EPJA50, 10(2014).

DP: Dipole Polarizability
^{208}Pb AT PRL2011

Constraints on *J* and *L*

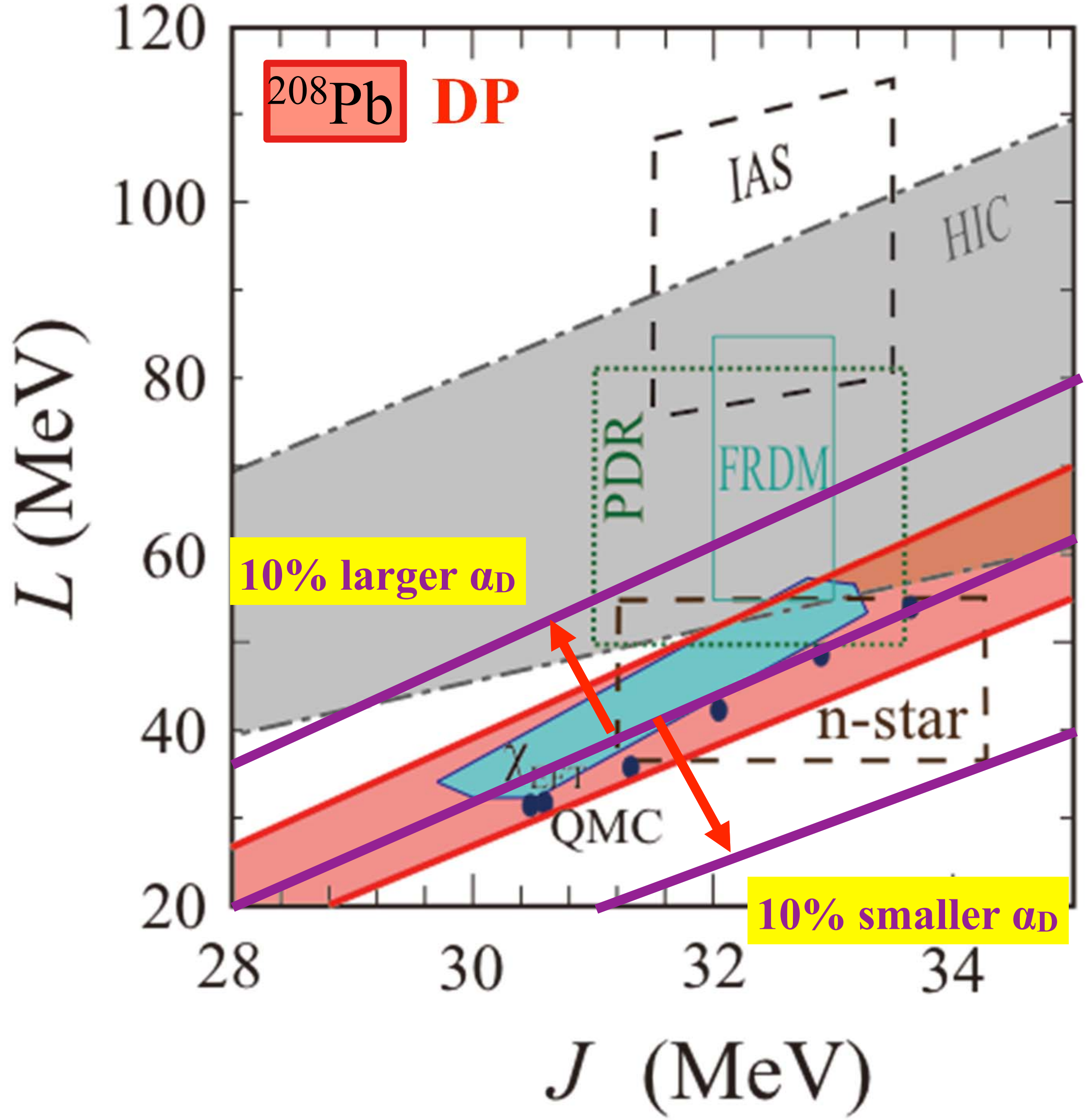

The α_D data determine the scale of the J-axis of the constraint band.

The χ_{EFT} and QMC calculations are consistent with the information that is extracted from α_D.

χ_{EFT}: Chiral Effective Field Theory, Tews PRL2013

QMC: Quantum Monte-Carlo Calc. Gandolfi, EPJA50, 10(2014).

DP: Dipole Polarizability ^{208}Pb AT PRL2011

QMC

S. Gandolfi, J. Carlson et al., EPJA50, 10 (2014)

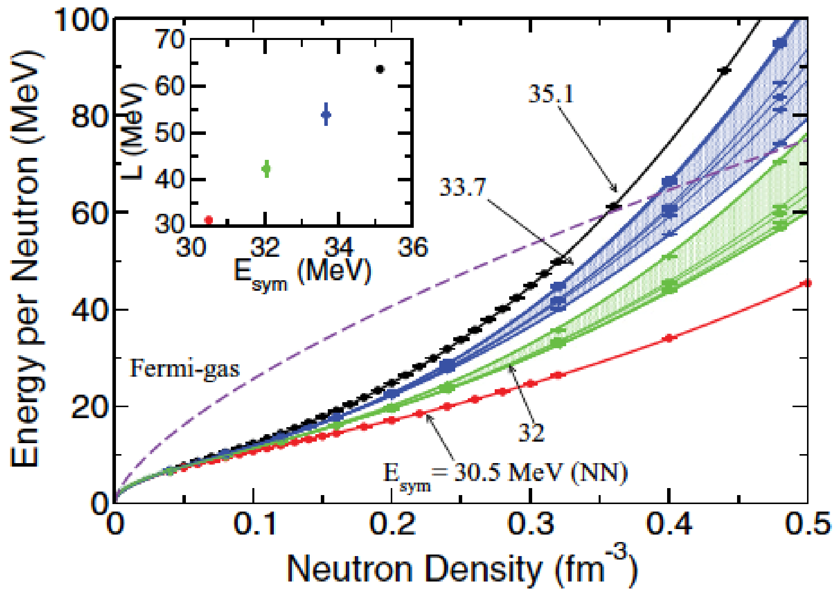

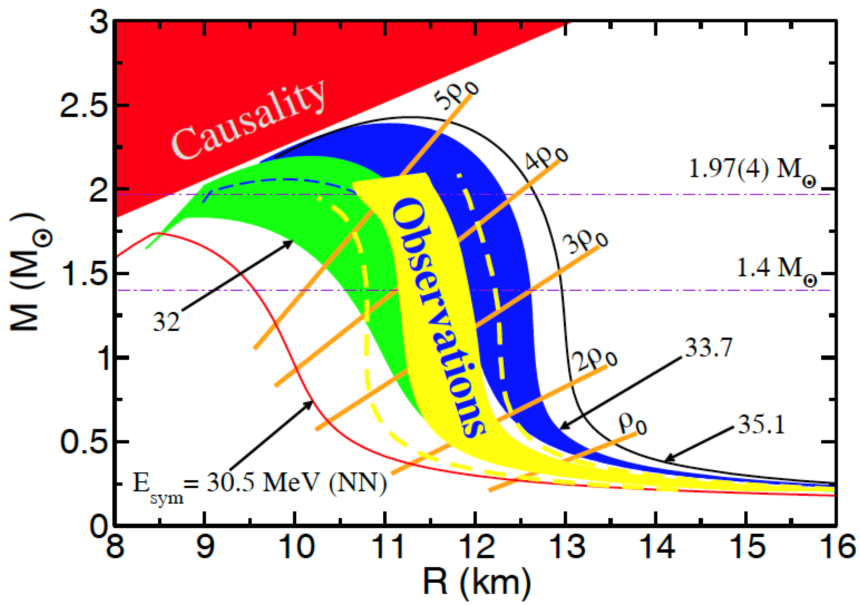

χEFT

I. Tews, K. Hebeler et al., PRL110, 032504(2013)

K. Hebeler et al., et al., EPJA50, 11 (2014)

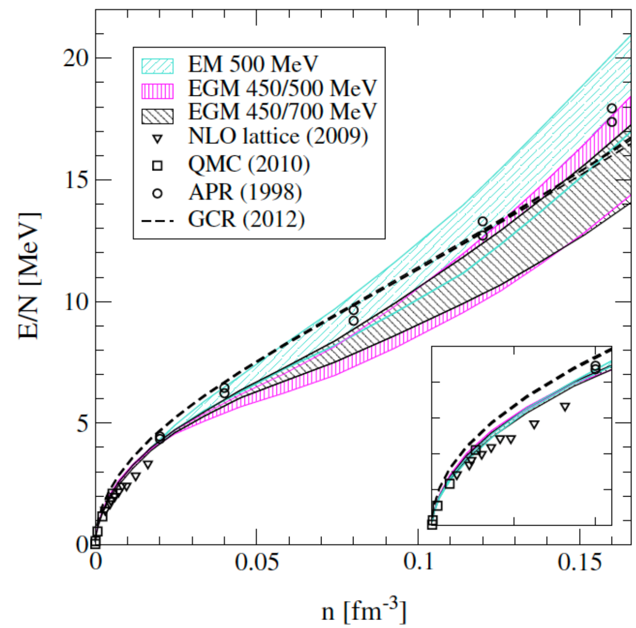

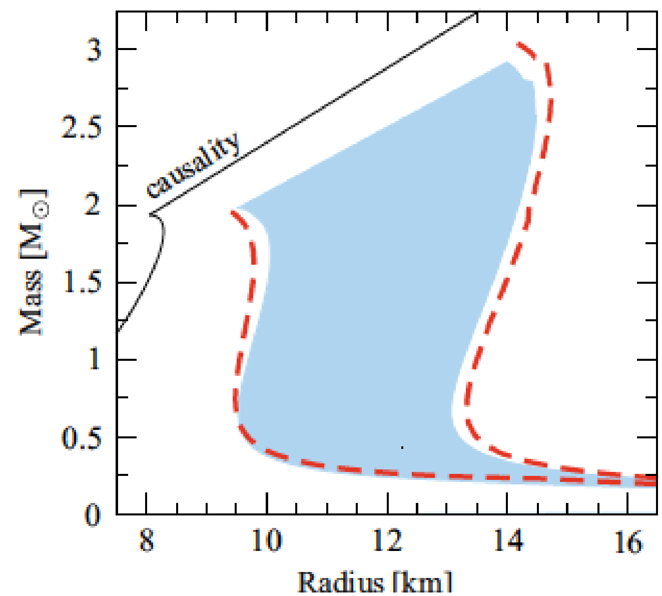

Relativistic Mean-field Calculation

F.T. Fattoyev et al., PRL120, 172702(2018)

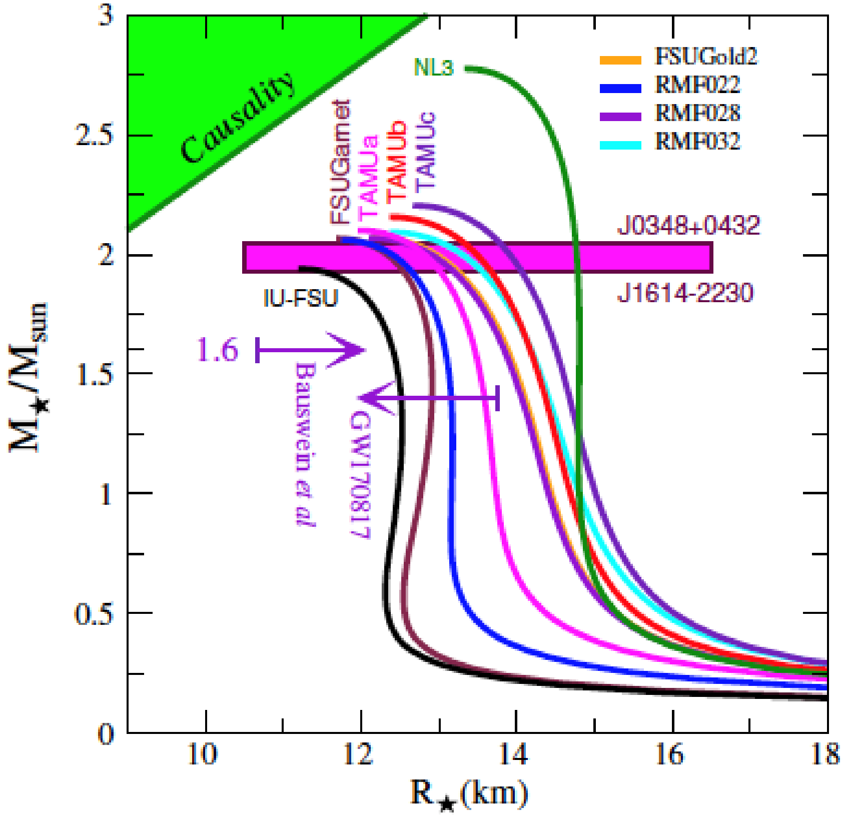

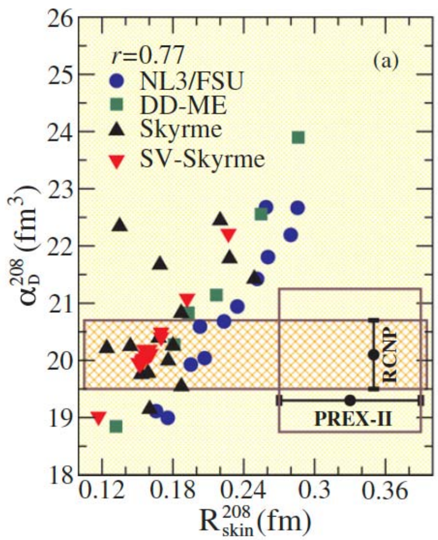

C.J. Horowitz et al., JPG41, 093001(2014)
S. Abrahamyan et al., PRL108, 112502 (2012).
PREX@JLab

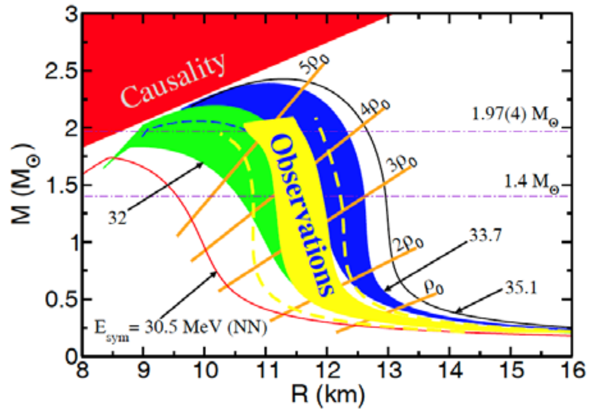

S. Gandolfi, J. Carlson et al.,
EPJA50, 10 (2014)
QMC 理論計算

A. Brown and A. Schwenk et al.,
PRC89, 011307R (2014).
Shell Model & 3NF

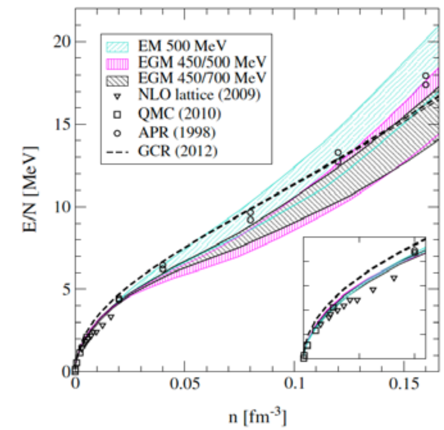

I. Tews, K. Hebeler et al.,
PRL110, 032504(2013)
χEFT 理論計算

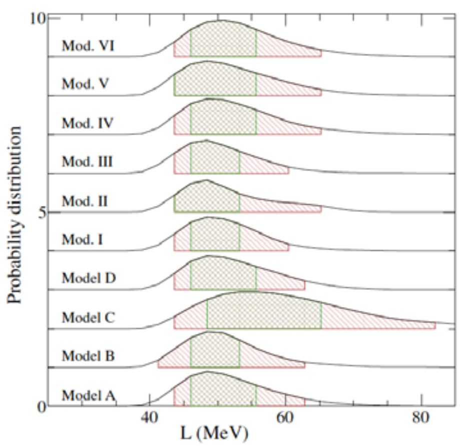

A.W. Steiner et al., AJL 765, L5(2013)
中性子星の観測の解析

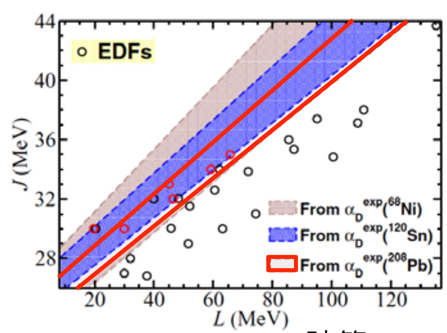

EDF & mean field 計算

X. Roca-Maza, G. Colo, N. Paar,
J. Piekarewicz et al., PRC92, 064304 (2015).
W. Nazarewicz, P.-G. Reinhard et al.,
EPJA50, 20 (2014)

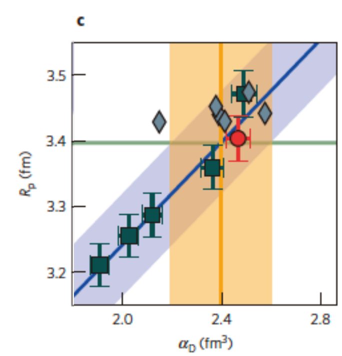

G. Hagen et al., Nature Phys.
12, 186 (2016)
Coupled Cluster 計算

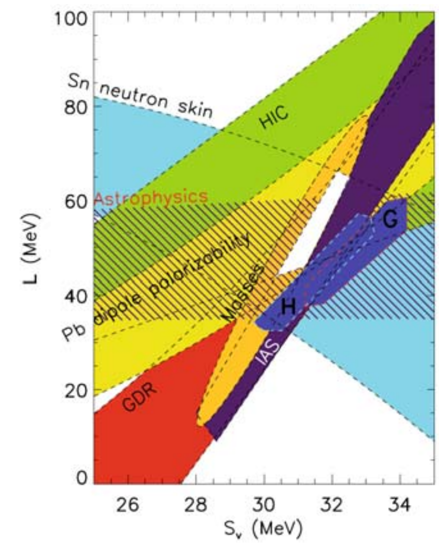

M. Lattimer et al., EPJA50, 40 (2014)
中性子星の物理

中性子星の半径と質量の関係

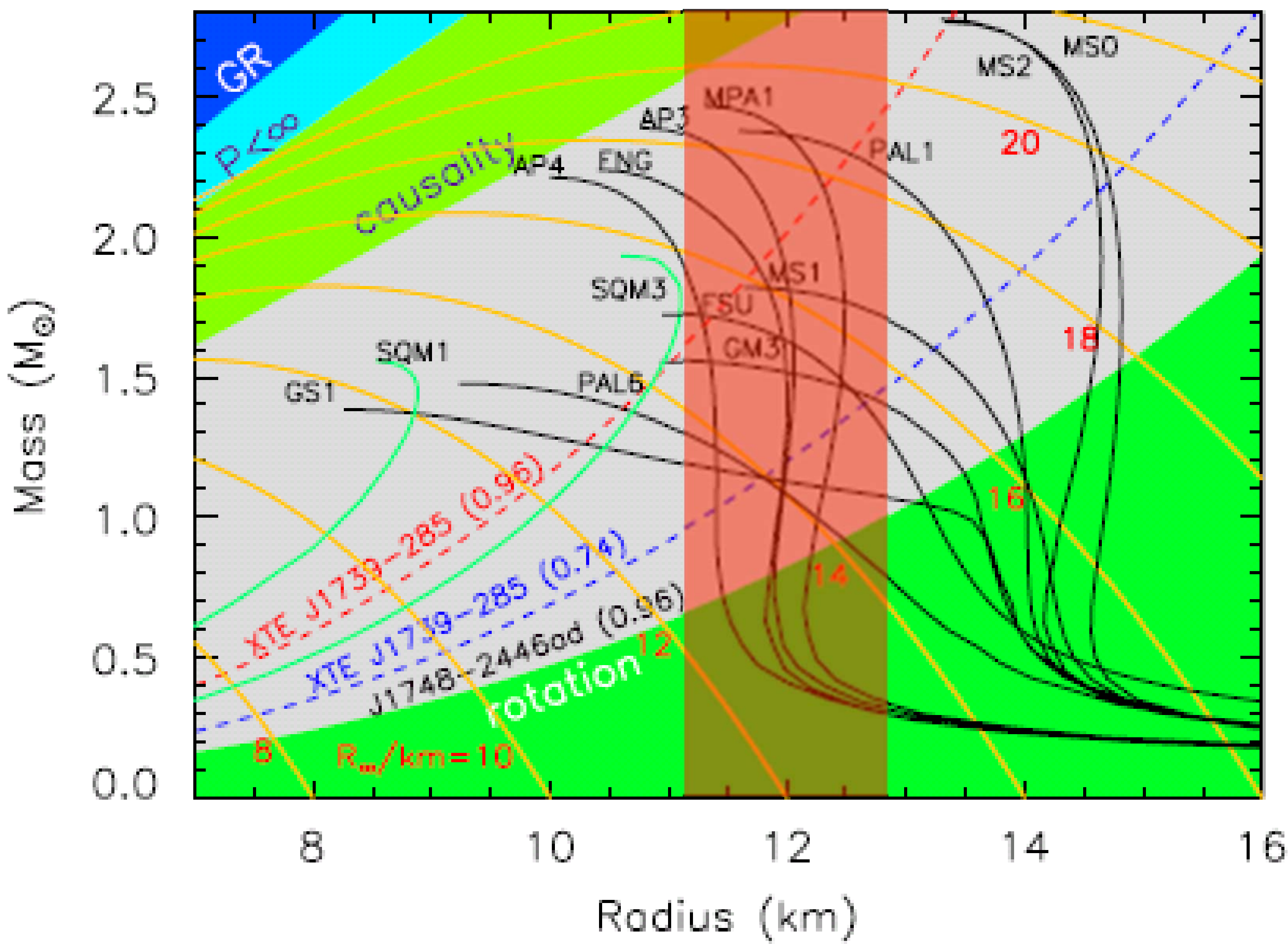

Neutron Star Merger GW170817

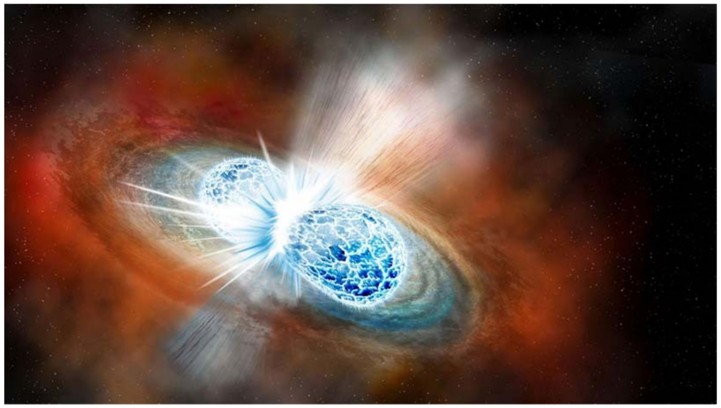

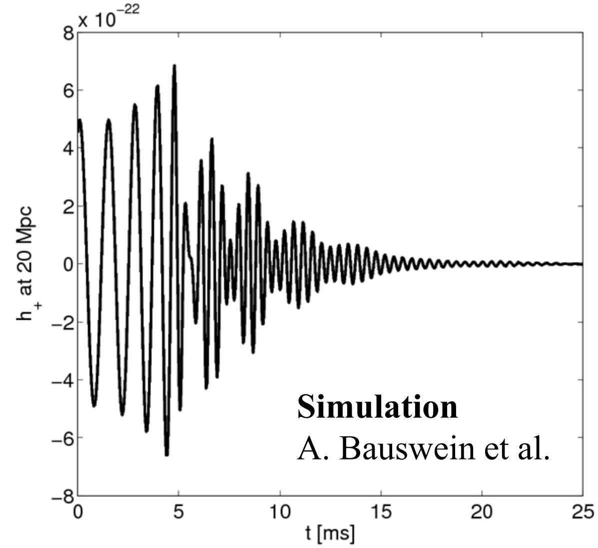

GW170817
PRL119, 161101(2017)

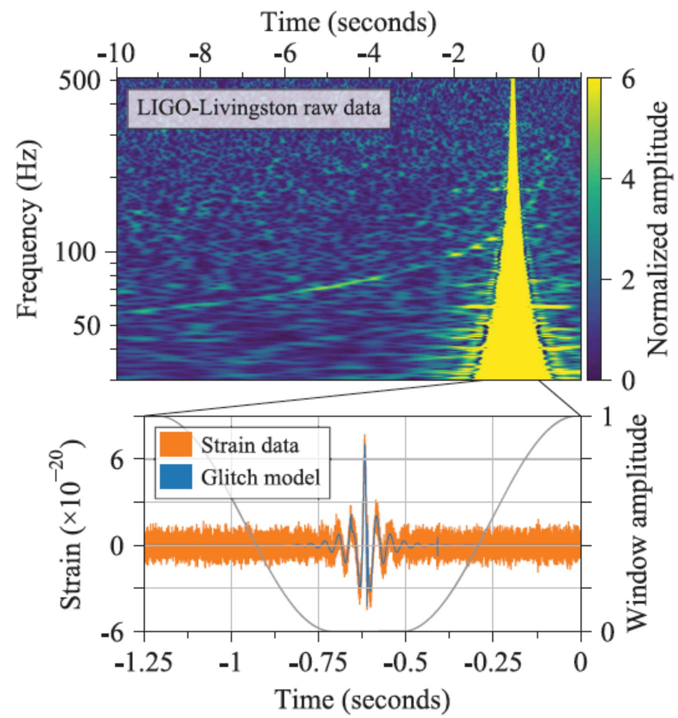

LIGO

Neutron Star Merger GW170817

PRL119, 161101(2017)

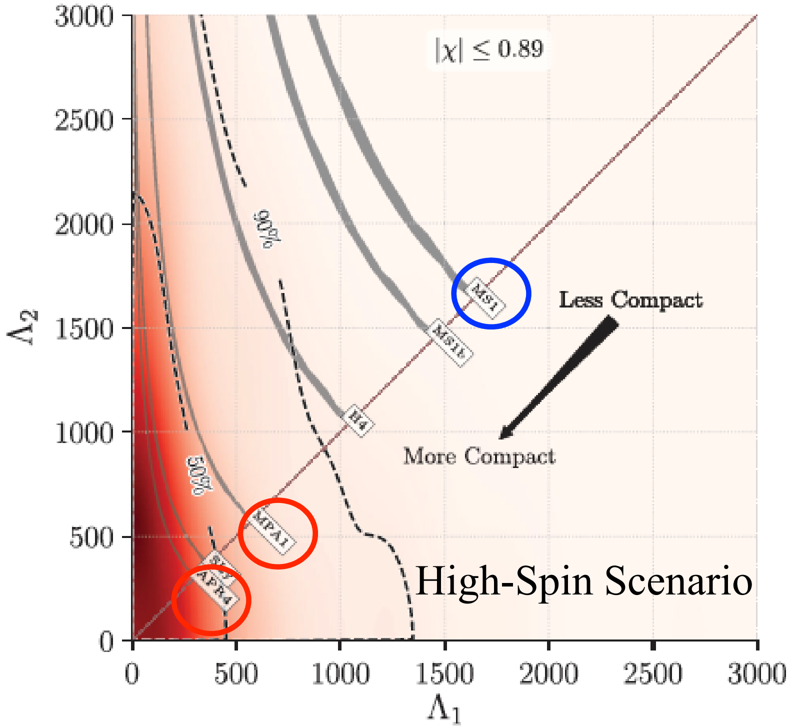

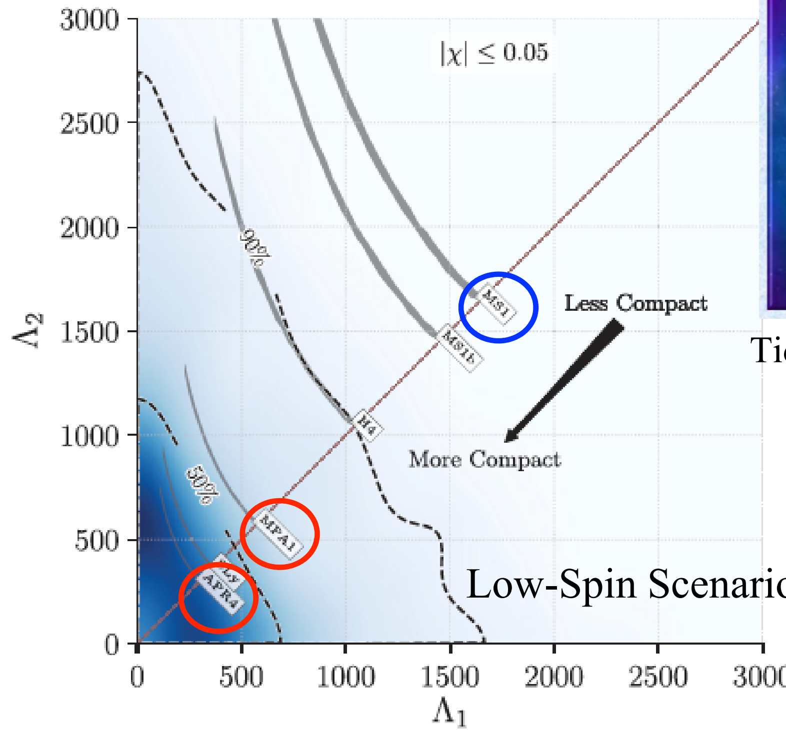

Tidal Deformatio

Tidal Deformation Parameters

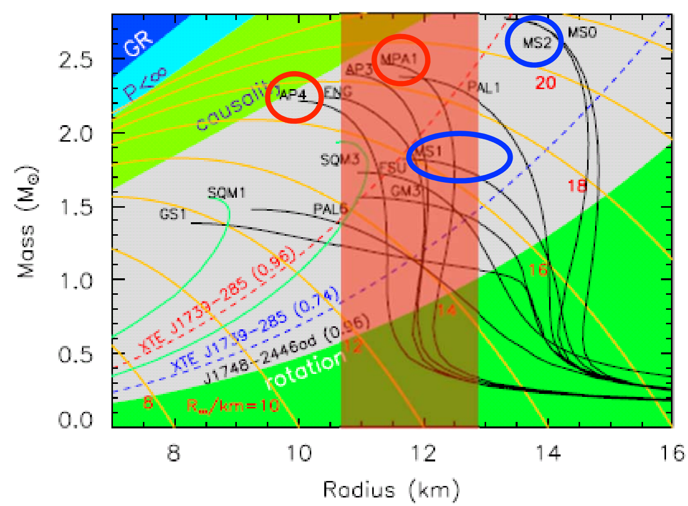

Constraints from the N-Star Merger GW

PRL119, 161101(2017)

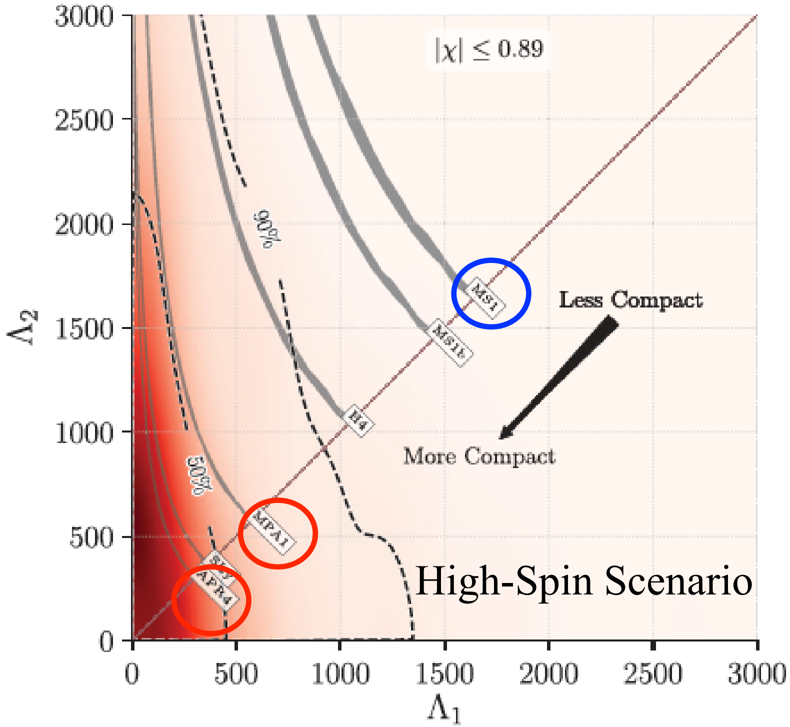

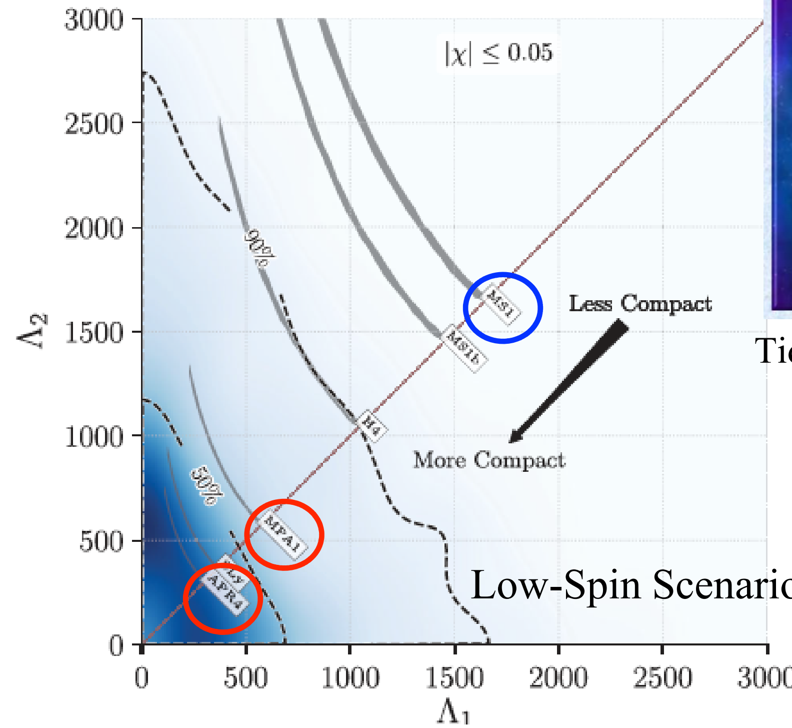

Tidal Deformatio

Tidal Deformation Parameters

N-Star Radius (1.4M$_\odot$)

$R^{1.4}$ < 13.76 km F.J. Fattoyev et al., PRL120, 172702(2018)

12.00 < $R^{1.4}$ < 13.45 km E.R. Most et al., PRL120, 261103(2018)

9.0 < $R^{1.4}$ < 13.6 km I. Tews et al., talk in the next session

N-star merger GW analysis is giving constraints on the nuclear EOS that are consistent with the study of atomic nuclei.

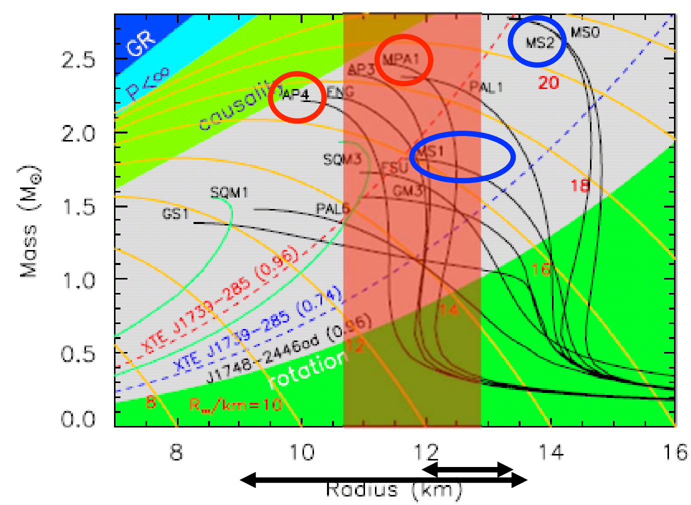

Summary

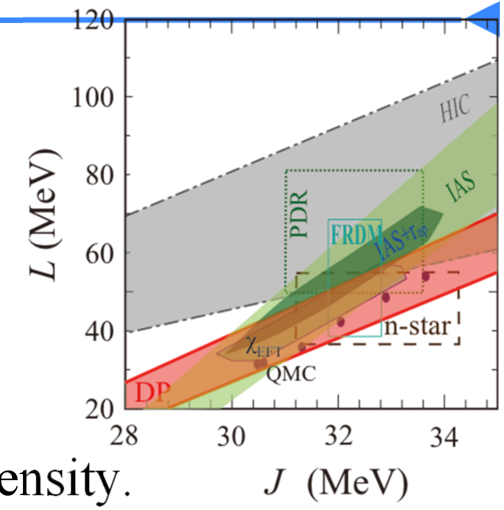

- The **electric dipole polarizability** (EDP) of ^{208}Pb, ^{120}Sn, and ^{48}Ca were measured precisely with Coulomb excitation by proton scattering.
- Constraint bands in the *J*-*L* plane has been determined that describes the **symmetry energy** at and below the saturation density.
- The result from the laboratory nuclear experiments is consistent with the information from GW170817. Further observation of N-Star merger GW's are anticipated.
- EoS at higher than the saturation density need to be studied by Heavy-Ion-Collision measurements in combination with neutron-star observations and neutron-star merger GW observations.
- Study of nuclear responses and giant resonances is important to study the nuclear matter properties: further possible extensions to radioactive nuclei, *e.g.* by (p,p') and (α,α') with an active target system.

Campaign experiments in Oct. – Dec. 2016 at RCNP

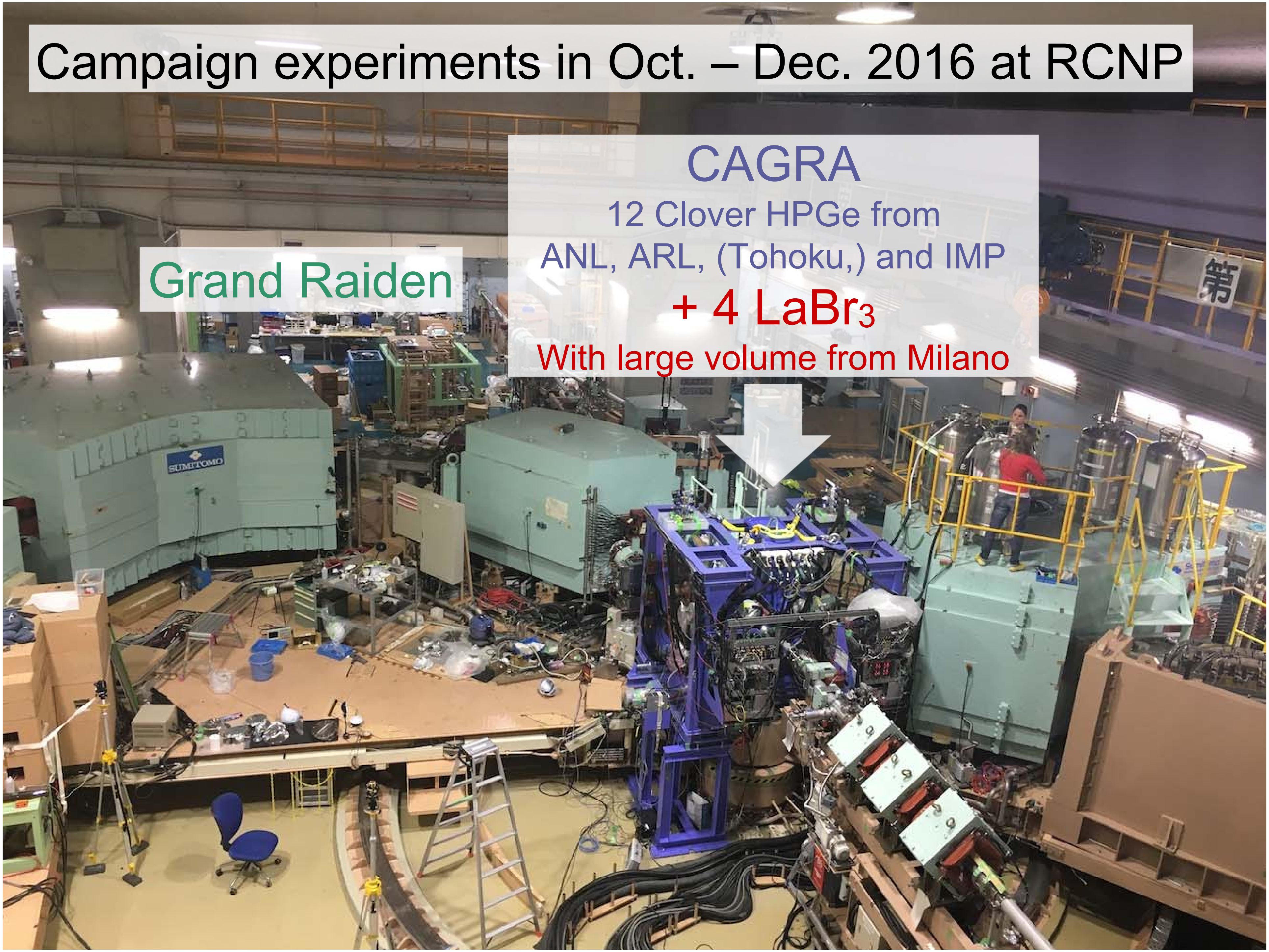

CAGRA+GR Campaign Exp. Oct-Dec 2016

1. **Structure of the PDR *1** (α,α'γ) and (p,p'γ) on ^{64}Ni, ^{90,94}Zr, ^{120,124}Sn, ^{206,208}Pb
2. Inelastic ν-nucleus response
3. Super-deformed states, high-spin states

*1 A. Bracco, F. Crespi, V. Derya, M.N. Harakeh, T. Hashimoto, C. Iwamoto, P. von Neumann-Cosel, N. Pietralla, D. Savran, A. Tamii, V. Werner, and A. Zilges *et al.*

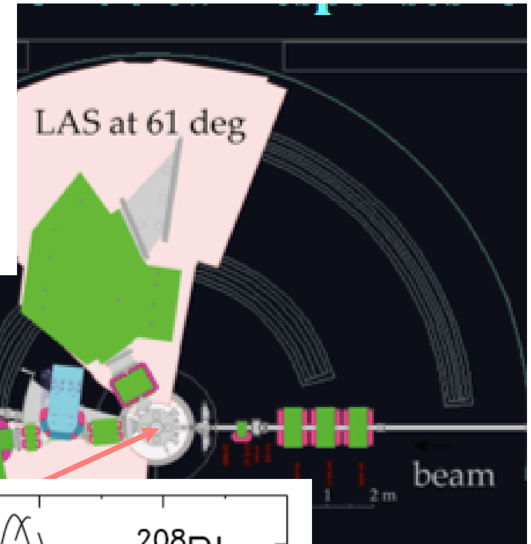

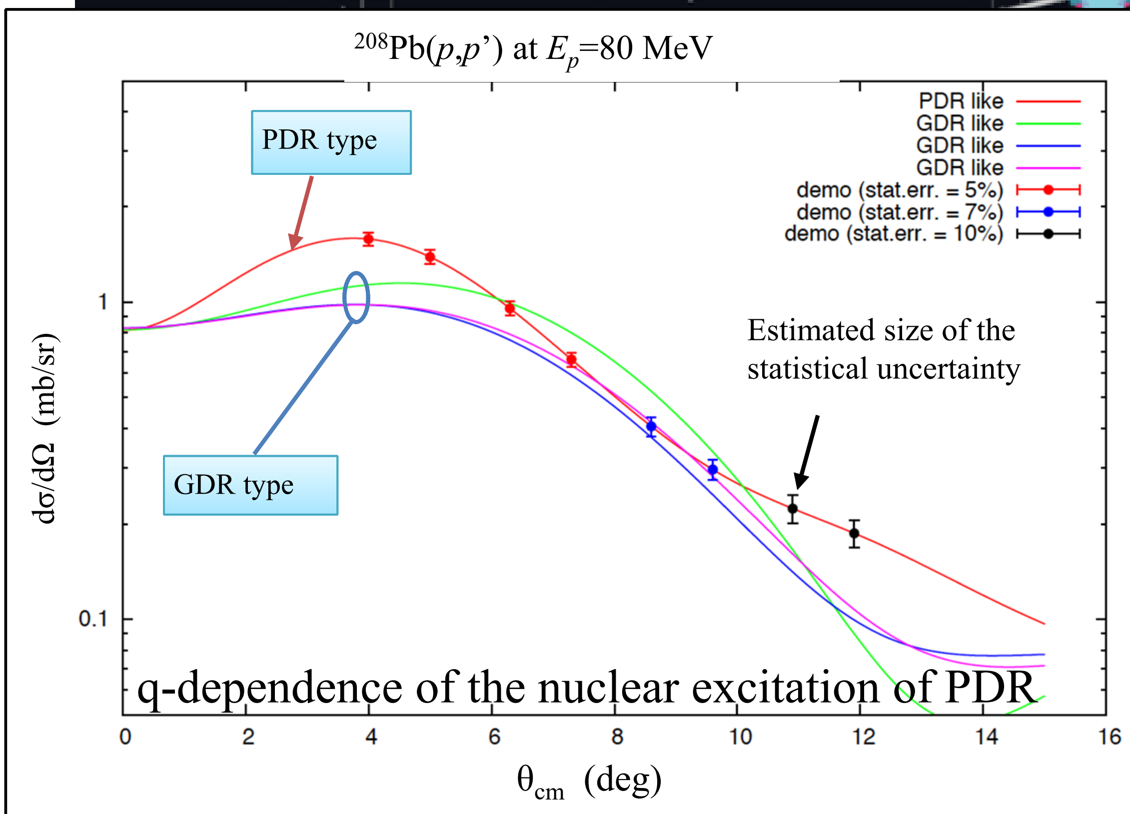

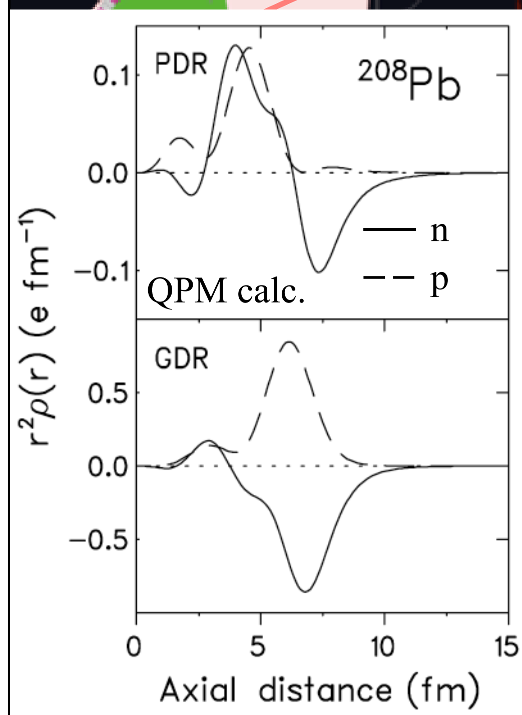

Fine Structure and Damping Mechanism of the GDR

Photo-absorption by ^{208}Pb

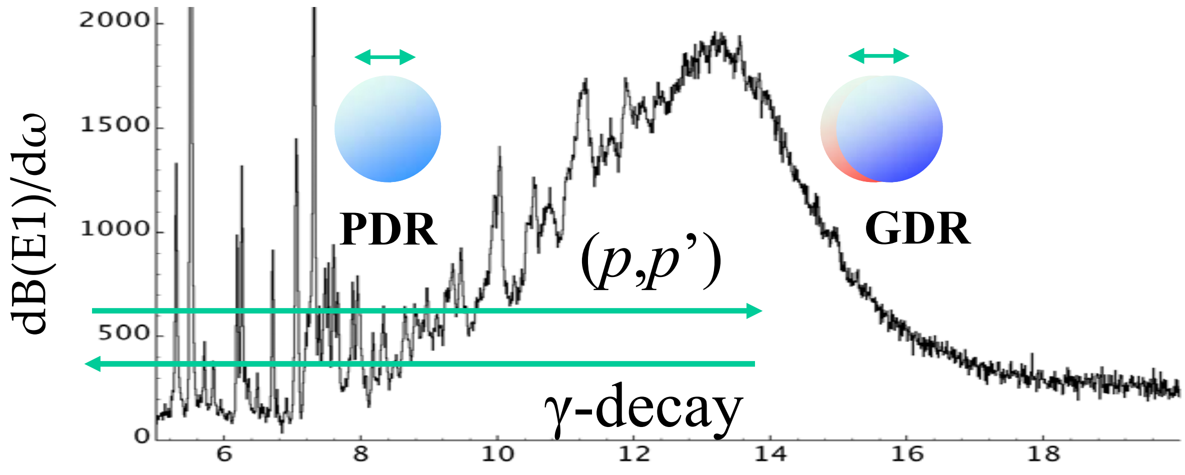

RCNP-E498

performed in July 2018

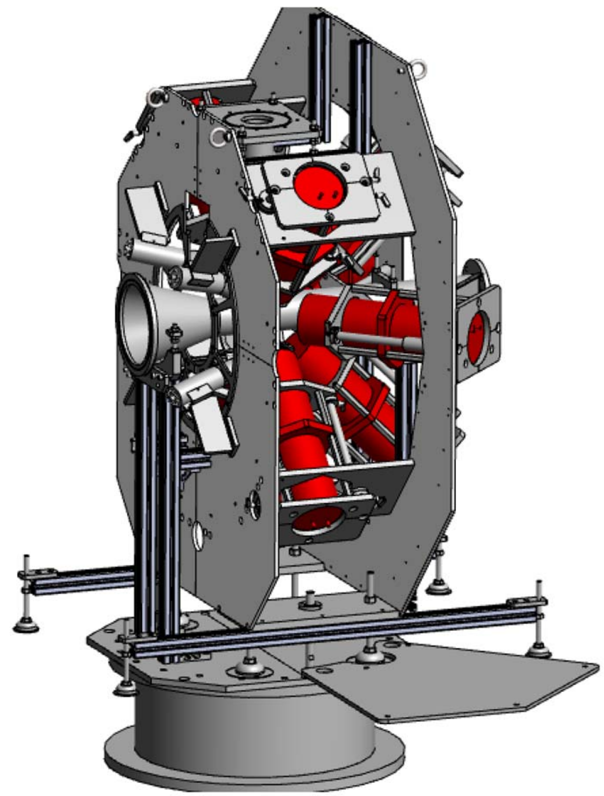

E498 set up with Large volume $LaBr_3$ detectors from Milano

Dumping mechanism of the giant resonances:

Gamma decay from GDR:

Summary

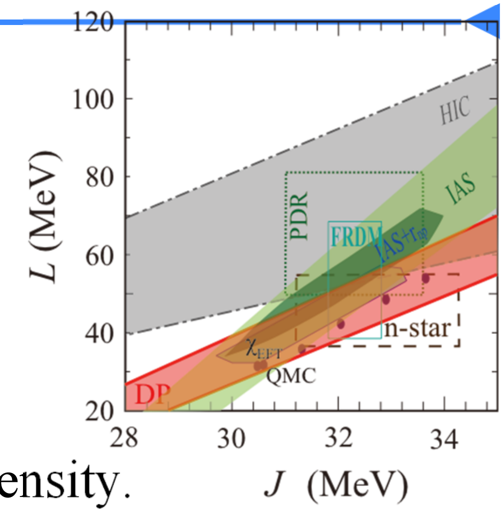

- The **electric dipole polarizability** (EDP) of ^{208}Pb, ^{120}Sn, and ^{48}Ca were measured precisely with Coulomb excitation by proton scattering.
- Constraint bands in the *J*-*L* plane has been determined that describes the **symmetry energy** at and below the saturation density.
- The result from the laboratory nuclear experiments is consistent with the information from GW170817. Further observation of N-Star merger GW's are anticipated.
- EoS at higher than the saturation density need to be studied by Heavy-Ion-Collision measurements in combination with neutron-star observations and neutron-star merger GW observations.
- Study of nuclear responses and giant resonances is important to study the nuclear matter properties: further possible extensions to radioactive nuclei, *e.g.* by (p,p') and (α,α'), with an active target system.

^{208}Pb RCNP-282 Collaboration

RCNP, Osaka University
A. Tamii, H. Matsubara, H. Fujita, K. Hatanaka,
H. Sakaguchi Y. Tameshige, M. Yosoi and J. Zenihiro

IKP, TU-Darmstadt
P. von Neumann-Cosel, A-M. Heilmann,
Y. Kalmykov, I. Poltoratska, V.Yu. Ponomarev,
A. Richter and J. Wambach

KVI, Univ. of Groningen
T. Adachi and L.A. Popescu

IFIC-CSIC, Univ. of Valencia
B. Rubio and A.B. Perez-Cerdan

Sch. of Science Univ. of Witwatersrand
J. Carter and H. Fujita

iThemba LABS
F.D. Smit

Texas A&M Commerce
C.A. Bertulani

GSI
E. Litivinova

Dep. of Phys., Osaka University
Y. Fujita

Dep. of Phys., Kyoto University
T. Kawabata

CNS, Univ. of Tokyo
K. Nakanishi,
Y. Shimizu and Y. Sasamoto

CYRIC, Tohoku University
M. Itoh and Y. Sakemi

Dep. of Phys., Kyushu University
M. Dozono

Dep. of Phys., Niigata University
Y. Shimbara

^{120}Sn RCNP-316 Collaboration

T. Hashimoto[†], A. M. Krumbholz[1], A. Tamii[2], P. von Neumann-Cosel[1], N. Aoi[2], O. Burda[2], J. Carter[3], M. Chernykh[2], M. Dozono[4], H. Fujita[2], Y. Fujita[2], K. Hatanaka[2], E. Ideguchi[2], N. T. Khai[5], C. Iwamoto[2], T. Kawabata[6], D. Martin[1], K. Miki[1], R. Neveling[7], H. J. Ong[2], I. Poltoratska[1], P.-G. Reinhard[8], A. Richter[1], F.D. Smit[6], H. Sakaguchi[2,4], Y. Shimbara[9], Y. Shimizu[4], T. Suzuki[2], M. Yosoi[1], J. Zenihiro[4], K. Zimmer[1]

[†]Institute for Basic Science, Korea
[1]IKP, Technische Universität Darmstadt, Germany
[2]RCNP, Osaka University, Japan
[3]Wits University, South Africa
[4]RIKEN, Japan
[5]Institute for Nuclear Science and Technology (INST), Vietnam
[6]Kyoto University, Japan
[7]iThemba LABs, South Africa
[8]Institut Theoretical Physik II, Universität Erlanen-Nürnberg, Germany
[9]CYRIC, Tohoku University, Japan

Collaboration ^{48}Ca

Experiment: Darmstadt-Osaka
Theory: Darmstadt-Tennessee-TRIUMF

S. Bacca (TRIUMF)
S. Bassauer (TUD)
J. Birkhan (Darmstadt)
G. Hagen (ORNL)
H. Matsubara (RCNP)
M. Miorelli (TRIUMF)
P. von Neumann-Cosel (TUD)
T. Papenbrock (U Tennessee)
N. Pietralla (TUD)
A. Richter (TUD)
A. Schwenk (TUD)
A. Tamii (RCNP)

CAGRA+GR Campaign Exps. in Oct-Dec 2016

Participants from abroad

Mike Carpenter	ANL
Agnieszka Czeszumska	Berkley
Dimiter Balabanski	ELI-NP
Shumpei Noji	FRIB
Denis Savran	GSI
Maria Kmiecik	IFJ-PAN, Krakow
Mateusz Krzysiek	IFJ-PAN, Krakow
Michal Lukasz Ciemala	IFJ-PAN, Krakow
Adam Maj	IFJ-PAN, Krakow
Barbara Wasilewska	IFJ-PAN, Krakow
Sandrine Courtin	IPHC – CNRS, Strasbourg
Guillaume Fruet	IPHC – CNRS, Strasbourg
Daniele Montanari	IPHC – CNRS, Strasbourg
Simon Glynn Pickstone	Koeln
Mark Spieker	Koeln
Julius Wilhelmy	Koeln
Muhsin Harakeh	KVI
Nives Blasi	Univ. Milano, INFN
Angela Bracco	Univ. Milano, INFN
Franco Camera	Univ. Milano, INFN
Fabio Crespi	Univ. Milano, INFN
Oliver Wieland	Univ. Milano, INFN
Daniel Basin	NSCL
Juan Carlos Zamora Cardona	NSCL
Samuel Israel Lipschutz	NSCL
Jaclyn Marie Schmitt	NSCL
Chris Sullivan	NSCL
Rachel Charlotte Taverner Titus	NSCL
Remco Godfried Theo Zegers	NSCL
Carol Guess	Swarthmore College
Emily Hudson	Swarthmore College
Charles Kacir	Swarthmore College
Sergej Bassauer	TU-Darmstadt
Tobias Klaus	TU-Darmstadt
Peter von Neumann-Cosel	TU-Darmstadt
Gerhart Steinhilber	TU-Darmstadt
Volker Werner	TU-Darmstadt
Lindsay Donaldson	Univ. Witwatersrand
Adam Sebastian Brown	Univ. York
David Jenkins	Univ. York
Paul John Davies	Univ. York
Luke Morris	Univ. York

Participants from Japan

Nori Aoi	RCNP
Atsushi Tamii	RCNP
Eiji Ideguchi	RCNP
Yoshitaka Fujita	RCNP
Hirohiko Fujita	RCNP
Ong Hooi Jin	RCNP
Johann Isaak	RCNP
Nobuyuki Kobayashi	RCNP
Fang Yongde	RCNP
Kumar Raju	RCNP
Satoshi Adachi	RCNP
Azusa Inoue	RCNP
Tetsuya Yamamoto	RCNP
Yasutaka Yamamoto	RCNP
Hang Thi Ha	RCNP
Takeshi Koike	Tohoku Univ.
Yuni Watanabe	Tokyo Univ.
Chiriro Iwamoto	CNS

Contributors in commissioning experiments.

Calem Hoffman	ANL
Satoru Terashima	Beihang Univ.
Lei Yu	Beihang Univ.
Motonobu Takaki	CNS
Masatoshi Itoh	CYRIC
Takashi Hashimoto	IBS
Hiroyuki Fujioka	Kyoto Univ.
Takahiro Kawabata	Kyoto Univ.
Noritsugu Nakatsuka	Kyoto Univ.
Akane Sakaura	Kyoto Univ.
Yassid Ayyad	LBNL
Ou Iwa	Okayama Univ.
Makoto Sakuda	Okayama Univ.
Atsuko Odahara	Osaka Univ.
Shinnosuke Yoshida	Osaka Univ.
Phaik Ying Chan	RCNP
Guillaume Gey	RCNP
Gaku Isago	RCNP
Takeshi Ito	RCNP
Masaki Miura	RCNP
Hirotaka Suzuki	RCNP
Tomokazu Suzuki	RCNP
Mana Tanaka	RCNP
Hidetada Baba	RIKEN
Natsumi Ichige	Tohoku Univ.
Kenjiro Miki	Tohoku Univ.
Hirokazu Tamura	Tohoku Univ.
Tomoyuki Ozaki	Tokyo Inst. Tech.
Yasuhiro Togano	Tokyo Inst. Tech.

Technical Staff

Hidetomo P. Yoshida	RCNP
Keiichi Nagayama	RCNP
Michio Uraki	RCNP

We gratefully appreciate the support from RCNP and the accelerator group.

Thank you

for your attention

Backup Slides

Dipole Polarizability of ^{48}Ca

where the EDF and ab-initio calculations meet

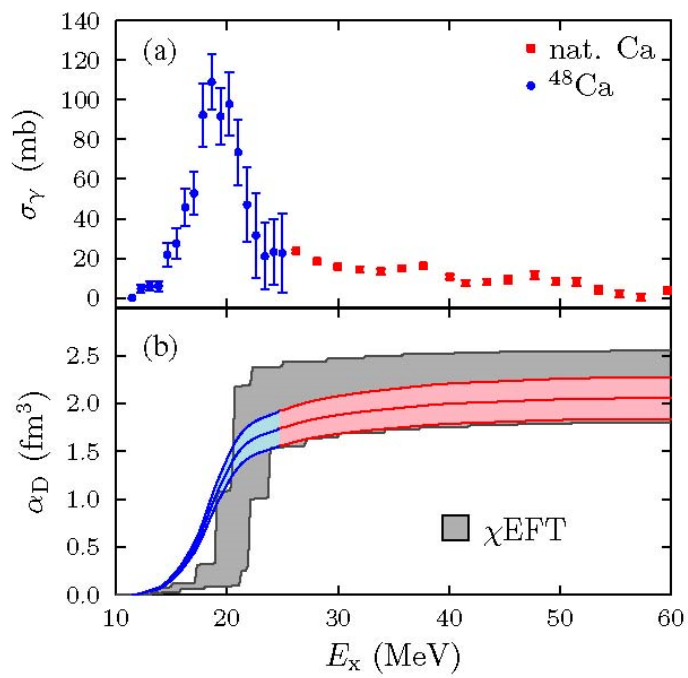

J. Birkhan et al., PRL118_252501(2017)

Theory: Darmstadt-Tennessee-TRIUMF

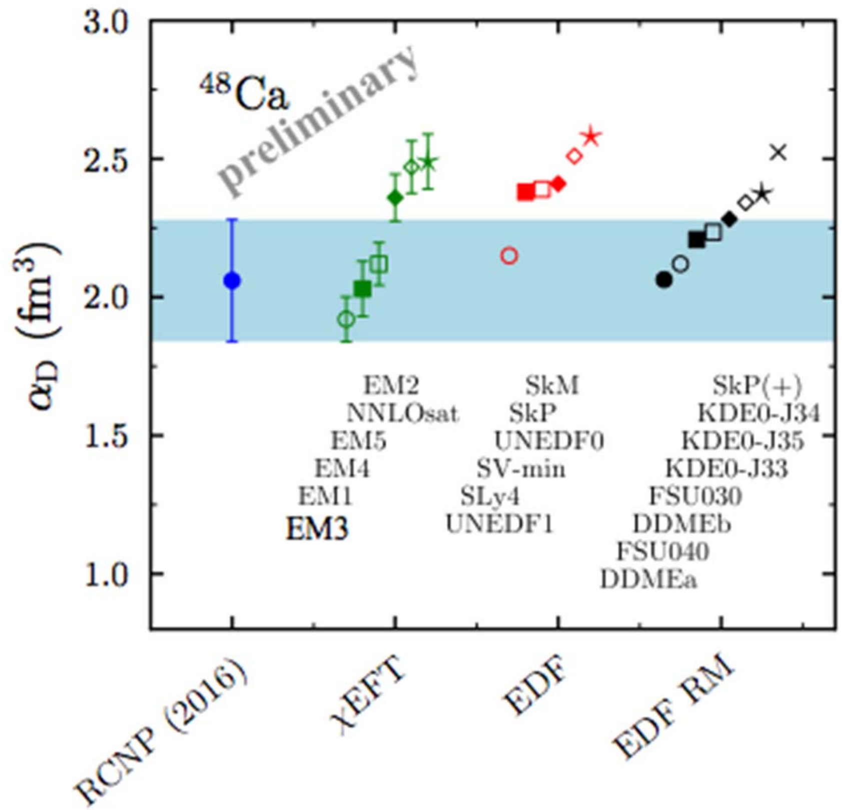

A dedicated new measurement is approved for a smaller uncertainty.

Constraints on *J* and *L*

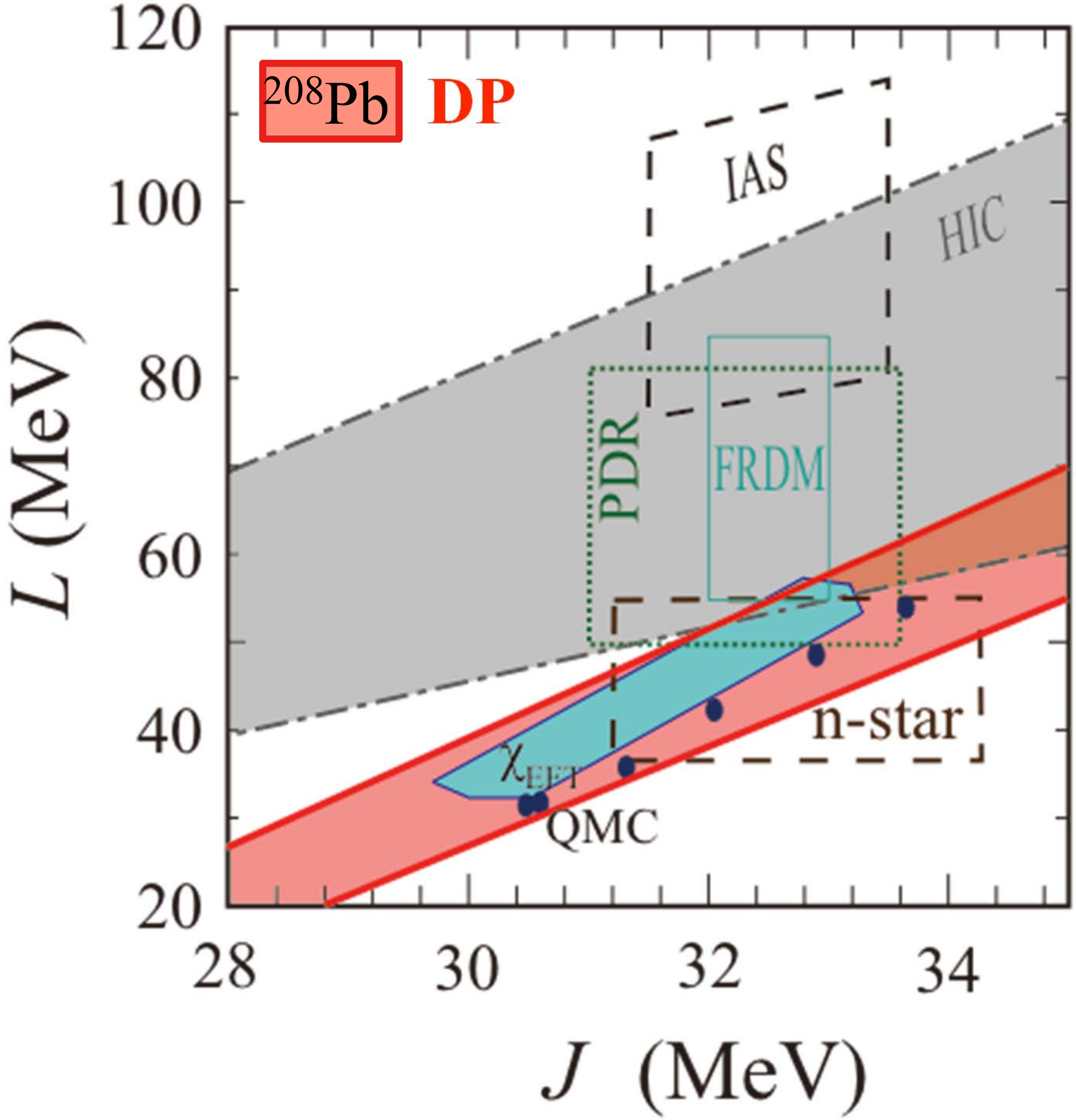

Tsang PRC2012

HIC: Heavy Ion Collision Analysis
Tsang PRL2009

IAS: Isobaric Analog State Energy
Danielewicz&Lee NPA2009

PDR: Pygmy Dipole Resonance in ^{132}Sn, ^{68}Ni, Carbone PRC2010

FRDM: Finite Range Droplet Model
Moller PRL2012

n-star: Quiescent Low-Mass X-ray Binaries, Stainer PRL2012

χ_{EFT}: Chiral Effective Field Theory, Tews PRL2013

QMC: Quantum Monte-Carlo Calc.
Gandolfi, EPJA50, 10(2014).

DP: Dipole Polarizability
^{208}Pb AT PRL2011

IAS: Isobaric Analog State Energy
Danielewicz&Lee NPA2014

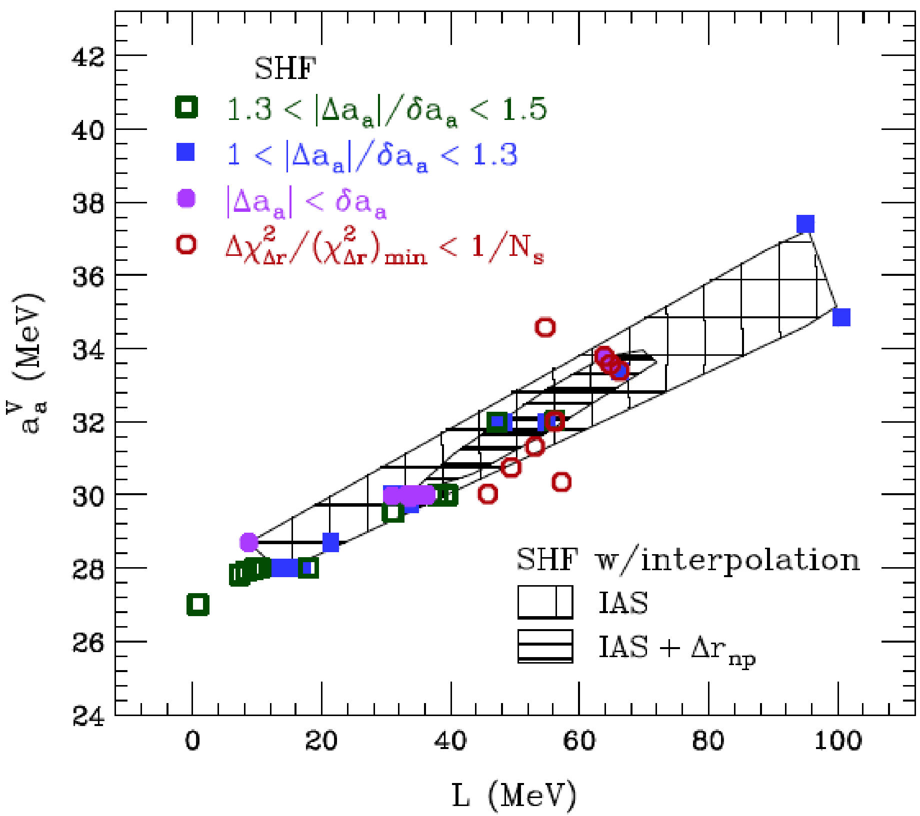

quoted neutron-skin studies

Nucleus	Reference	Data source	Δr_{np} [fm]	Δr_{np}^{GF} [fm]
^{48}Ca	Friedman [93]	pionic atoms	0.13 ± 0.06	
	Gils et al. [94]	elastic α scattering	0.175 ± 0.050	
	Ray [95]	elastic $\bar{p}$ scattering	0.229 ± 0.050	
	Clark et al. [96]	elastic p scattering	0.103 ± 0.040	
	Shlomo et al. [97]	elastic p scattering	0.10 ± 0.03	
	Gibbs et al. [98]	elastic π scattering	0.11 ± 0.04	
		combined results	0.129 ± 0.053*	0.218 ± 0.015
^{50}Ti	Gils et al. [94]	elastic α scattering	0.031 ± 0.040	0.133 ± 0.011
^{64}Ni	Ray [95]	elastic $\bar{p}$ scattering	0.167 ± 0.050	0.102 ± 0.015
^{116}Sn	Ray [95]	elastic $\bar{p}$ scattering	0.146 ± 0.050	0.103 ± 0.015
^{124}Sn	Ray [95]	elastic $\bar{p}$ scattering	0.252 ± 0.050	0.184 ± 0.021
^{204}Pb	Zenihiro et al. [99]	elastic p scattering	0.178 ± 0.059	0.161 ± 0.024
^{206}Pb	Zenihiro et al. [99]	elastic p scattering	0.180 ± 0.064	
	Starodubsky et al. [100]	elastic p scattering	0.181 ± 0.045	
		combined results	0.181 ± 0.037	0.172 ± 0.024
^{207}Pb	Starodubsky et al. [100]	elastic p scattering	0.186 ± 0.041	0.178 ± 0.024
^{208}Pb	Starodubsky et al. [100]	elastic p scattering	0.197 ± 0.042	
	Ray [95]	elastic $\bar{p}$ scattering	0.16 ± 0.05	
	Clark et al. [96]	elastic p scattering	0.119 ± 0.045	
	Zenihiro et al. [99]	elastic p scattering	0.211 ± 0.063	
	Friedman [93]	elastic π^+ scattering	0.11 ± 0.06	
	Friedman [93]	pionic atoms	0.15 ± 0.08	
		combined results	0.159 ± 0.041*	0.179 ± 0.023

any average effects of asymmetry on the reactions competing with a variety of physical effects subject to modeling uncertainties. In this paper we attempt to learn about the average effects of neutron–proton asymmetry on nuclear energies, exploiting excitation energies to isobaric analog states and to reach the conclusions in as model-independent manner as possible. Our early efforts in this direction have been reported in [1–3]. As we progress, we find that we need to reassess our strategy.

Constraints on *J* and *L*

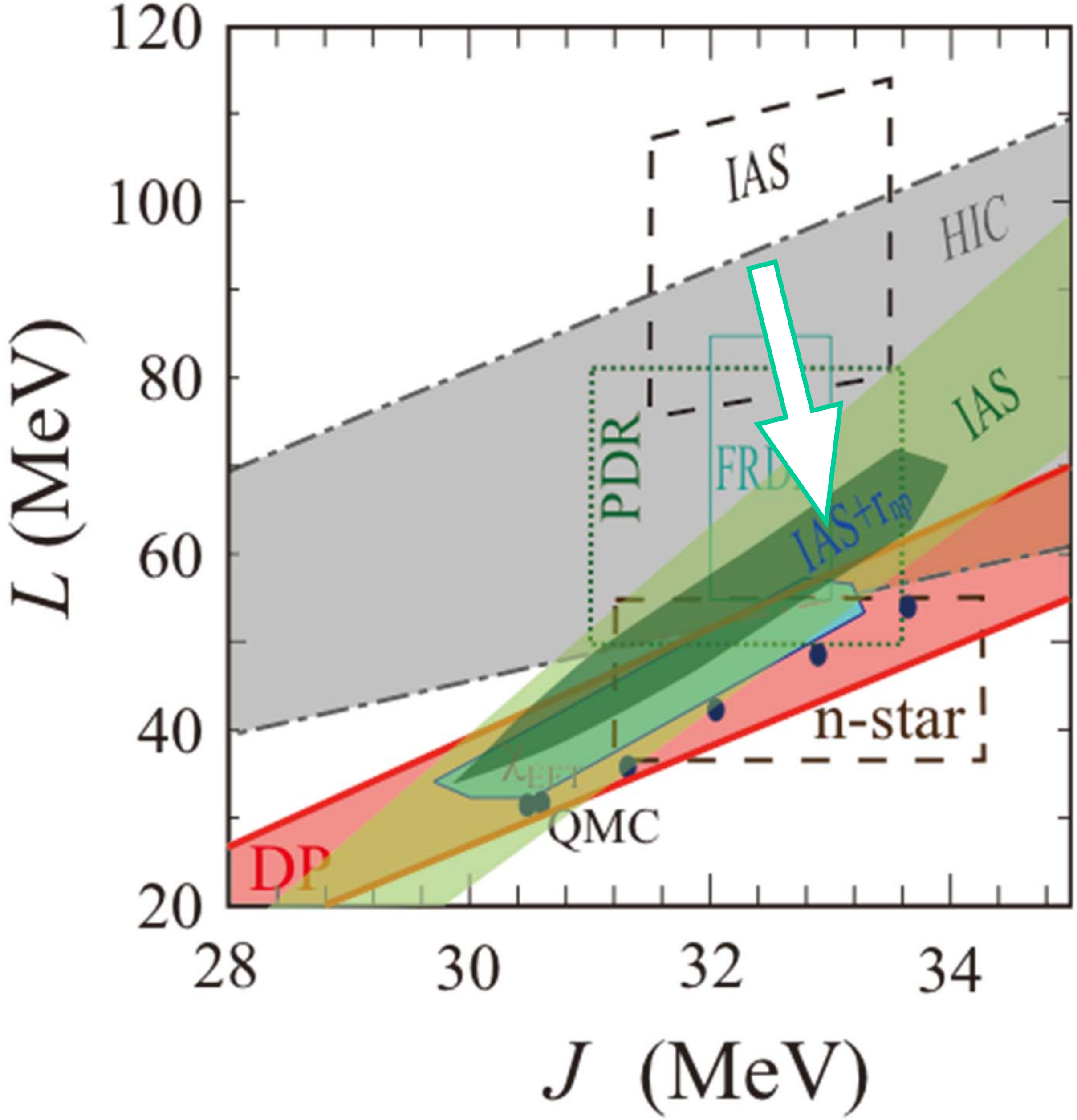

Tsang PRC2012

HIC: Heavy Ion Collision Analysis
Tsang PRL2009

IAS: Isobaric Analog State Energy
Danielewicz&Lee **NPA2009→2014**

PDR: Pygmy Dipole Resonance in
^{132}Sn, ^{68}Ni, Carbone PRC2010

FRDM: Finite Range Droplet Model
Moller PRL2012

n-star: Quiescent Low-Mass X-ray
Binaries, Stainer PRL2012

χEFT: Chiral Effective Field Theory,
Tews PRL2013

QMC: Quantum Monte-Carlo Calc.
Gandolfi, EPJA50, 10(2014).

DP: Dipole Polarizability
^{208}Pb AT PRL2011

Constraints on J and L

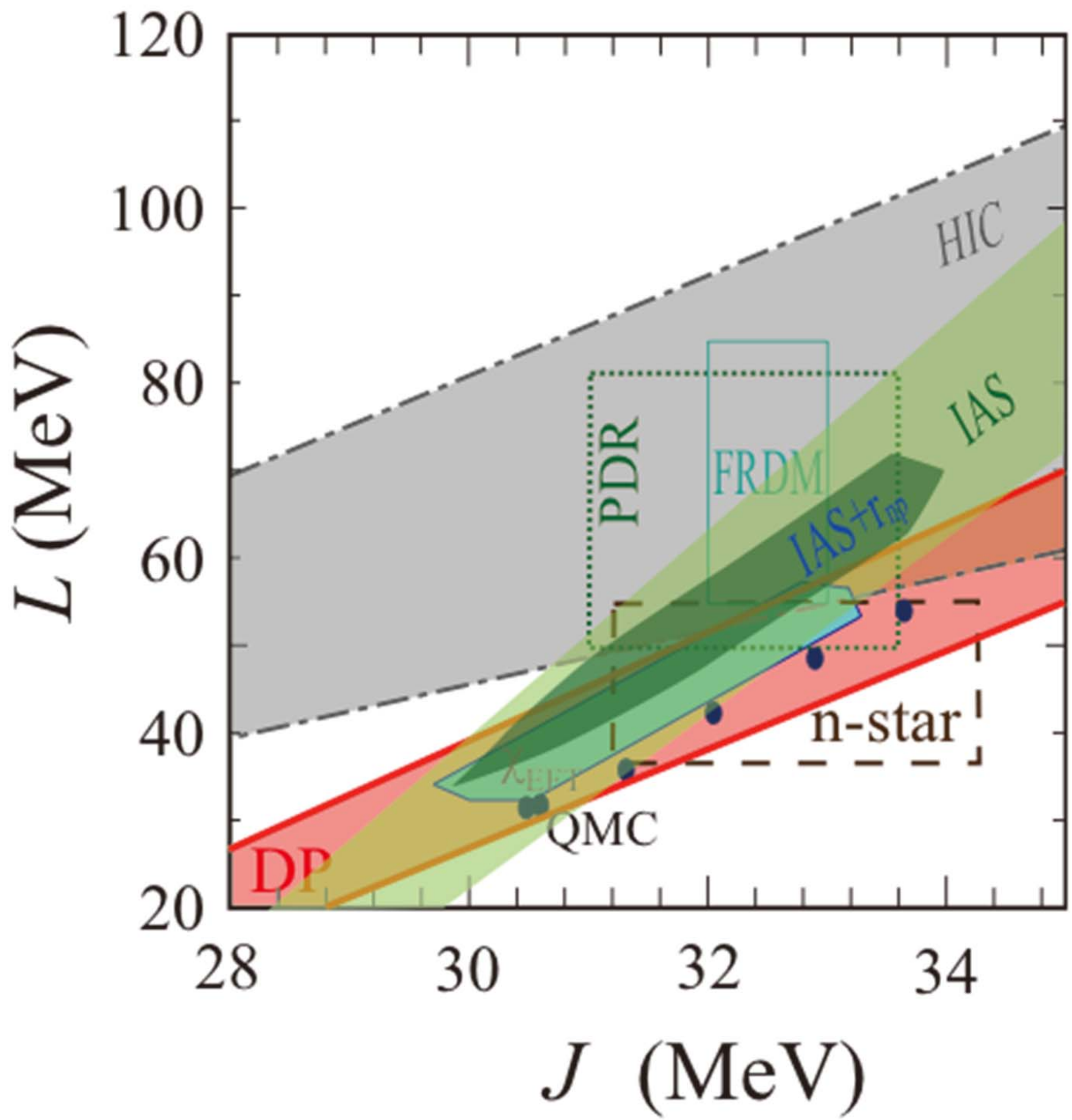

Tsang PRC2012

HIC: Heavy Ion Collision Analysis
Tsang PRL2009

IAS: Isobaric Analog State Energy
Danielewicz&Lee NPA2014

PDR: Pygmy Dipole Resonance in
^{132}Sn, ^{68}Ni, Carbone PRC2010

FRDM: Finite Range Droplet Model
Moller PRL2012

n-star: Quiescent Low-Mass X-ray
Binaries, Stainer PRL2012

χ_{EFT}: Chiral Effective Field Theory,
Tews PRL2013

QMC: Quantum Monte-Carlo Calc.
Gandolfi, EPJA50, 10(2014).

DP: Dipole Polarizability
^{208}Pb AT PRL2011

LA-UR-16-26401 Sagawa and Moller

The optimal values of the asymmetry variables J and L that we obtained from the mass model FRDM (2012) study are

$$J = 32.3 \pm 0.5 \ \text{MeV}$$
$$L = 53.5 \pm 15 \ \text{MeV}$$

with the minimum rms deviation of σ <560 keV as shown in Fig. 2. The above optimal L value is somewhat smaller than the value in Ref. [3], because we have implemented a more accurate calculation of the zero-point fluctuation effect, see [2] for more details.

FRDM: Finite Range Droplet Model
Moeller ADNTD2016

Constraints on *J* and *L*

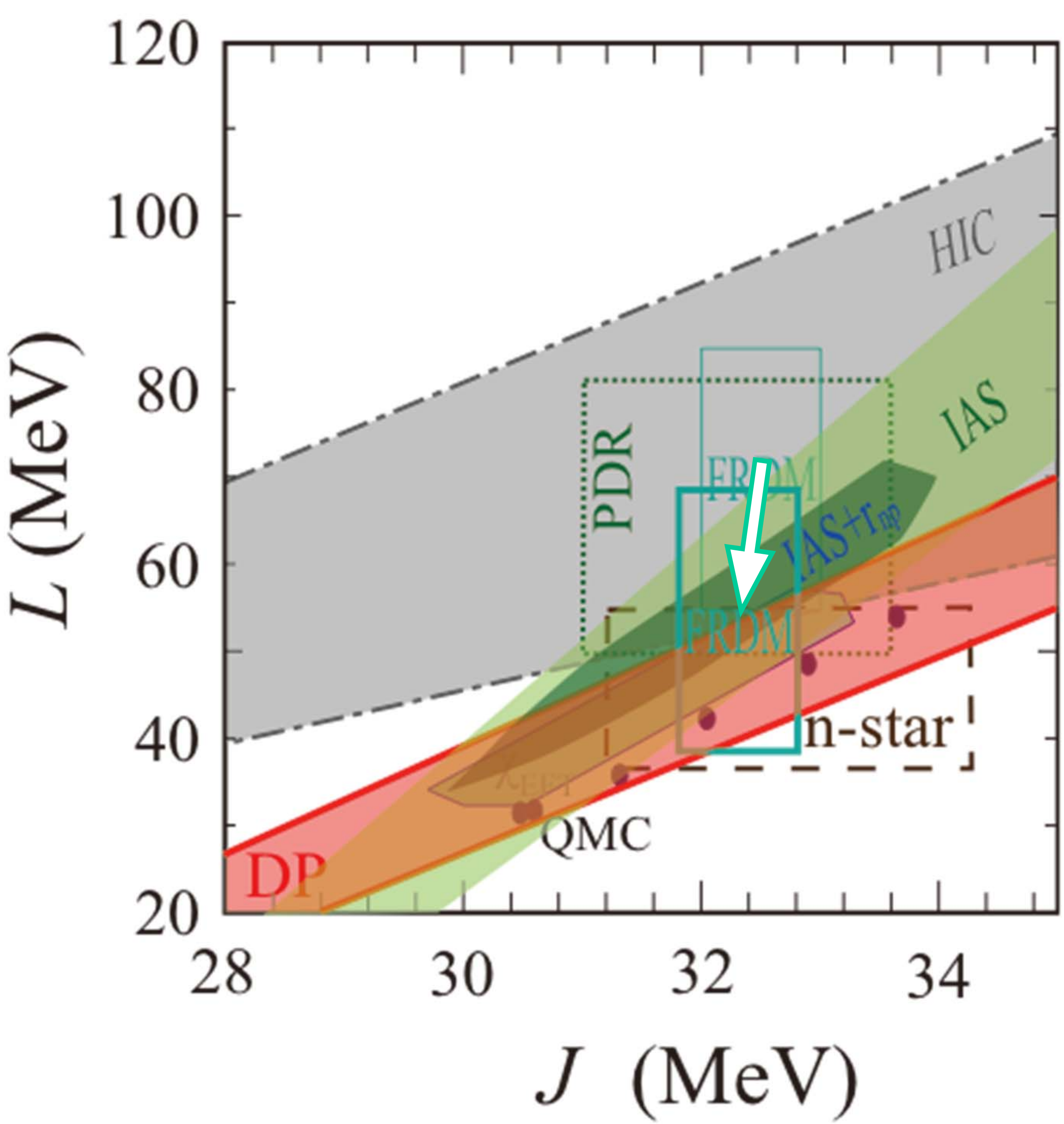

Tsang PRC2012

HIC: Heavy Ion Collision Analysis
Tsang PRL2009

IAS: Isobaric Analog State Energy
Danielewicz&Lee NPA2014

PDR: Pygmy Dipole Resonance in
^{132}Sn, ^{68}Ni, Carbone PRC2010

FRDM: Finite Range Droplet Model
Moller **PRL2012→ADNTD2016**

n-star: Quiescent Low-Mass X-ray
Binaries, Stainer PRL2012

χEFT: Chiral Effective Field Theory,
Tews PRL2013

QMC: Quantum Monte-Carlo Calc.
Gandolfi, EPJA50, 10(2014).

DP: Dipole Polarizability
^{208}Pb AT PRL2011

Constraints on J and L

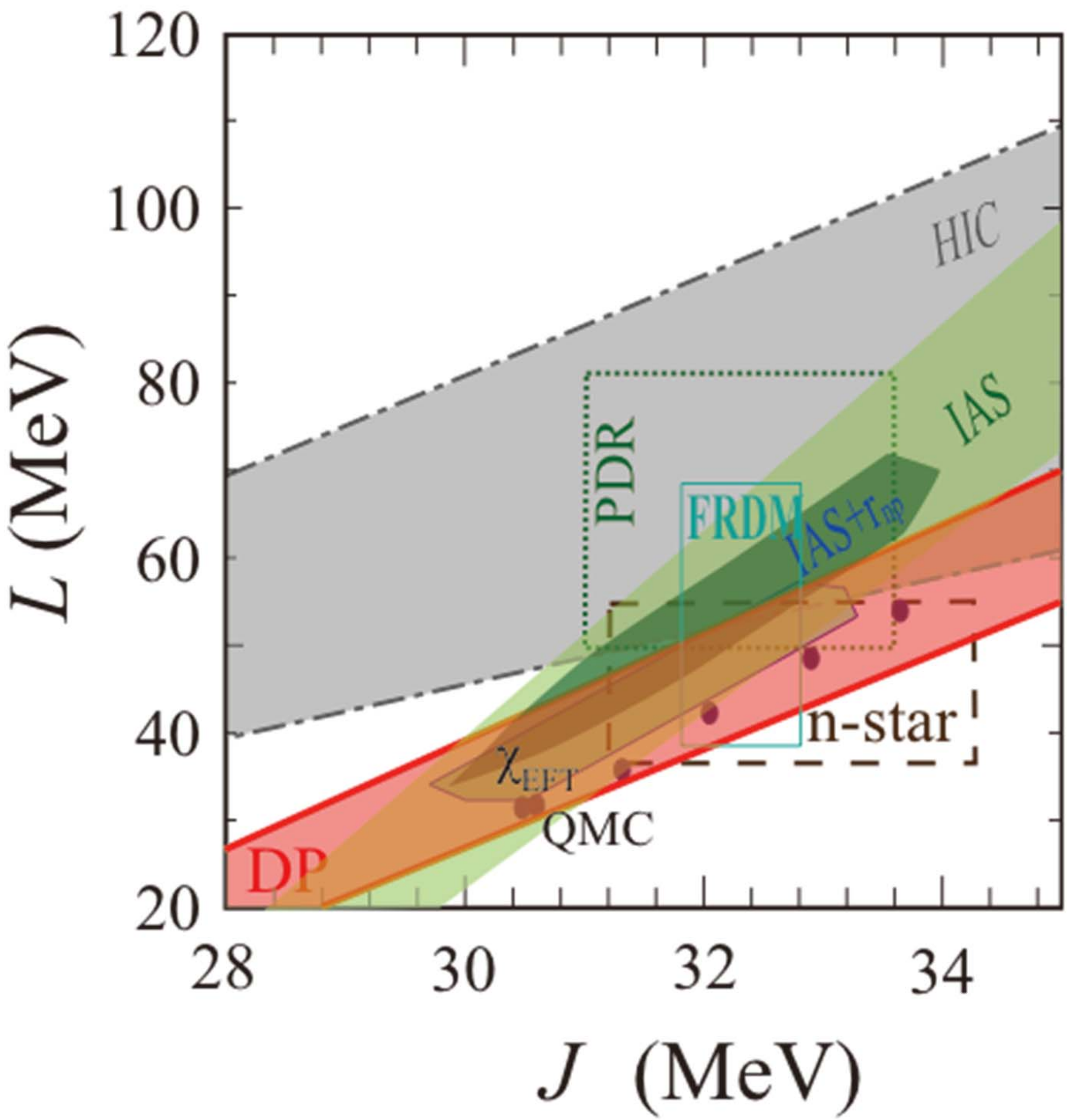

Tsang PRC2012

HIC: Heavy Ion Collision Analysis
Tsang PRL2009

IAS: Isobaric Analog State Energy
Danielewicz&Lee NPA2014

PDR: Pygmy Dipole Resonance in ^{132}Sn, ^{68}Ni, Carbone PRC2010

FRDM: Finite Range Droplet Model
Moller ADNTD2016

n-star: Quiescent Low-Mass X-ray Binaries, Stainer PRL2012

χEFT: Chiral Effective Field Theory,
Tews PRL2013

QMC: Quantum Monte-Carlo Calc.
Gandolfi, EPJA50, 10(2014).

DP: Dipole Polarizability
^{208}Pb AT PRL2011

PDR: Pygmy Dipole Resonance in ^{132}Sn, ^{68}Ni, Carbone PRC2010

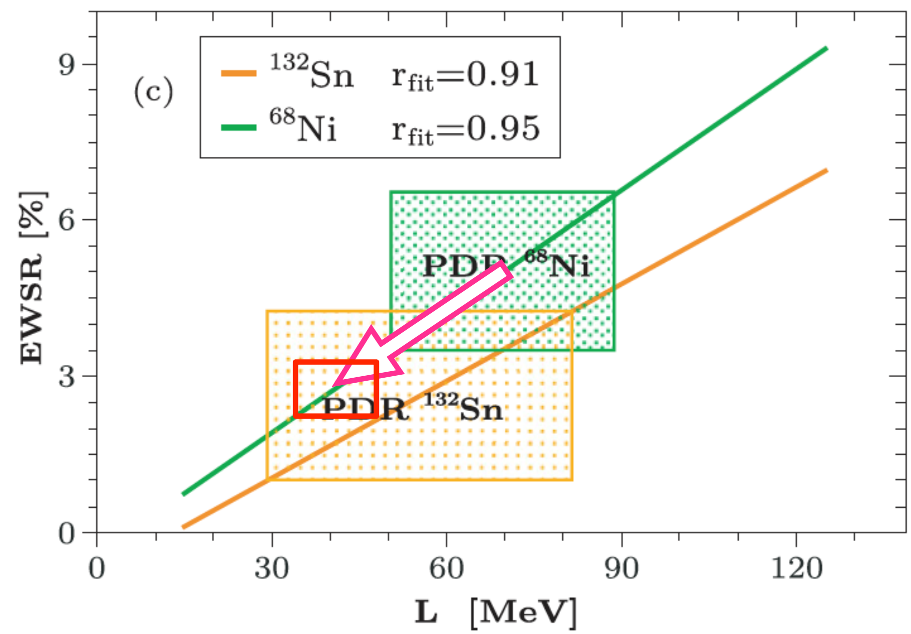

Wieland: PRL2009

In summary, we have here presented the first experimental search of a pygmy resonance in the neutron-rich ^{68}Ni nucleus using the virtual photon scattering technique. Evidence is found for the presence of sizeable strength energetically located below the GDR and centered at ≈11 MeV with approximately 5% of the EWSR strength.

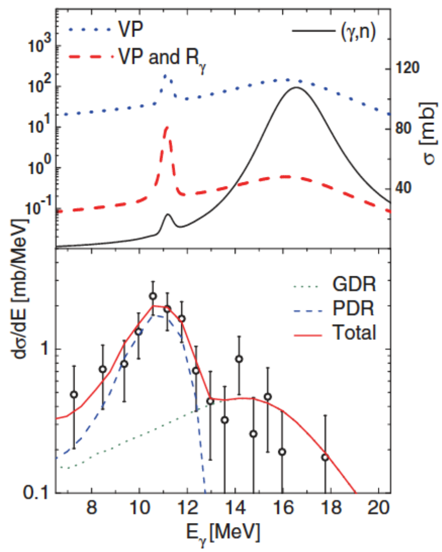

Rossi: PRL2013

TABLE I. GDR and PDR parameters for ^{68}Ni from fit to $E1$ strength, as shown in Fig. 3. Included as well are the GDR and PDR parameters from the literature.

			This work	Literature	Reference
GDR	E_m	[MeV]	17.1(2)	17.84	[30]
	Γ	[MeV]	6.1(5)	5.69	[30]
	S_{EWSR}	[%]	98(7)	100	
PDR	E_m	[MeV]	9.55(17)	11.0(5)	[25,31]
	σ	[MeV]	0.51(13)	<1	[25]
	S_{EWSR}	[%]	2.8(5)	5.0(1.5)	[13,25]

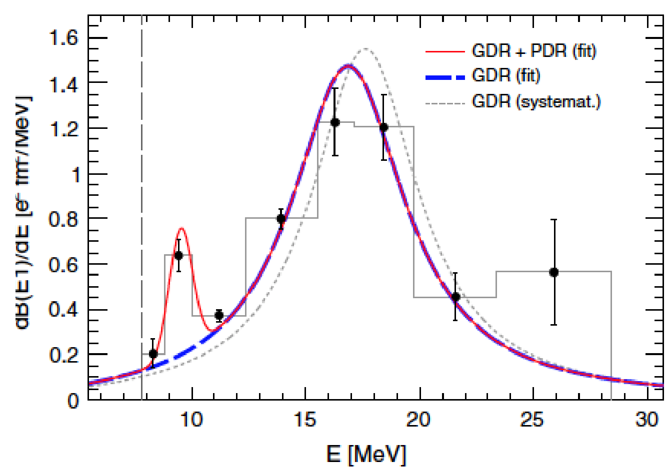

Constraints on J and L

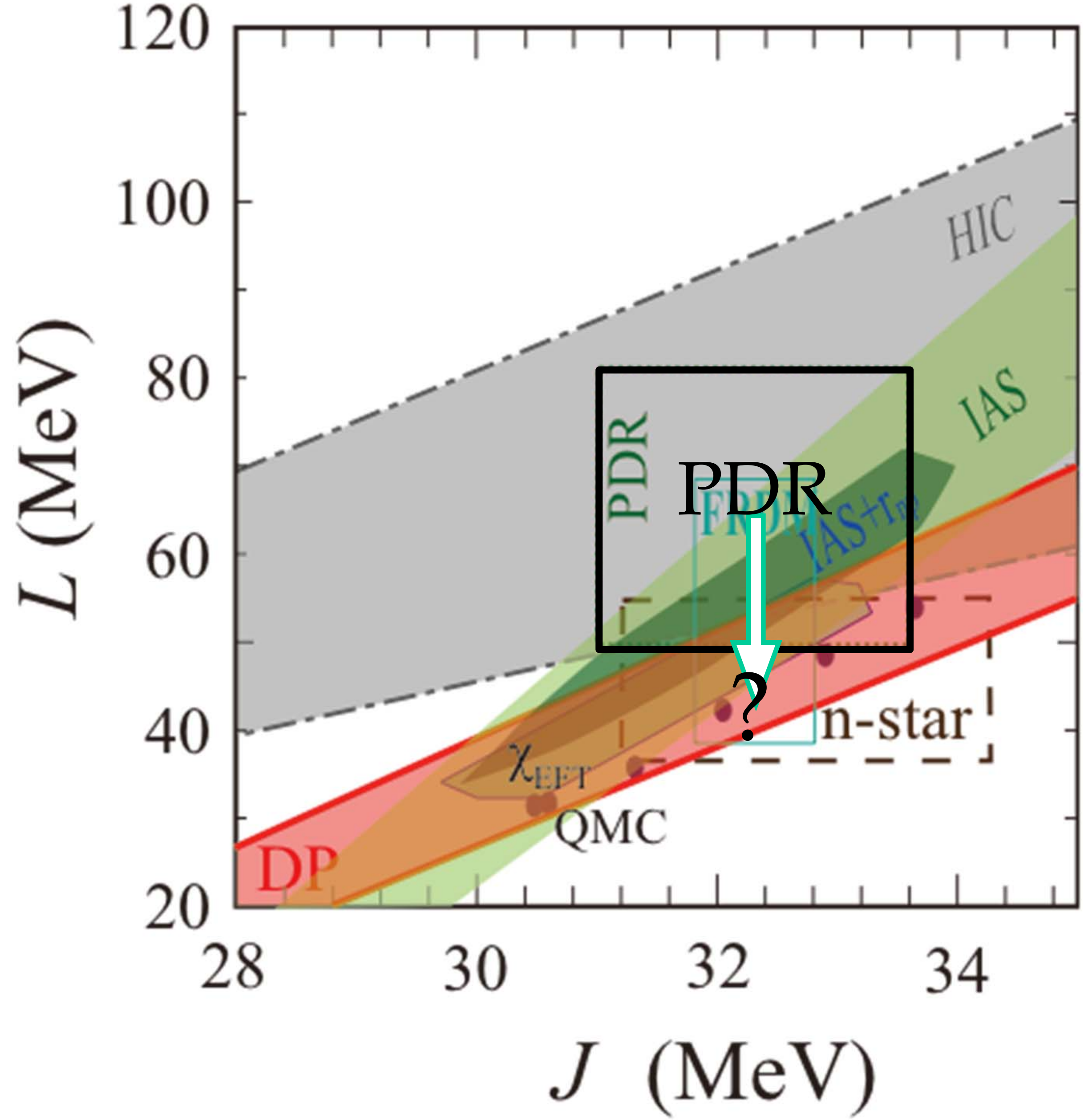

Tsang PRC2012

HIC: Heavy Ion Collision Analysis
Tsang PRL2009

IAS: Isobaric Analog State Energy
Danielewicz&Lee NPA2014

PDR: Pygmy Dipole Resonance in
^{132}Sn, ^{68}Ni, Carbone **PRC2010→?**

FRDM: Finite Range Droplet Model
Moller ADNTD2016

n-star: Quiescent Low-Mass X-ray
Binaries, Stainer PRL2012

χ_{EFT}: Chiral Effective Field Theory,
Tews PRL2013

QMC: Quantum Monte-Carlo Calc.
Gandolfi, EPJA50, 10(2014).

DP: Dipole Polarizability
^{208}Pb AT PRL2011

Fine Structure of the Giant Resonances
and
the Nuclear Level Density

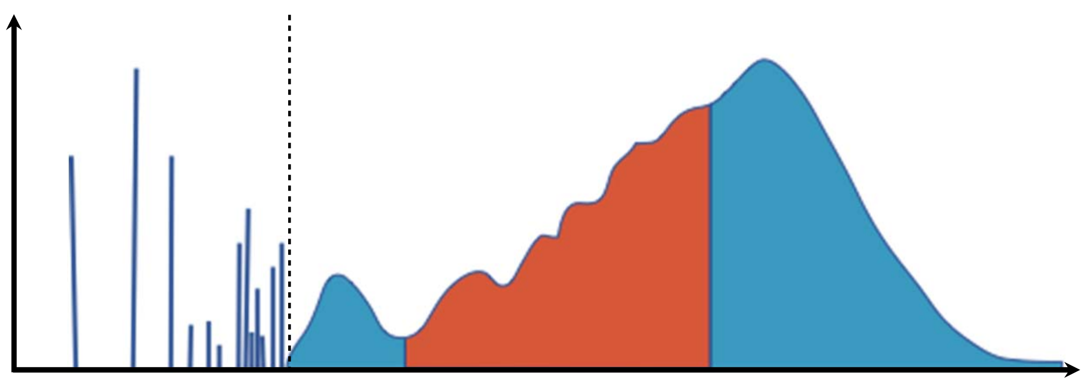

Fine Structure of the GDR

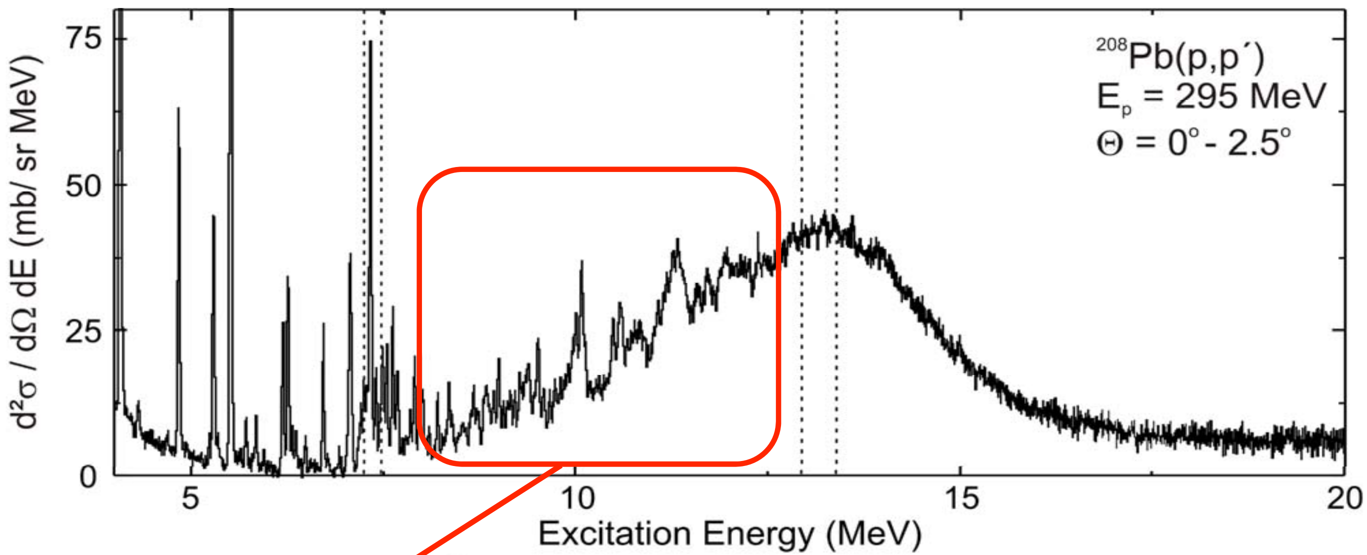

Fine structure of the GDR is clearly observed.

→ Energy dissipation and damping

Gamma decay measurement of the GDR will be one of interesting probes to study the damping mechanism of the GDR.

See e.g. J. Beene et al., PRC41, 920 (1990)

Fine Structure of the GDR

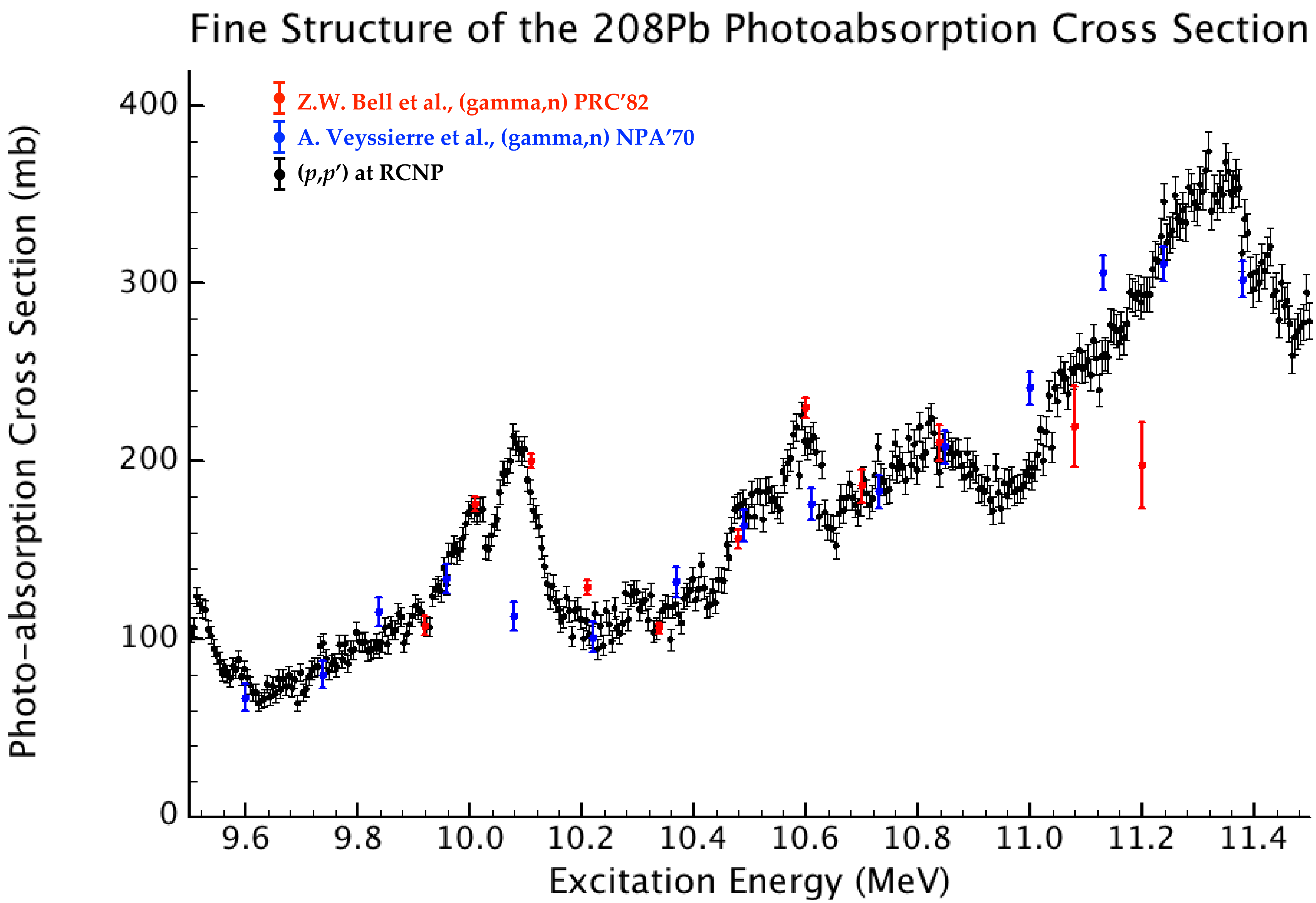

Requirement: an energy resolution of 20-30 keV or better

Fine Structure of the GDR

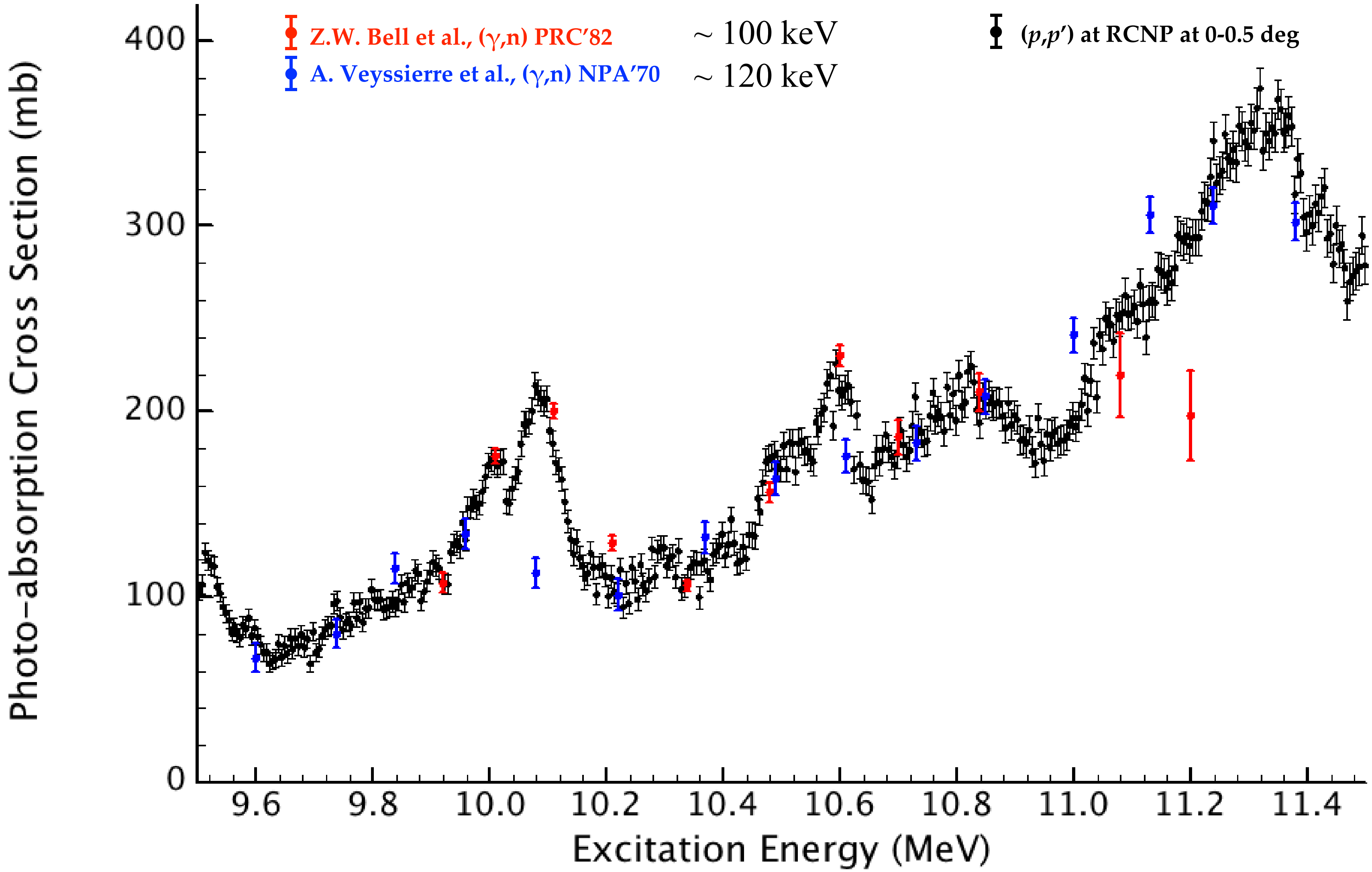

20-30 keV resolution is required.

Fine Structure of the GDR

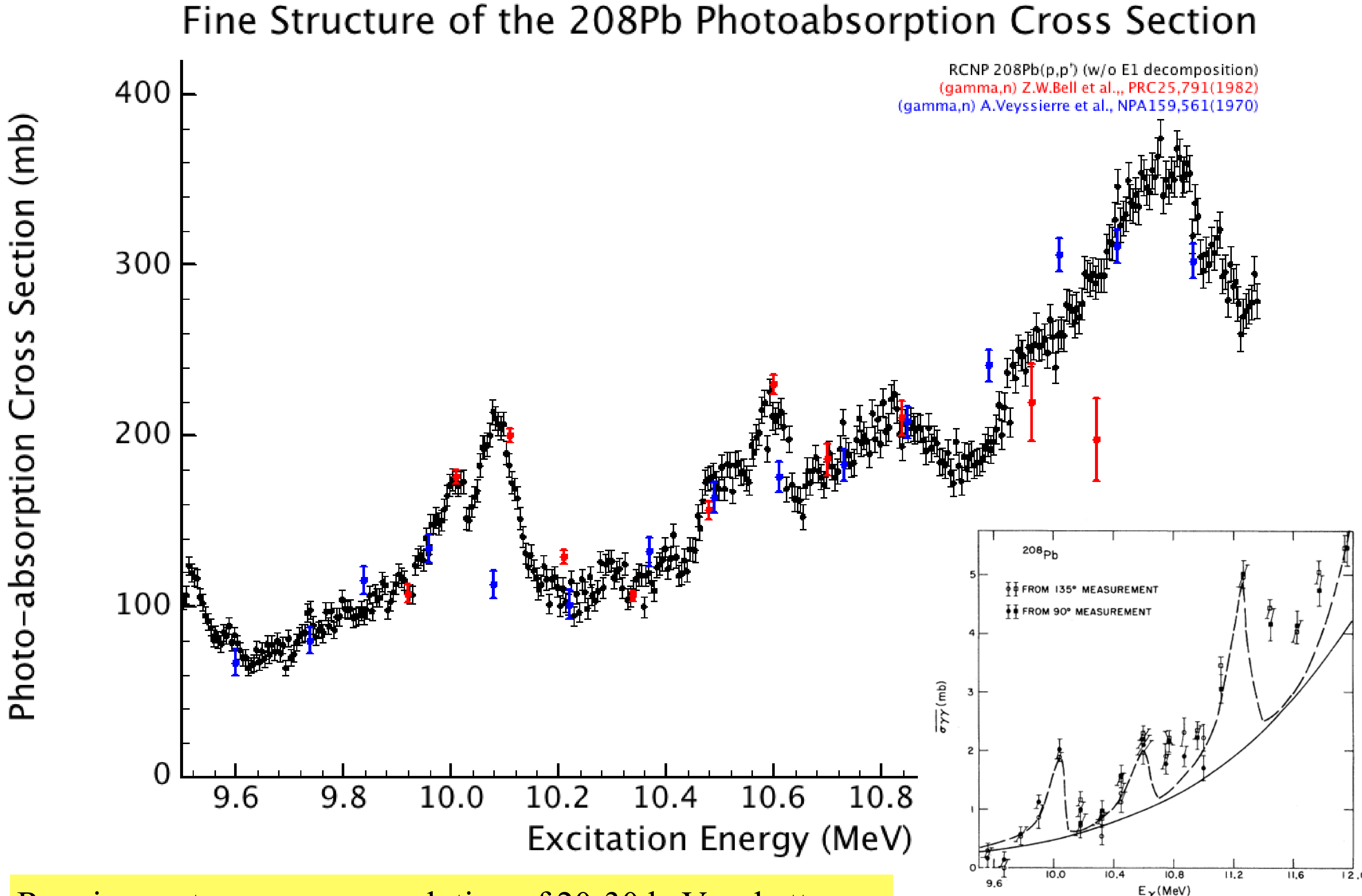

Requirement: an energy resolution of 20-30 keV or better

Fine Structure of the GDR

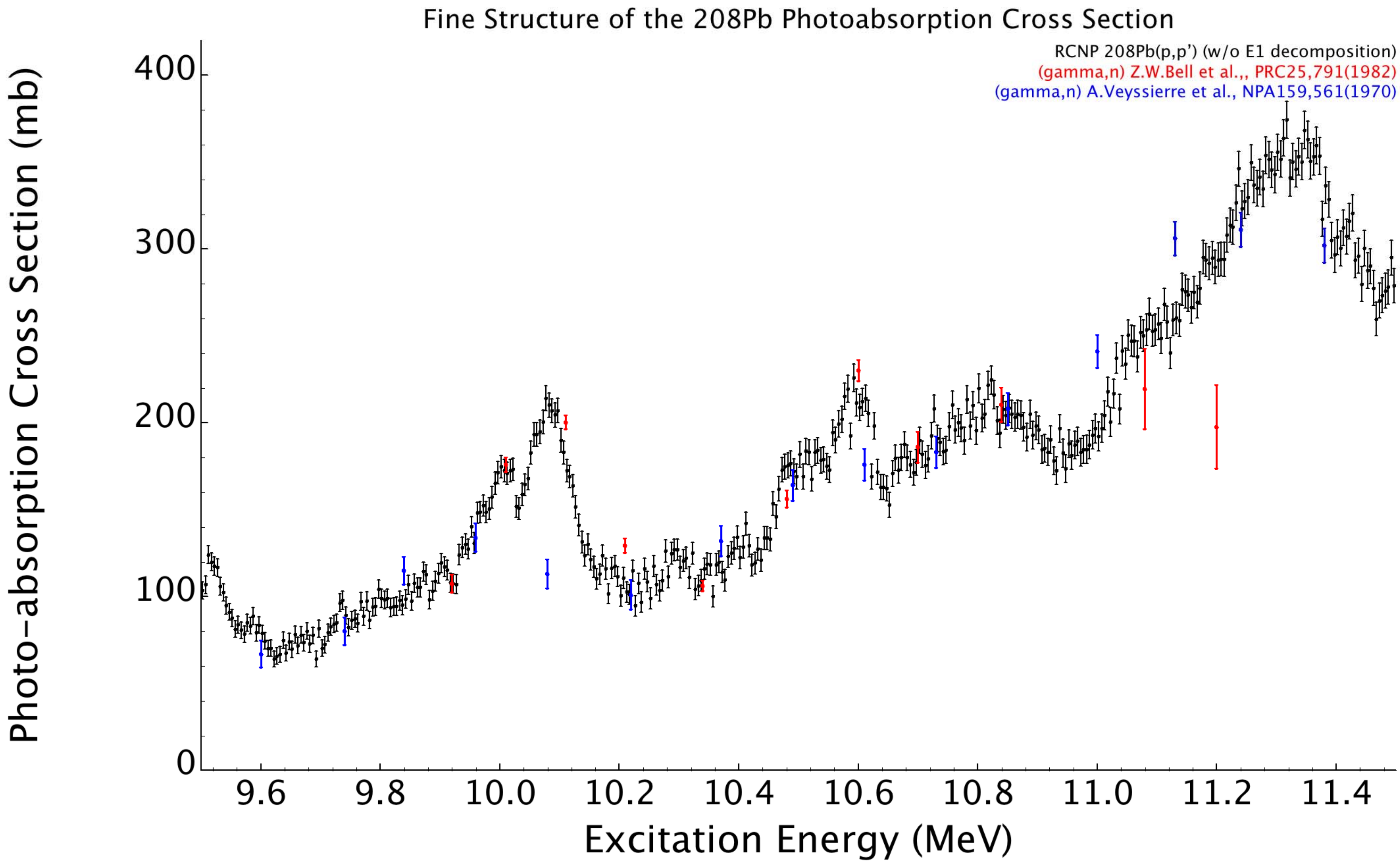

Requirement: an energy resolution of 20-30 keV or better

Nuclear Level Densities

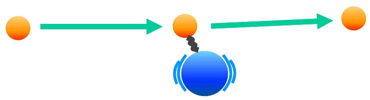

extracted by fluctuation analysis using auto-correlation function

I. Poltoratska et al., PRC89, 054322 (2014)

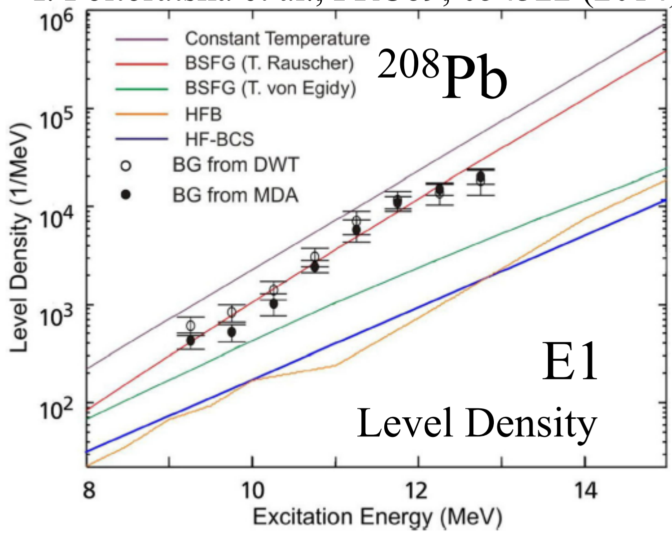

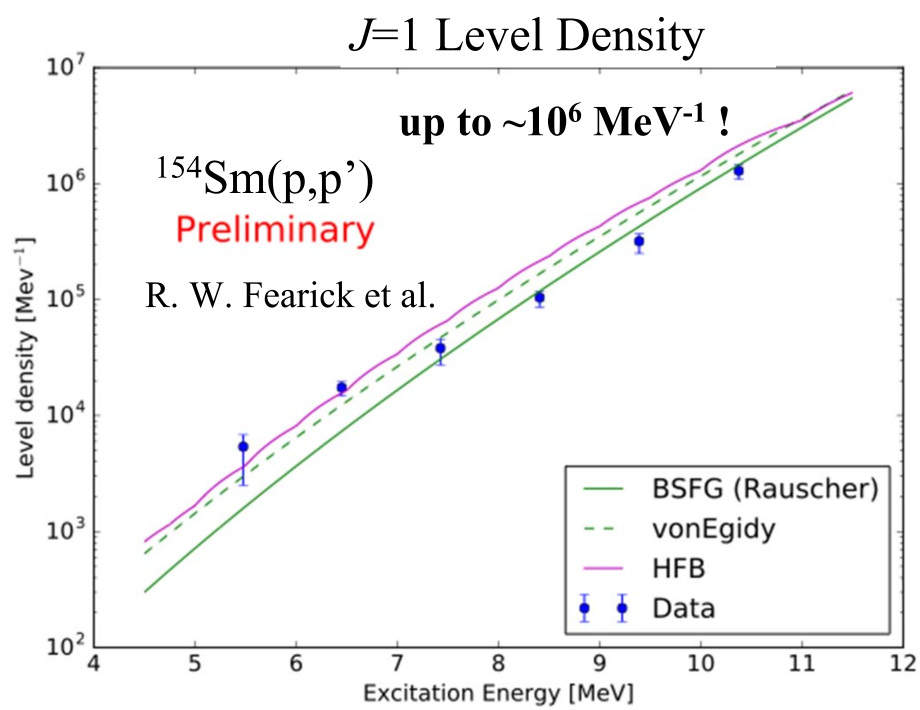

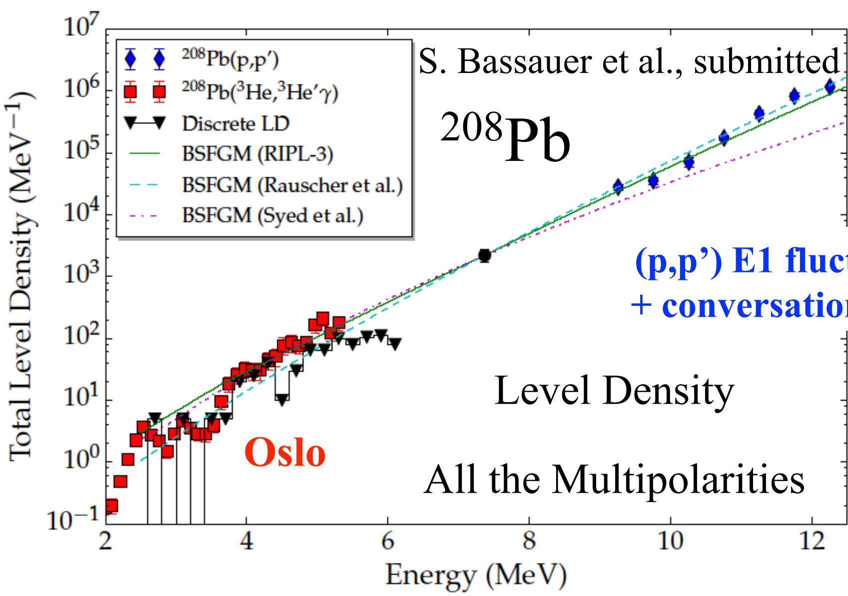

(p,p') E1 fluctuation analysis
+ conversation to total (theo.)

Oslo method: Plenary talk by A.-C. Larsen

Gamma-Decay
of
Electric Dipole Excitations

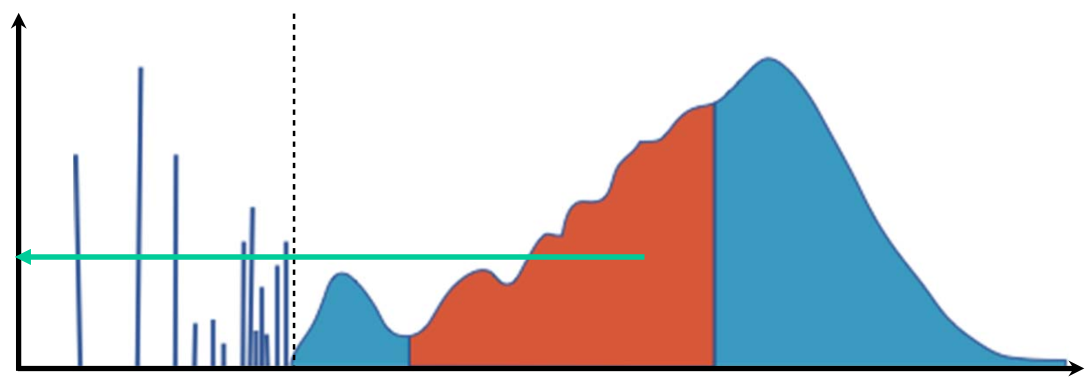

CAGRA+GR Campaign Exp. Oct-Dec 2016

1. **Structure of the PDR *1** (α,α’γ) and (p,p’γ) on ^{64}Ni, ^{90,94}Zr, ^{120,124}Sn, ^{206,208}Pb
2. Inelastic ν-nucleus response
3. Super-deformed states, high-spin states

*1 A. Bracco, F. Crespi, V. Derya, M.N. Harakeh, T. Hashimoto, C. Iwamoto, P. von Neumann-Cosel, N. Pietralla, D. Savran, A. Tamii, V. Werner, and A. Zilges *et al.*

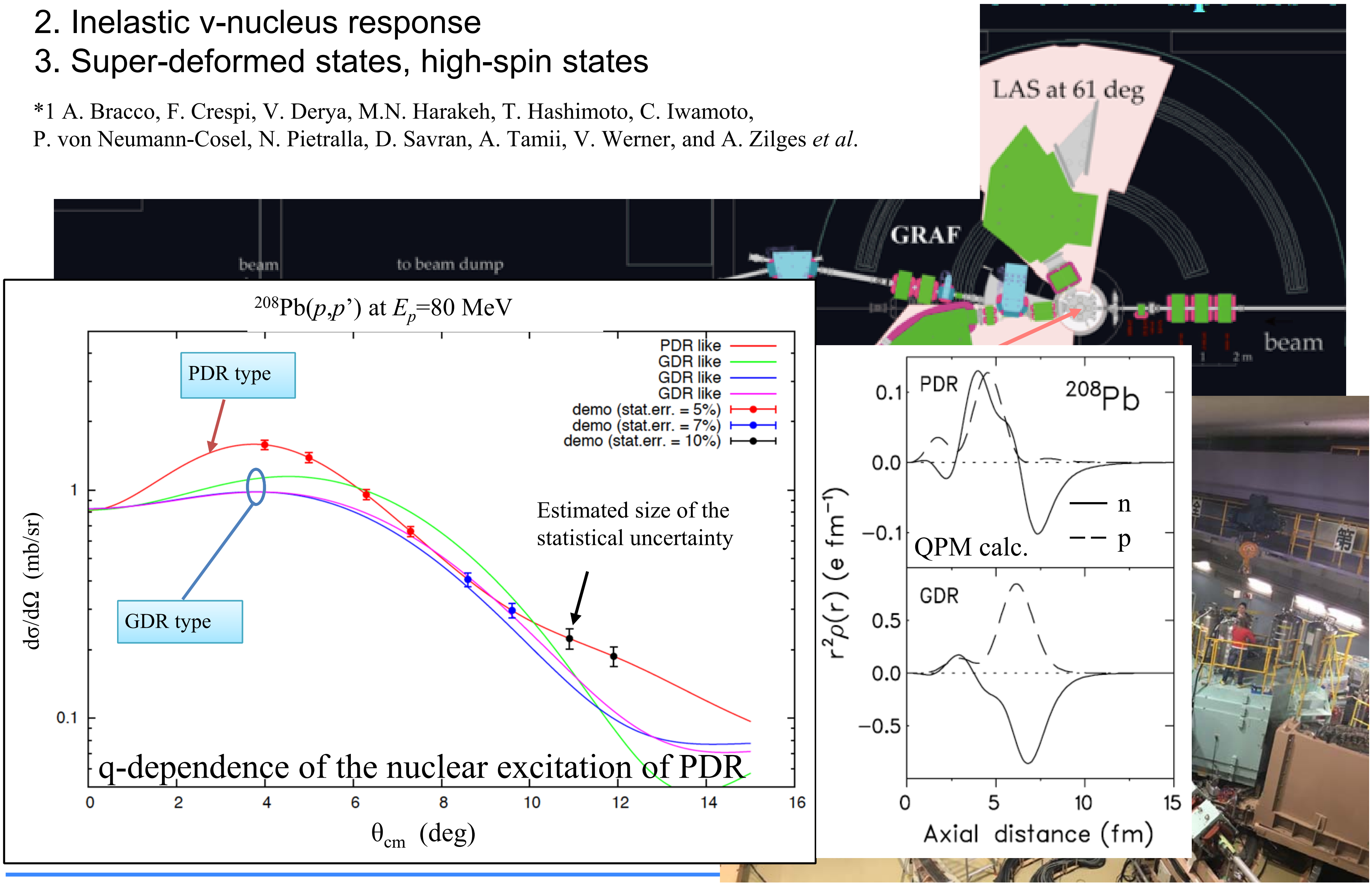

Fine Structure of GDR and its direct g.s. gamma decay

(measurement in July 2018 for ^{90}Zr)

fine structure of GDR

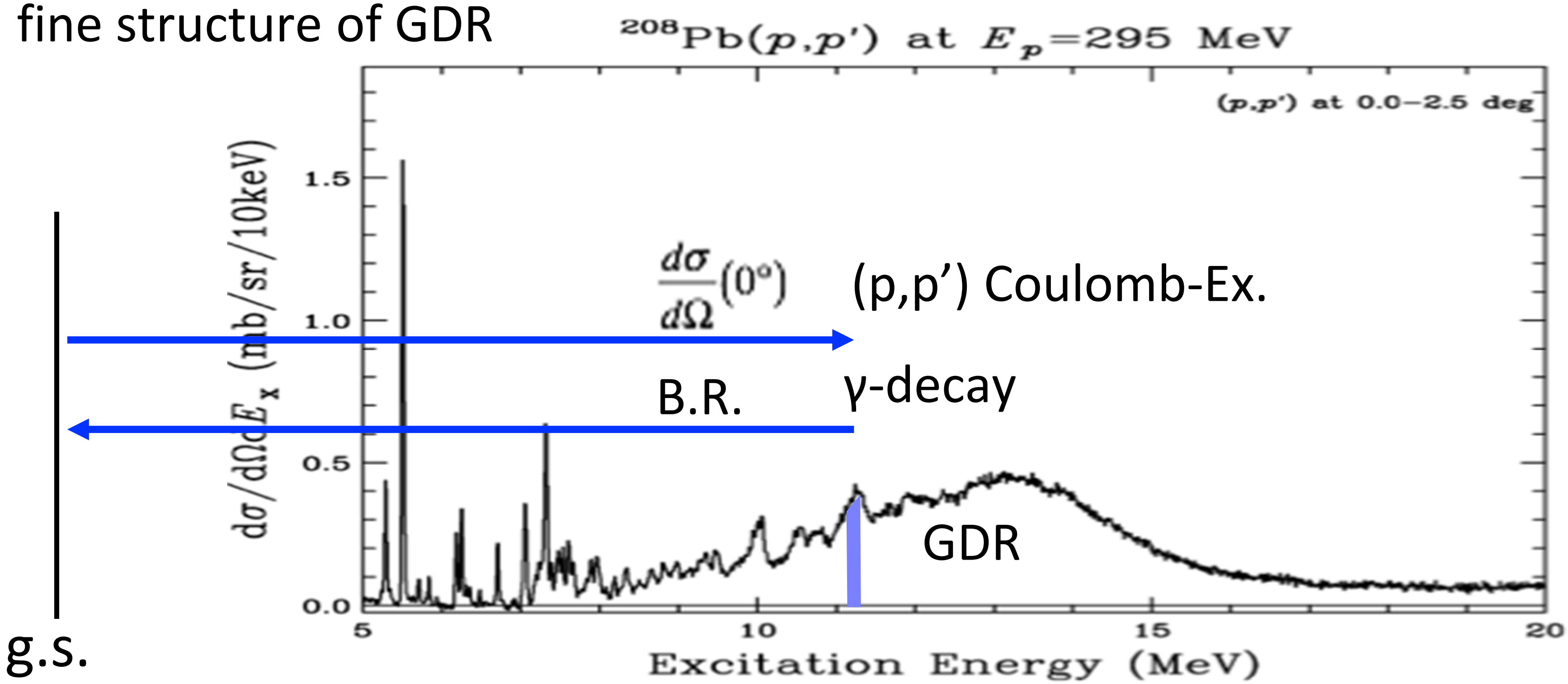

$$\frac{d\sigma}{d\Omega}(0^\circ) \rightarrow B(E1) \rightarrow \Gamma_0$$

$$B.R. = \frac{\Gamma_0}{\Gamma}$$

The total width Γ will be determined for each part of the GDR.

pioneering works:

J. R. Beene et al.,PRC41, 920(1990)

A. Bracco et al., PRC39, 725(1989)

Damping Mechanism of the GDR

γ_0: gamma-decay to the ground state

viscosity between the *n/p* fluids

$$B_{\gamma_0} = \frac{\Gamma_{\gamma_0}}{\Gamma}$$

measured by γ-decay

$$\Gamma_{\gamma_0} = \frac{2J_0+1}{2J+1} E_x^3 B(E1)\uparrow$$

measured by (Coulomb) excitation

Characteristic width Γ can be studied across the IVGDR

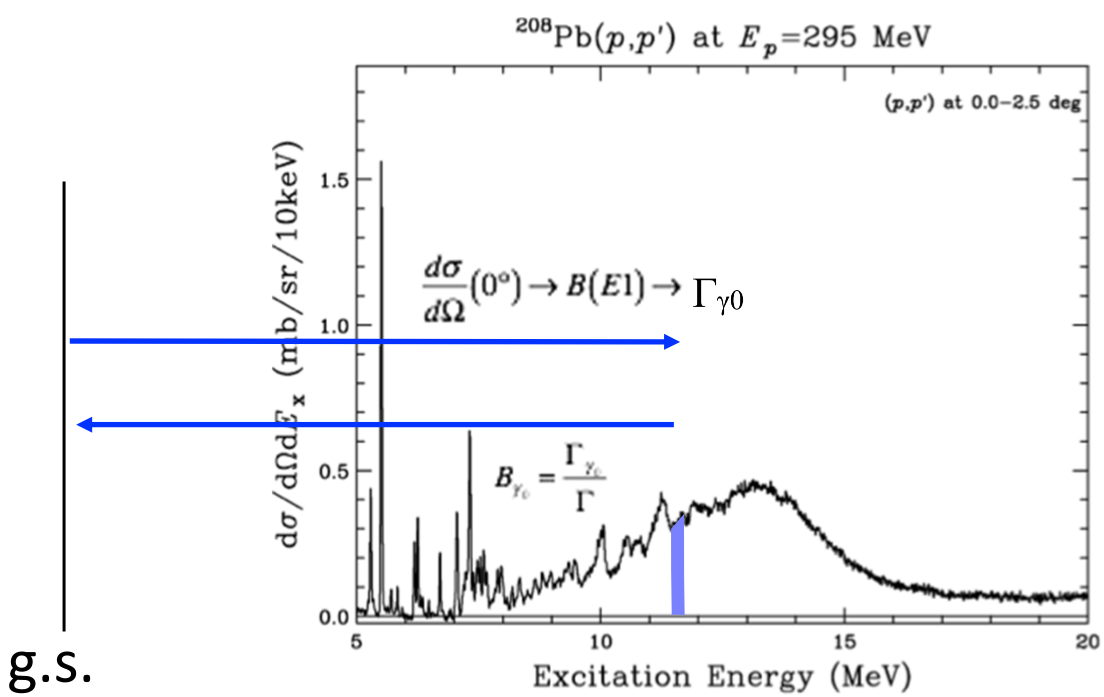

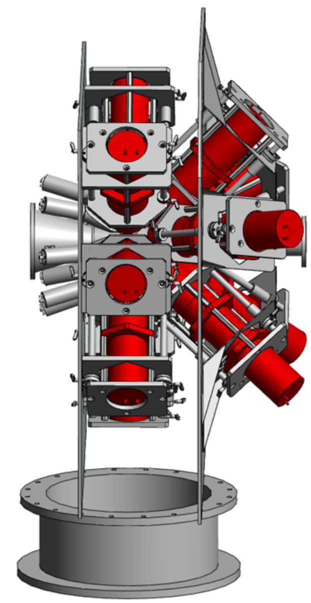

S. Nakamura

RCNP-E498 in July 2018

measurement for ^{90}Zr

LaBr3 scintillator array (Scylla)

Damping Mechanism of the GDR in ^{90}Zr

(July 2018 at RCNP)

RCNP/Milano/TU-Darmstadt Collaboration

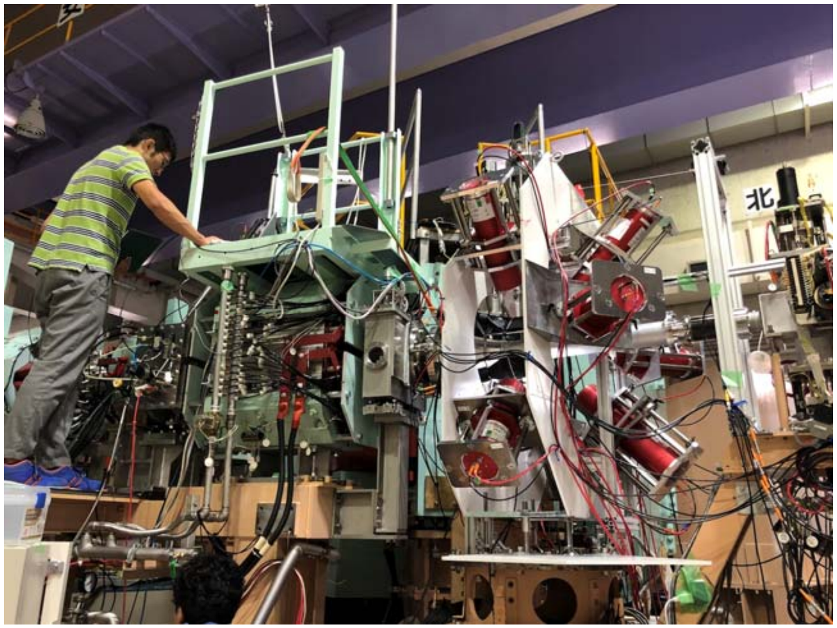

S. Nakamura working on the LaBr3 gamma-detector array (Scylla)

A part of the E498 collaborators

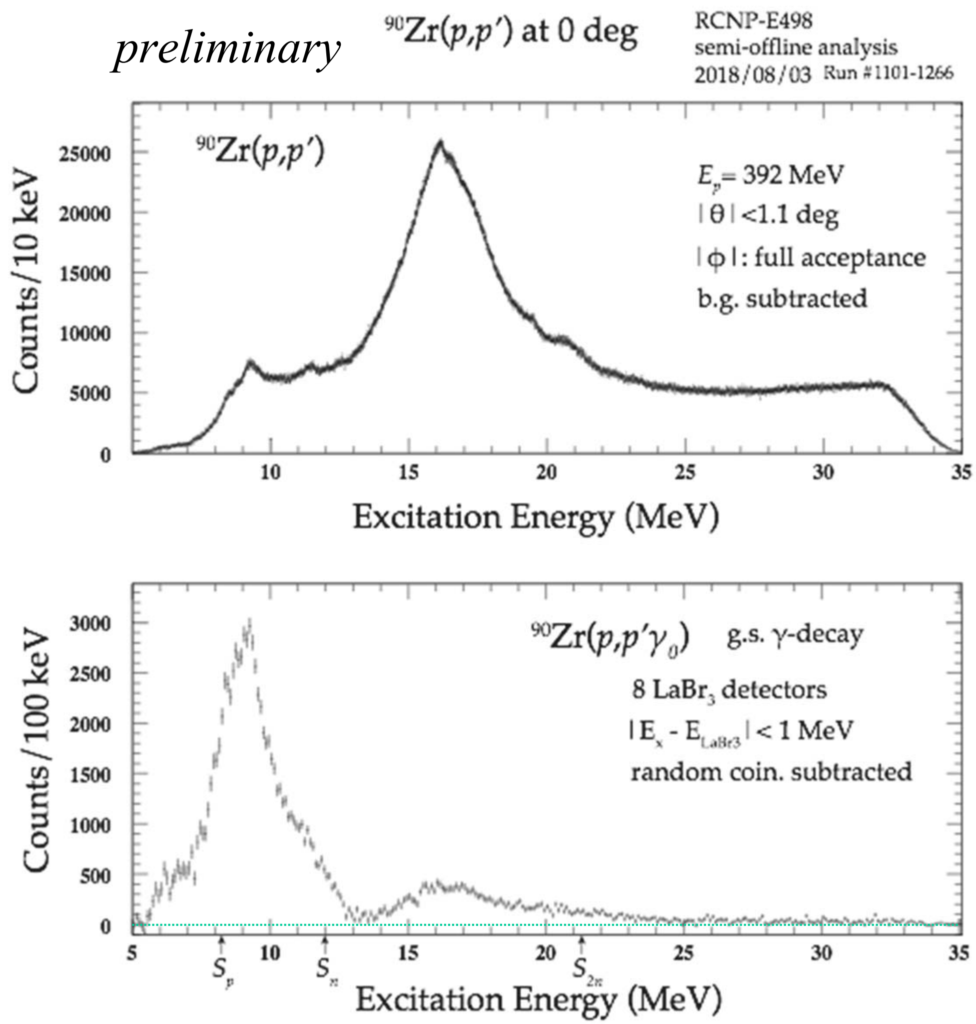

Nuclear Viscosity: damping of the resonances (width)

The damping of a resonance is induced by the viscosity. (friction between nucleons of different motions)

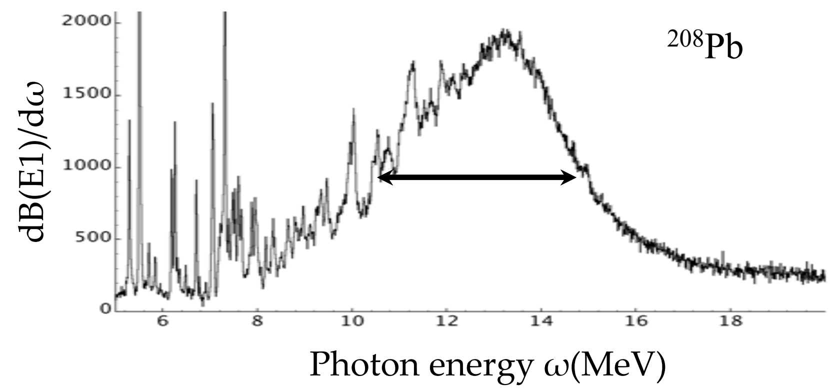

Systematic understanding of the width and the fine-structures of the resonances. (also at higher temperatures)

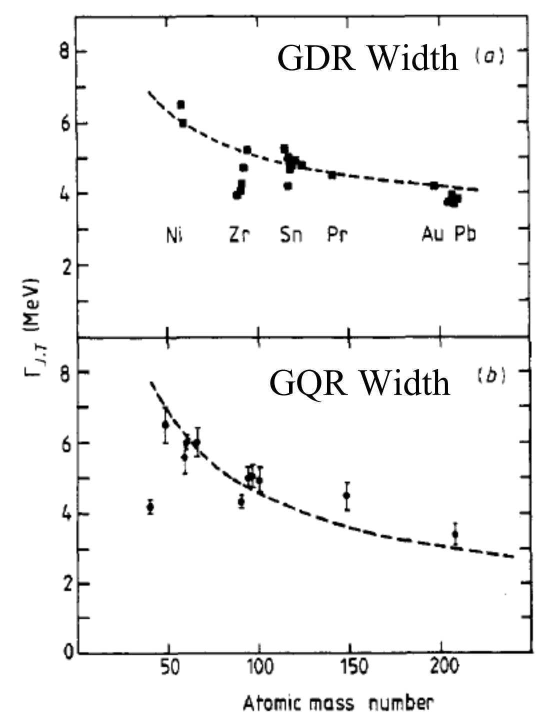

Navier-Stokes equations of viscous two fluids

$$\frac{\partial \mathbf{v}_p}{\partial t} = -\frac{1}{\rho_{p,0}} \nabla P_p + \nu \nabla^2 \mathbf{v}_p + \frac{1}{3} \nu \nabla \nabla \cdot \mathbf{v}_p - \gamma \frac{\rho_{n,0}}{\rho_{n,0} + \rho_{p,0}} (\mathbf{v}_p - \mathbf{v}_n)$$

$$\frac{\partial \mathbf{v}_n}{\partial t} = -\frac{1}{\rho_{n,0}} \nabla P_n + \nu \nabla^2 \mathbf{v}_n + \frac{1}{3} \nu \nabla \nabla \cdot \mathbf{v}_n + \gamma \frac{\rho_{p,0}}{\rho_{n,0} + \rho_{p,0}} (\mathbf{v}_p - \mathbf{v}_n).$$

N. Auerbach and A. Yeverechyahu, Ann. Phys. 1975

J. Wambach, Rep. Prog. Phys. 1988

RCNP-E498 July 2018

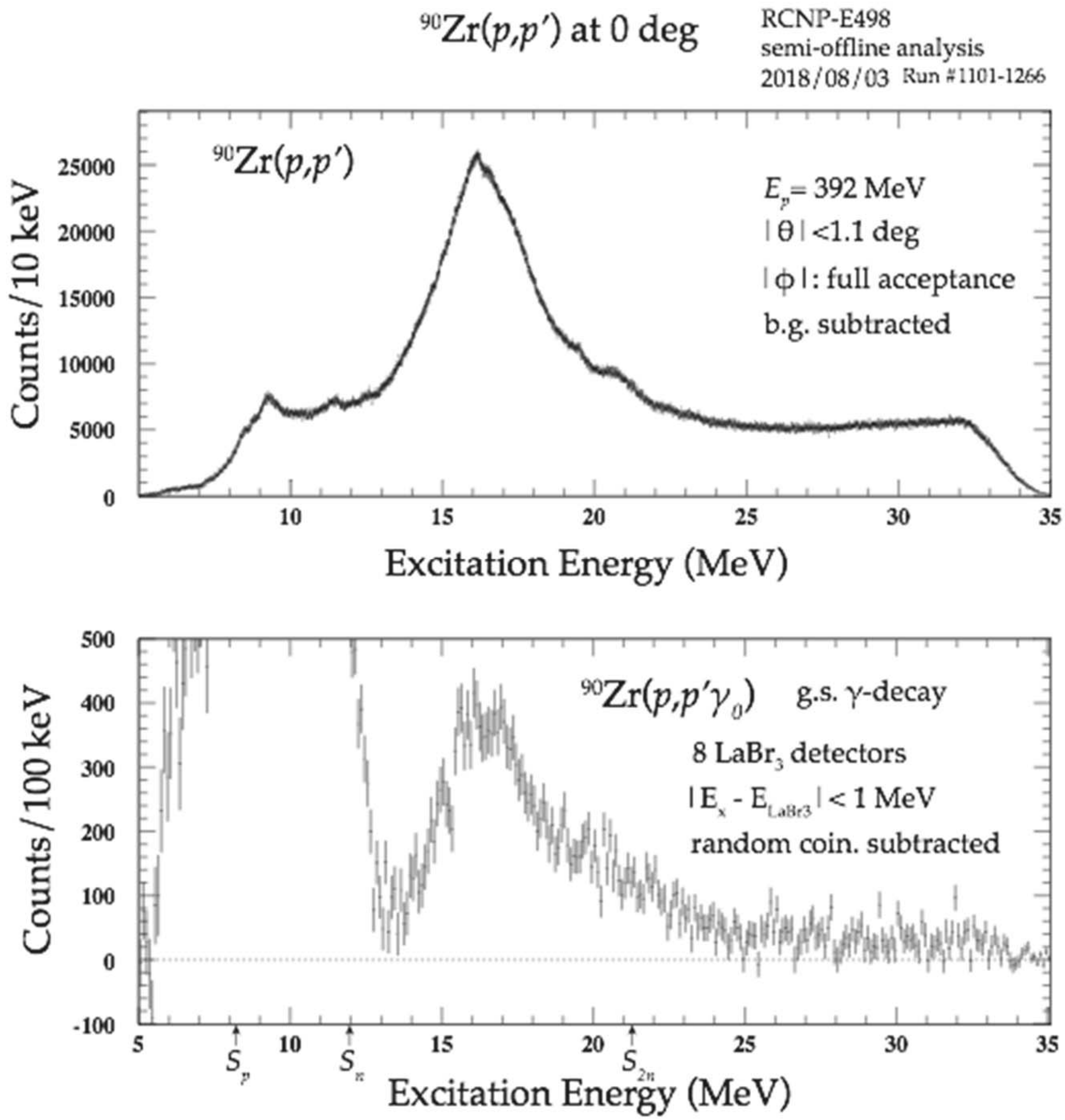

Summary

- The electric dipole polarizability (EDP) is sensitive to the symmetry energy parameters of the nuclear EOS at the saturation density.

- EDP is a well defined quantity, saturating quickly at ~30 MeV in ^{208}Pb.

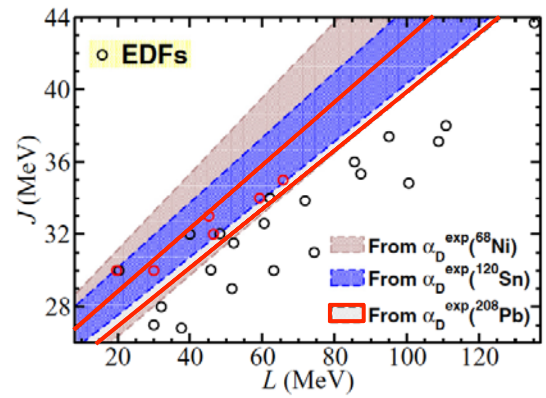

- The EDPs have been experimentally determined precisely for ^{208}Pb and ^{120}Sn (and for ^{68}Ni at GSI). Constraint bands on the symmetry energy parameters, *J* and *L*, has been extracted.

- The EDP of 48Ca has been extracted. A dedicated experiment for smaller exp. uncertainty is planned in 2020.

- Gamma-coincidence projects are on going.

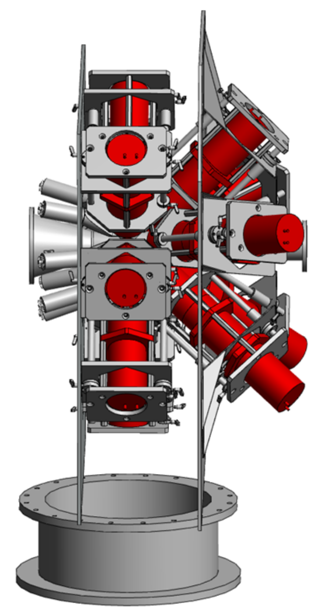

Neutron Skin Thickness of ^{208}Pb

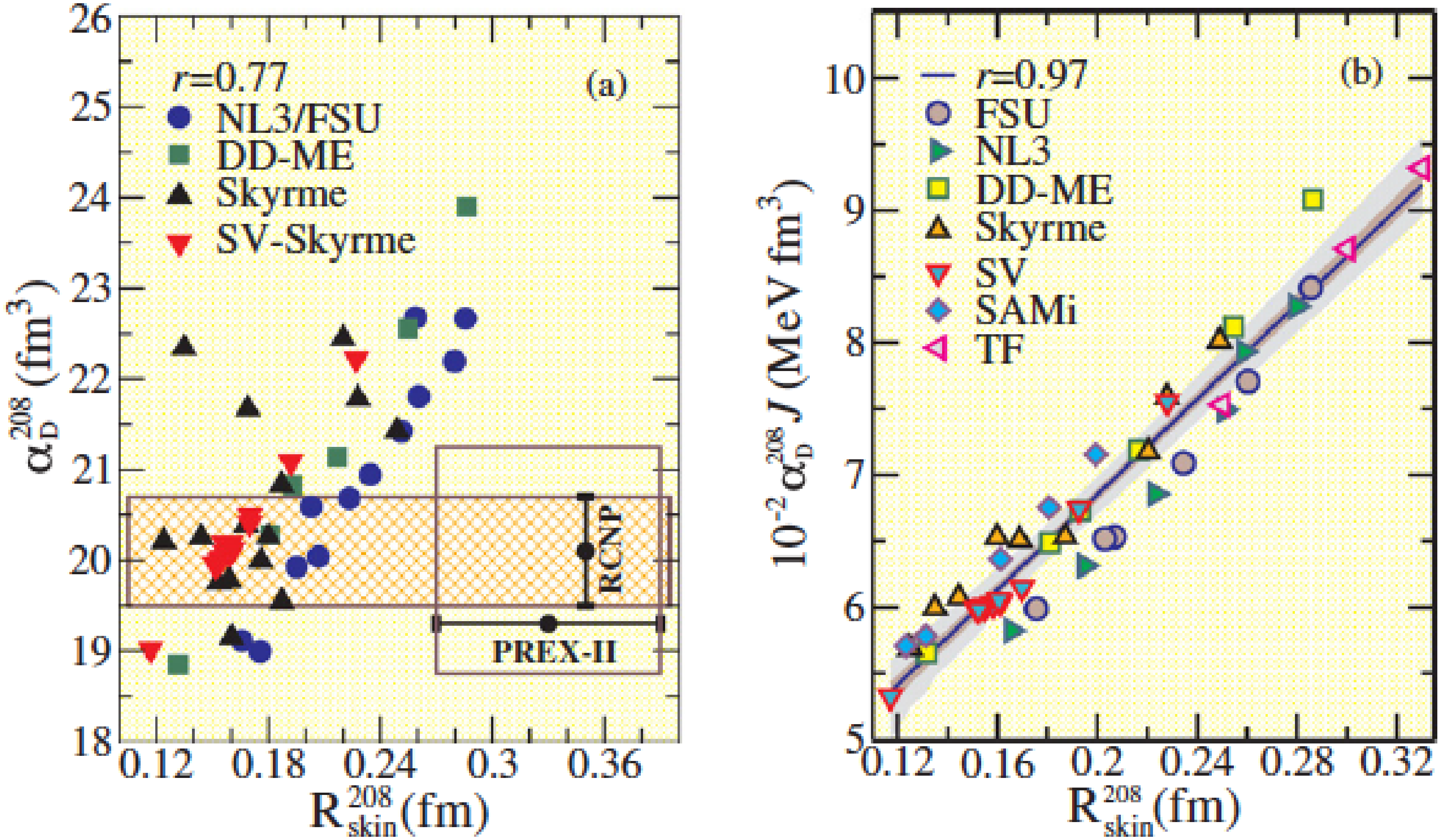

X. Roca-Maza et al., PRC88, 024316 (2013)

C.J. Horowitz et al., JPG41, 093001 (2014)